National Library
of Canada

Canadian Theses Service

Ottawa, Canada
K1A 0N4

Bibliothèque nationale
du Canada

Service des thèses canadiennes

## NOTICE

The quality of this microform is heavily dependent upon the quality of the original thesis submitted for microfilming. Every effort has been made to ensure the highest quality of reproduction possible.

If pages are missing, contact the university which granted the degree.

Some pages may have indistinct print especially if the original pages were typed with a poor typewriter ribbon or if the university sent us an inferior photocopy.

Previously copyrighted materials (journal articles, published tests, etc.) are not filmed.

Reproduction in full or in part of this microform is governed by the Canadian Copyright Act, R.S.C. 1970, c. C-30.

## AVIS

La qualité de cette microforme dépend grandement de la qualité de la thèse soumise au microfilmage. Nous avons tout fait pour assurer une qualité supérieure de reproduction.

S'il manque des pages, veuillez communiquer avec l'université qui a conféré le grade.

La qualité d'impression de certaines pages peut laisser à désirer, surtout si les pages originales ont été dactylographiées à l'aide d'un ruban usé ou si l'université nous a fait parvenir une photocopie de qualité inférieure.

Les documents qui font déjà l'objet d'un droit d'auteur (articles de revue, tests publiés, etc.) ne sont pas microfilmés.

La reproduction, même partielle, de cette microforme est soumise à la Loi canadienne sur le droit d'auteur, SRC 1970, c. C-30.

NL-339 (r. 88/04)

Canada

# SEDIMENTOLOGY OF AN ANCIENT CLASTIC NEARSHORE SEQUENCE, LOWER CRETACEOUS BOOTLEGGER MEMBER, NORTH-CENTRAL MONTANA

by

ROBERT WILLIAM CHARLES ARNOTT

©

A THESIS
SUBMITTED TO THE FACULTY OF GRADUATE STUDIES AND RESEARCH
IN PARTIAL FULFILMENT OF THE REQUIREMENTS FOR THE DEGREE
OF
DOCTOR OF PHILOSOPHY

GEOLOGY

EDMONTON, ALBERTA
FALL 1987

Permission has been granted to the National Library of Canada to microfilm this thesis and to lend or sell copies of the film.

The author (copyright owner) has reserved other publication rights, and neither the thesis nor extensive extracts from it may be printed or otherwise reproduced without his/her written permission.

L'autorisation a été accordée à la Bibliothèque nationale du Canada de microfilmer cette thèse et de prêter ou de vendre des exemplaires du film.

L'auteur (titulaire du droit d'auteur) se réserve les autres droits de publication; ni la thèse ni de longs extraits de celle-ci ne doivent être imprimés ou autrement reproduits sans son autorisation écrite.

ISBN 0-315-40862-6

THE UNIVERSITY OF ALBERTA

**RELEASE FORM**

NAME OF AUTHOR ROBERT WILLIAM CHARLES ARNOTT

TITLE OF THESIS SEDIMENTOLOGY OF AN ANCIENT CLASTIC NEARSHORE SEQUENCE, LOWER CRETACEOUS BOOTLEGGER MEMBER, NORTH-CENTRAL MONTANA

DEGREE FOR WHICH THESIS WAS PRESENTED DOCTOR OF PHILOSOPHY

YEAR THIS DEGREE GRANTED FALL 1987

Permission is hereby granted to the UNIVERSITY OF ALBERTA LIBRARY to reproduce single copies of this dissertation and to lend or sell such copies for private, scholarly or scientific research purposes only.

The author reserves other publication rights, and neither the thesis nor extensive extracts from it may be printed or otherwise reproduced without the author's written permission.

(SIGNED) R. W

PERMANENT ADDRESS:

46 RADFORD ST.
HAMILTON, ONTARIO
L8S 3E6

DATED October 5 1987

THE UNIVERSITY OF ALBERTA

FACULTY OF GRADUATE STUDIES AND RESEARCH

The undersigned certify that they have read, and recommend to the Faculty of Graduate Studies and Research, for acceptance, a thesis entitled SEDIMENTOLOGY OF AN ANCIENT CLASTIC NEARSHORE SEQUENCE, LOWER CRETACEOUS BOOTLEGGER MEMBER, NORTH-CENTRAL MONTANA submitted by ROBERT WILLIAM CHARLES ARNOTT in partial fulfilment of the requirements for the degree of DOCTOR OF PHILIOSOPHY.

..............................

Supervisor

..............................

..............................

..............................

..............................

Date October 5/87

# DEDICATION

This thesis is dedicated to my wife Siobhan, and to whom I dedicate much more than this thesis.

When you take up a pencil and sharpen it up
When they're kicking the fence and still nothing will budge
When the words are in mobile until you sit down
Then to feel their worth keeping they're not easily found
And you know in some strange unexplainable way
You must really have something, something, something fighting hiding away
And hope to say

Peter Townshend (The Who) (1978)

# ABSTRACT

The late Albian to early Cenomanian Bootlegger Member is the uppermost of four members making up the Blackleaf Formation of north-central Montana. In the study areas near Great Falls and on the northwest slopes of Mt. Lebanon in the Sweetgrass Hills, the Bootlegger Member represents marine depositional conditions associated with the initial transgressive stage of the Greenhorn Cyclothem. It conformably overlies and onlaps terrestrial deposits of the Vaughn Member toward the west, and merges with the Mowry Shale to the east. It is unconformably overlain by black shales of the Upper Cretaceous Floweree Member of the Marias River Formation.

Strata of the Bootlegger Member comprise a number of stacked sedimentary sequences. Each sequence is characterised by a thick shoaling-upward sequence, truncated on its upper surface by a planar transgressive which is commonly overlain by a thin transgressive lag deposit. The thick basal portion of each sequence suggests eastward strandline progradation (regressive conditions) while the upper surface represents the subsequent transgression. Strandline migration and development of the Bootlegger sequences were thought to have resulted from episodic uplift and subsidence of the ancestral Sweetgrass Arch, which may have acted as a forebulge. Uplift was associated with accelerated Cordilleran thrusting while subsidence recorded thrust quiescence and lithospheric foundering due to sediment loading and elastic lithospheric relaxation.

Physical and biogenic structures characterising the Bootlegger Member are indicative of a storm-dominated, nearshore environment. Particularly interesting is the occurrence of a sedimentary structure called "gently undulating parallel lamination" (GUP lamination). This structure is characterised by parallel lamination which exhibits a subdued undulation

(spacing-to-height ratio of 50-100, or more), and palaeocurrent indicators (grain fabric, ripples *etc.*) indicating offshore sediment transport. GUP lamination, which is the dominant structure characterising the lower shoreface, is interpreted to be deposited from upper-flow-regime, unidirectionally-dominated, combined flow. In a seward direction, the reduced abundance of GUP lamination matched with an increase of hummocky cross-stratification may suggest the waning of unidirectionally-dominated and an increase in oscillatory-dominated combined flow as a function of depth, or more appropriately distance from the palaeoshoreline.

# ACKNOWLEDGEMENTS

This dissertation was carried out under the supervision of Drs. S.G. Pemberton and F.J. Hein, with funding (to both supervisors) from the Natural Sciences and Engineering Research Council of Canada. Additional financial support was provide by Shell Resources Canada Ltd. and the Hamilton-Wentworth Police Association and are appreciatively acknowledged.

I would like to thank the many people, in particular Drs. S.G. Pemberton, F.J. Hein, B.M. Hand and J.B. Southard, R.A. Burwash, J.F. Lerbekmo and J. England whose comments and reviews have greatly enhanced the quality of this work. In addition, I would like to thank Dr. B.M. Hand for the opportunity to work on the flume at Syracuse University. This project drove home many of the concepts concerning sediment transport and sediment-fluid interaction, and has greatly enhanced my knowledge and appreciation of physical sedimentology. Also I would like to extend my most sincere thanks to Dr S.G. Pemberton for reasons too numerous to count.

Very special thanks is extended to Mr. Mark "Fingers" Fingland for his friendship and very competent assistance during the summer's field work. Also, I would like to thank Mr. Blair Mattison for spending time in the field and helping with the identification of the Bootlegger trace fossils.

I would also like to extend my sincere gratitude to all those with whom I have played and have been associated with in Canadian waterpolo, as it was and still is you who have kept me sane during all these years of "post-secondary education".

Lastly, and most importantly, I would like to thank my brother Paul, whose infectious enthusiasm of these things we call rocks ignited my initial intrique into the science of geology.

# TABLE OF CONTENTS

Chapter Page

I. Introduction 1

References 5

II. Influence of the Sweetgrass Arch on sedimentation of the Bootlegger Member, north-central Montana 6

References 17

III. Sedimentology of a Cretaceous storm-dominated, nearshore sequence and the origin of Gently Undulating, Parallel Lamination (GUP lamination) 31

References 51

IV. Palaeoshoreline and lithologic unit mapping of the Bootlegger Member, north-central Montana 76

References 98

V. Amalgamating physical and biogenic sedimentary structures: A case study; Bootlegger Member, north-central Montana 123

References 138

VI. General Discussion and Conclusions 161

References 169

VII. A. Appendix I(A) The anisotropy of magnetic susceptibility 171

B. Appendix I(B) Data on magnetic susceptibility and anisotropy of magnetic susceptibility 189

VIII. A. Appendix II Flume data from sediment fallout experiments 205

IX. A. Appendix III Structural geology of the Bootlegger Member 231

X. A. Appendix IV Measure palaeocurrent directional data 244

# LIST OF TABLES

TABLE VII(B)-1: Summary table of hydrodynamic conditions during specific upper-plane-bed sediment-fallout flume experiments 217

TABLE VII(B)-2: Grain-imbrication data from specific upper-plane-bed flume runs. Imbrication was analysed by using anisotropy of magnetic susceptibility 219

TABLE VII(B)-3: Summary table of bed accretion rate during specific upper-plane-bed sediment-fallout runs 222

TABLE IX-1: Palaeocurrent data from both the Great Falls and Mt. Lebanon study areas in north-central Montana 247

TABLE IX-2: Pebble imbrication measurements of Sequence 3 conglomerate: Little Willow Ranch Section 260

TABLE IX-3: Pebble imbrication measurements of Sequence 3 conglomerate: Little Belt Creek - Section 2(a) 264

# LIST OF FIGURES

FIGURE II-1: Location map of the area near Great Falls in north-central Montana 24

FIGURE II-2: Correlation chart of Upper and Lower Cretaceous strata in northwestern United States and south-central Alberta (modified after Stelck and Armstrong, 1981) 26

FIGURE II-3: Generalized section of the Bootlegger Sequences east and west of Great Falls:
Eastern area represents sections near Belt
Western area represents sections near Gordon and on Taft Hill (the symbol "F" means the presence of abundant fish scales and fish bones) 28

FIGURE II-4: Location map of the constituent elements making up the Sweetgrass Arch in north-central Montana and southern portion of the Bow Island Arch of southern Alberta 30

FIGURE III-1: Location map of the Ulm Pishkun and surrounding area near Great Falls, Montana 59

FIGURE III-2: Correlation chart of Upper and Lower Cretaceous strata in northwestern United States and south-central Alberta (modified after Stelck and Armstrong, 1981) 61

FIGURE III-3(A): Sharp contact between Unit 1 and Unit 2 (staff is 1.5 m long) 63

FIGURE III-3(B): Interbedded bentonitic shale and siltstone (Unit 1) 63

FIGURE III-4(A): Gently-undulating, parallel laminated sandstones (GUP lamination) of Unit 2 (outcrop is approximately 10 m high) 65

FIGURE III-4(B): Asymmetric ripple cap above GUP laminated sandstone bed 65

FIGURE III-4(C): Interbedded wave and current rippled sandstone and shale sandwiched between two GUP lamnated beds (scale bar is 10 cm long) 65

FIGURE III-4(D): Low angle truncation surfaces within and between individual GUP laminated beds 65

FIGURE III-4(E): HCS at the base of Unit 2 (beneath hammer), over and underlain by GUP laminated sandstones 65

FIGURE III-4(F): Sharp contact between Unit 2 and Unit 3 (just above person's head) 65

FIGURE III-5(A): Medium-scale cross-stratified sandstones of Unit 3 67

FIGURE III-5(B): Thin slabby sandstones (swash lamination) of Unit 5. Note low angle truncation surfaces (width of photo is approximately 1.5 m) 67

FIGURE III-6(A): Cross-sectional palaeo-reconstruction of the Ulm Pishkun study area 69

FIGURE III-6(B): Palaeocurrent rose diagrams for each depositional environment (Cosets = medium-scale, 3-D bedform (dune) coset measurements) 71

FIGURE III-7: The axial trace of the South Arch through the Great Falls study area (Inset shows the constituent elements (South Arch and Kevin-Sunburst Dome) of the ancestral Sweetgrass Arch plus the Bow Island Arch of south-central Alberta 73

FIGURE III-8(A): Gutter cast and numerous flute marks on the sole of a GUP laminated bed 75

FIGURE III-8(B): Directional scour fill (current flowed from left to right) 75

FIGURE III-8(C): Deep, rippled scoured surfaces incised into the top of GUP laminated beds 75

FIGURE IV-1: Location map of the Great Falls and Sweetgrass Hills study areas in north-central Montana 107

FIGURE IV-2: Correlation chart of Upper and Lower Cretaceous strata in northwestern United States and south-central Alberta (modified after Stelck and Armstrong, 1981) 109

FIGURE IV-3: Diagrammatic sketch of the five Bootlegger sequences in the Great Falls study area and four sequences in the Sweetgrass Hills study area 111

FIGURE IV-4: Sweetgrass Arch of north-central Montana 113

FIGURE IV-5: Idealised Bootlegger Sequence 115

FIGURE IV-6(A): Interbedded siltstone/sandstone and shale of Unit 1 (scale bar is 2 cm) 117

FIGURE IV-6(B): Hummocky cross-stratified sandstone interbedded within shale of Unit 1 117

FIGURE IV-6(C): Sharp contact between Unit 1 and Unit 2 lithologies at the Ulm Pishkun (staff is 1.5 m long) 117

FIGURE IV-6(D): Gently undulating, parallel lamination (GUP lamination) (note subtle undulation and low-angle truncations) (scale bar is 10 cm) 117

FIGURE IV-6(E): Medium-scale, cross-stratified sandstones of Unit 3 117

FIGURE IV-6(F): Massive (faint parallel laminated) sandstone characterising the foreshore (Unit 4) (scale bar is 20 cm) 117

FIGURE IV-7(A): Symmetric wave ripples (λ=1.0 m, amplitude=7cm) overlain with a veneer of chert pebbles capping Sequence 3 near Belt, Montana 119

FIGURE IV-7(B): Coarse-grained, arkosic channel-fill overlying and incised into Unit 1 lithologies (Black Horse Lake, Montana) (scale bar is 1m) 119

FIGURE IV-8(A, C, E, G, I): Palaeoshoreline positions of Sequence 1, 2,3 and 4 respectively 121

FIGURE IV-8(B, D, F, H, J): Stratigraphic fence diagrams of Sequences 1,2,3 and 4 respectively 121

FIGURE V-1: Location map of the Taft Hill study area near Great Falls, Montana. (1) Ulm Pishkun study area; (2) Missile Tower study area 142

FIGURE V-2: Correlation chart of Upper and Lower Cretaceous strata in northwestern United States and south-central Alberta (modified after Stelck and Armstrong, 1981) 144

FIGURE V-3: Idealised shoaling-upward lithologic sequence at the Taft Hill study area. Also included are the observed environmental ranges of some common biogenic structures 146

FIGURE V-4(A): Intensely bioturbated, interbedded bentonitic shale and siltstone characterising the shallow offshore-shelf (scale bar represents 7 cm) 148

FIGURE V-4(B): Sharp contact between the shallow offshore-shelf and the overlying lower shoreface at the Ulm Pishkun study area (scale bar is 25 cm long) 148

FIGURE V-4(C): Gently undulating, parallel lamination characteristic of the lower-shoreface depositonal environment. Note numerous low-angle truncations (scale bar represents 15 cm) 148

FIGURE V-4(D): Medium-scale, cross-bedded sandstones representing the upper shoreface 148

FIGURE V-4(E): Abundant gently undulating, parallel lamination and interbedded medium-scale, cross-bedded sandstones of the surf zone (scale bar is 0.90 m long) 148

FIGURE V-4(F): Swash-laminated sandstones deposited in a foreshore environment (scale bar is 0.25 m long) 148

FIGURE V-5(A): Boxwork morphology of*Ophiomorpha nodosa* burrow (scale bar is 3.5 cm long) 150

FIGURE V-5(B): Branching*Thalassinoides* burrow cast (scale bar is 1.3 cm long) 150

FIGURE V-5(C): Abundant *Lockeia* burrow casts formed by the proposed activity of bivalves (scale bar is 0.9 cm long) 150

FIGURE V-5(D): Basal bedding plane view of *Cylindrichnus* burrows (top of bed is into the photo) (scale bar is 1.8 cm long) 150

FIGURE V-5(E): Circular *Berguaria* burrow cast formed by an ancient burrowing sea anemone (scale bar is 0.75 cm long) 150

FIGURE V-5(F): One very large and several smaller *Planolites beverlyensis* burrows (scale bar is 5 cm long) 150

FIGURE V-6(A): Cross-sectional view of a *Polycladichnus* burrow within a gently-undulating, parallel laminated bed. Note the presence of an amalgamated bed contact immediately above the *Polycladichnus* burrow (scale bar is 2.5 cm long) 152

FIGURE V-6(B): An escape structure created by the vertical burrowing activity of a buried animal following the rapid emplacement of the bed 152

FIGURE V-6(C): Abundant *Palaeophycus* burrow casts (scale bar is 3.0 cm long) 152

FIGURE V-6(D): Cross-sectional view of a *Teichichnus* burrow (scale is 8.0 mm long) 152

FIGURE V-7: Anomalous abundance of vertical burrows, in this case *Ophiomorpha nodosa* , observed along particular laterally continuous horizons at the Ulm Pishkun study area. These horizons are interpreted to represent temporary depositonal hiatuses which rendered the bed susceptible to anomalous degrees of bioturbation (scale bar represents 4 cm) 154

FIGURE V-8: Diagrammatic sketch of the Ulm Pishkun and Missile Tower study areas. Note the thinner lower shoreface deposits and the occurrence of the *Diplocraterion* unit at the top of the lower shoreface at the Missile Tower study area 156

FIGURE V-9(A): *Diplocraterion* unit occurring at the top of the lower shoreface at the Missile Tower study area 158

FIGURE V-9(B): *Rosselia* burrows occurring within the *Diplocraterion* unit at the Missile Tower study area. The occurrence of these two forms indicates the progressive evolution of a soft ground to a semi-consolidated substrate (scale bar is 1.2 cm long) 158

FIGURE V-9(C): Three distinct *Arenicolites* structures within the*Diplocraterion* unit at the Missile Tower study area. *Arenicolites* are soft-ground burrows occurring within a unit containing abundant semi-consolidated burrow forms (*Diplocraterion*) 158

FIGURE V-9(D): Laterally migrating limb of a *Arenicolites* burrow observed in the *Diplocraterion* unit at the Missile Tower study area 158

FIGURE V-9(E): Large, scratch-marked*Thalassinoides* burrow cast occurring on the base of the *Diplocraterion* unit at the Missile Tower study area (scale bar is 2 cm long) 158

FIGURE V-9(F): Abundant ropy textured *Palaeophycus* burrow casts observed on the base of the *Diplocraterion* unit at the Missile Tower study area (scale bar is 6 cm long) 158

FIGURE 10: Diagrammatic sketches of the development of Bootlegger Member strata at the (1) Ulm Pishkun and (2) Missile Tower study areas. Details of Figures 10A to 10D are given in the text.
(A) Palaeotopography at the close of Vaughn Member time; topographic high in the Missile Tower area and a low in the Ulm Pishkun area.
(B) Drowning of Vaughn palaeotopography during transgression associated with the advance of the Greenhorn Sea. Transgression lead to the deposition of shallow offshore-shelf deposits at both study areas, but palaeotopography was retained.
(C) Shoreline progradation and the development of lower-shoreface depositional environments at both study areas. Sediment by-passing at the topographically higher Missile Tower area enabled the exclusive development of semi-consolidated substrate conditions and the invasion of *Diplocraterion* trace makers
(D) Removal of differential topography and the deposition of equally thick upper shoreface strata 160

FIGURE VI(A)-1: Photo and Diagrammatic sketch of the SI-2 Magnetic Anisotropy and Susceptibility Instrument 187

FIGURE VI(A)-2: Sample coordinate system used for measurements of anisotropy of magnetic susceptibility 188

FIGURE VII-1: Recirculating flume at Syracuse University (9 m x 54.5 cm) 224

FIGURE VII-2: Sediment fallout during experimental runs 224

FIGURE VII-3(A): Wide-angle view at the completion of a dune bedform run (Run 22) 226

FIGURE VII-3(B): Close-up of climbing dunes from Run 22 226

FIGURE VII-4(A): Plane bed run - RUN 17: (dA/dt = 1.49 cm/s) 228

FIGURE VII-4(B): Plane bed run - RUN 20: (dA/dt = 3.0 cm/s) 228

FIGURE VII-4(C): Plane bed run - RUN 24: (dA/dt = 4.3 cm/s) 228

FIGURE VII-5: Development of climbing parallel bands as a result of climbing millimetre-height bedforms formed under upper-plane-bed conditions 230

FIGURE VIII-1: Location map of the Sweetgrass Hills and Great Falls in north-central Montana 235

FIGURE VIII-2: The constituent elements of the Sweetgrass Arch in north-central Montana (Kevin-Sunburst Dome and South Arch) plus the southern portion of the Bow Island Arch of south-central Alberta 235

FIGURE VIII-3: Diagrammatic of the bedding orientations on the northeast slope of Belt Butte 237

FIGURE VIII-4: Photo of the western slope of Belt Butte. Lower arrow points to the "belt" of basal Bootlegger strata (5 m thick), while the upper arrow points to the Arrow Creek Bentonite (11 m thick) 239

FIGURE VIII-5: Diagrammatic sketch of the structure developed on the northeast side of Belt Butte 241

FIGURE VIII-6: Location of Mt. Lebanon on the east side of East Butte within the Sweetgrass Hills 243

FIGURE IX-1: Location map of all study locations in the Great Falls study area from which palaeocurrent information was obtained 246

FIGURE IX-2: A Schmidt Net representation of the rotated palaeocurrent data from Mt. Lebanon 259

FIGURE IX-3: Rose diagram of pebble imbrication data of conglomerate cropping out at the Little Willow Ranch study area 263

FIGURE IX-4: Rose diagram of pebble imbrication data of conglomerate cropping out at the Little Belt Creek study area 267

# INTRODUCTION

The late Albian to early Cenomanian Bootlegger Member is the uppermost of four stratigraphic members composing the Lower Cretaceous Blackleaf Formation of north-central Montana (Cobban *et al.*, 1959, 1976; Cannon, 1966). By definition the Bootlegger Member is completely marine and represented deposition during the initial transgressive stages of the Greenhorn Cyclothem into this area of north-central Montana (Vuke, 1984). The Bootlegger Member overlies and onlaps westward with terrestrial deposits of the Vaughn Member, while merging eastward with the deep basinal Mowry Shale of east-central Montana. The type section of the Bootlegger Member crops out along the south face of Bootlegger Escarpment near the city of Great Falls and represents one of several study locations in this area of north-central Montana. Additional outcrops were studied on the northwest slopes of Mt. Lebanon in the Sweetgrass Hills.

The text of this thesis is comprised of four papers. The ordering of the papers is such that terminology used in each paper has been defined and discussed in the previous paper(s) (*eg.* the influence of the Sweetgrass Arch; gently undulating, parallel lamination *etc.*).

Detailed analysis of the regional nature of the Bootlegger Member in the Great Falls area indicates the recurring development of shoaling-upward depositional conditions during Bootlegger time (Arnott, 1987). These recurring conditions resulted in the development of five vertically stacked, shoaling-upward, clastic sequences observed throughout the entire Great Falls study area. In an idealized case a complete sequence is made up of strata deposited in a shallow-offshore shelf environment progressively overlain by lower shoreface, upper shoreface and finally foreshore strata. In the first paper (Influence of the

Sweetgrass Arch on sedimentation of the Bootlegger Member, north-central, Montana) the discussion deals mainly with the driving mechanism behind the development of cyclic Bootlegger sedimentation. In this paper the influence of the South Arch, the southern element of the Sweetgrass Arch whose crest lies close to the Great Falls study area, is inferred to be the controlling mechanism behind the development of the five Bootlegger Sequences.

Detailed lithologic facies analysis of one particular Bootlegger Member outcrop, the Ulm Pishkun (located approximatley 16 km west of the city of Great Falls), enabled an accurate delineation of the depositional environments within a storm-dominated, nearshore clastic sequence. In this the second paper (Sedimentology of a Cretaceous storm-dominated, nearshore sequence and the origin of gently undulating parallel lamination (GUP lamination)) the first half of the paper deals with the lithologic characteristics and depositional mechanisms defining five distinct depositional environments developed in a prograding, storm-dominated nearshore. Depositional environments include: shallow-offshore shelf, lower shoreface, upper shoreface, channellized surf zone and foreshore. Also included in the second paper is a discussion concerning the possible origin of a problematic sedimentary structure called "gently undulating parallel lamination", or in an abbreviated form, GUP lamination. This sedimentary structure, which dominates in the fine-grained sandstones of the lower shoreface, is characterised by gently undulating parallel lamination. The undulating nature of the lamination exhibits metre(s)-scale spacing, but height rarely exceeds 1-1.5 cm. Several characteristics of this lamination and the beds which it forms indicates deposition from upper-flow-regime, unidirectionally-dominated, combined flow. The development of this structure along with its possible hydrodynamic relationship with hummocky cross-stratification (HCS) (Harms *et al.*, 1975) is discussed in detail in the latter part of the second paper.

As discussed above the Bootlegger Member in the Great Falls area is comprised of five vertically stacked, shoaling-upward sequences. Similarly, Bootlegger Member strata cropping out in the Sweetgrass Hills at Mt. Lebanon is comprised of shoaling-upward sequences, but only three and the lower portion of a possible fourth were observed. At both study areas, nonetheless, shoaling-upward depositional characteristics were the result of eastward strandline progradation associated with uplift of the Sweetgrass Arch. Subsequent subsidence of the arch, related to sediment loading and elastic lithospheric relaxation, resulted in westward displacement of the strandline and the termination of the shoaling-upward sequence. The sequential history of strandline position during each of the five Bootlegger sequences in the Great Falls study area and the resultant depositional characteristics of these strata are dealt with in the third paper (Palaeoshoreline and lithologic mapping of the Bootlegger Member, north-central Montana).

The use of primary biogenic sedimentary structures as a palaeoenvironmental tool has until recently gone unnoticed. However, recently many studies have proven the importance of these structures in reconstructing palaeoenvironmental conditions present before, during and after sedimentation. By combining both the physical and biogenic evidence a better assessment of the ancient environmental conditions can be made. In the fourth paper (Combining physical and biogenic sedimentary structures: A case study ; Bootlegger Member, north-central Montana) the physical and biogenic evidence reported from two adjacent study areas (the Ulm Pishkun and the Missile Tower sections) are discussed. In this paper, both lines of evidence support similar interpretations concerning this ancient nearshore environment. However, the biogenic record illustrates a number of depositional hiatuses which are undetectable in the physical record.

The final portion of the thesis is a compilation of four appendices, each dealing with a specific subject eluded to in the main text. The first appendix is a discussion and tabulation of data concerned with the anisotropy of magnetic susceptibility. This phenomenon, which is exhibited by most sedimentary rocks, can be used to determine current direction and hydrodynamic conditions during sediment deposition. Unfortunately, due to the low magnetic content of most Bootlegger Member strata this procedure proved to be effective in only a few cases.

The second appendix is a presentation of data and results from flume experiments investigating the effect of sediment-fallout on equilibrium bedforms, and in particular its influence during upper plane bed conditions. Appendix II has been included because of the interpreted importance of upper-flow-regime plane bed conditions during the generation of gently undulating parallel lamination (GUP lamination). In the Great Falls area, most Bootlegger Member strata are flat lying, although exceptions do occur. These exceptions, *eg*. Belt Butte and the Sweetgrass Hills, are due to vertical uplift by post-depositional Tertiary intrusions. The third appendix outlines the structural elements which outcrop on the northeast side of the Belt Butte. The fourth appendix is a compilation of all the collected palaeocurrent data from the Great Falls and Mt. Lebanon study areas.

# REFERENCES

Arnott. R.W., 1987. Stratigraphy of the Lower Cretaceous Bootlegger Member near Great Falls, Montana and its relationship with the ancestral Sweetgrass Arch. Geological Association of Canada, Program with Abstracts, p. 22.

Cannon. J.L., 1966. Outcrop examination and interpretation of paleocurrent patterns of the Blackleaf Formation near, Great Falls, Montana. Billings Geologic Society Guidebook, 17th annual field conference, pp. 71-111.

Cobban, W.A., Erdmann, C.E., Lemke, R.W., Maughn, E.K., 1959. Revision of Colorado Group on Sweetgrass Arch, Montana. American Association of Petroleum Bulletin Geologists, v. 43, pp. 2786-2796.

--------, 1976. Type sections and stratigraphy of the members of the Blackleaf and Marias River Formations (Cretaceous) of the Sweetgrass Arch, Montana. U.S.G.S. Professional Paper 974, 66 p.

Harms, J.C., Southard, J.B., Spearing, D.R., Walker, R.G., 1975. Depositional environments as interpreted from primary structures and stratification sequences. Sociey of Economic Paleontologists and Mineralogists, Tulsa, Short Course No. 2, 161 p.

Vuke, S.M., 1984. Depositional environments of the Early Cretaceous Western Interior Seaway in southwestern Montana and the northern United States. *In* Stott, D.F., Glass, D.J., eds., The Mesozoic of middle North America. Canadian Society of Petroleum Geologists Memoir 9, pp. 127-144.

# INFLUENCE OF THE SWEETGRASS ARCH ON SEDIMENTATION OF THE BOOTLEGGER MEMBER, NORTH-CENTRAL MONTANA

## INTRODUCTION

The Cretaceous of western North America was marked by the long-term development of a Cordilleran thrust belt. Lithospheric loading in response to the progressive "piling-up" and eastward migration of the Cordilleran Fold and Thrust Belt caused the cratonic margin adjacent to the leading edge of this belt to subside (Price, 1973; Beaumont, 1981; Jordan, 1981). Subsidence resulted in the development of an asymmetric, elongate trough into which large amounts of clastic detritus were deposited during the Late Jurassic and Cretaceous. This trough, commonly called the Western Interior Seaway, reached its maximum extent during the early Turonian - middle Santonian and extended a distance of more than 4800 km from north to south and 1600 km from east to west (Kauffman, 1977).

Regression-transgression couplets have long been recognised in the Cretaceous of North America. The typical coarsening- to fining-upward sequences making up these couplets have been commonly attributed to eustatic fluctuations which control sedimentation. Numerous stratigraphic studies in both Canada and the United States have illustrated the common repetitive coarsening- to fining-upward sequences observed throughout this basin in both space and time (Kauffman, 1977; Vail *et al.*, 1977; Weimer, 1984; Merewether and Cobban, 1986). Vail *et al.* (1977) showed that some of these sedimentary cycles occurred worldwide (supercycles) reflecting global eustatic change. Similar sequences, although of a much smaller scale, have also been reported and related to more localized intrabasinal events (Vail *et al.*, 1977; Weimer, 1984; Kauffman, 1985; Cant and Hein, 1986).

This paper illustrates the effect of Cordilleran tectonism on the uplift/subsidence history of the ancestral Sweetgrass Arch, and the effect of these movements during deposition of the upper Albian - lower Cenomanian Bootlegger Member of the Blackleaf Formation near the city of Great Falls, Montana (Fig. 1). Within a period of approximately 2 my, episodic uplift and subsidence of the arch resulted in the development of five regressive/transgressive couplets making up the Bootlegger Member.

## GEOLOGY OF THE BOOTLEGGER MEMBER

The Bootlegger Member is the uppermost of four stratigraphic members that make up the late Lower Cretaceous to early Upper Cretaceous Blackleaf Formation in north-central Montana (Fig. 2) (Cobban *et al.*, 1959, 1976; Cannon, 1966; Stelck and Armstrong, 1981). The Bootlegger Member lies stratigraphically above terrestrial deposits of the Vaughn Member (regressive stage of the Kiowa-Skull Creek Cyclothem (Kauffman *et al.*, 1977)) and beneath deep basinal shales that make up the Floweree Member of the Marias River shales (transgressive stage of the Greenhorn Cyclothem (Hattin, 1964) ).

The Bootlegger Member represents the initial transgression of the Greenhorn Sea, associated with the Greenhorn Cyclothem, into the Great Falls area. It pinches out to the west as it onlaps terrestrial deposits of the Vaughn Member and merges to the east with the deep basinal Mowry shales of eastern Montana and the Black Hills (Cobban, 1951; Cobban *et al.*, 1959, 1976). The occurrence of the ammonite *Neogastroplites americanus* (Reeside and Cobban, 1960) dates the Bootlegger Member at approximately 96 Ma (Folinsbee *et al.*, 1963). An areally extensive bentonite known as the Clay Spur Bentonite, cropping-out at the top of the Mowry Member in southeastern Montana (Rubey, 1929; 1930), has been dated at 94 Ma (Folinsbee *et al.*, 1963). Therefore, the Bootlegger Member represents approximately 2 (~± 1) million years of geologic time (approximately 96 to 94 Ma). In the Great Falls area the Bootlegger Member is composed of five stacked sequences. Stratigraphically-upward each sequence is characterised by a steady increase in the sand/shale ratio and is abruptly truncated on its upper surface (Fig. 3).

The following is a generalization of the five Bootlegger sequences; a more complete report of these strata is in preparation (Arnott, in preparation). The base of each sequence is identified by the cropping-out of silty bentonitic shales with siltstone interbeds, interpreted to be deposited in a shallow offshore shelf environment. Stratigraphically-upward interbeds become coarser-grained, thicker and more abundant. Shallow offshore-shelf deposits are overlain by fine-grained sandstones deposited in a lower shoreface environment. Continuing upward through the sequence, if such strata are present, lower shoreface deposits are overlain by upper shoreface deposits which at two localities are overlain by foreshore deposits. The coarsening-upward portion of each of the five Bootlegger sequences illustrates shoaling-upward depositional conditions associated with progradation of the local strandline.

Abruptly truncating each coarsening-upward sequence is a typically planar transgressive surface usually capped with a thin, coarse-grained lag deposit. Each lag deposit is composed of sediment reworked from the underlying shoaling-upward sequence and was left behind during the marine transgression. Sequences where lag deposits are composed of pebble-sized chert clasts suggest the transgressive reworking and concentrating of possible beach or fluvial coarse-grained sediments. The lag deposit cropping-out at the top of Sequence 5, in addition to being granule sand size is also characterised by an anomalous abundance of fish scales and fish bones. This fossilliferous horizon has been termed the "Base of the Fish Scales" by petroleum geologists in Canada and represents a synchronous marker extending from at least northeastern British Columbia to southern Alberta, a distance of over 800 km (Stelck and Armstrong, 1981). Its similar association with *Neogastroplites americanus* in the Great Falls area would indicate the extension of this synchronous marker into at least north-central Montana, a distance of an additional 300 km.

In the western Great Falls study area strata of the Base of the Fish Scales crop-out above Sequence 4, thereby contrasting its occurrence above Sequence 5 in the eastern Great Falls study area (Fig. 3). Lack of Sequence 5 strata in the western Great Falls study area indicates the development of a markedly condensed stratigraphic section, which is probably the consequence of erosive bevelling and sediment reworking which occurred during Base of the Fish Scales time. Sediment reworking led to the concentration of fish remains and ultimately to the development of the Base of the Fish Scales marker.

Development of the thick shoaling-upward portion of each Bootlegger sequence indicated eastward shoreline progradation during eustatic still-stand or fall, although progradation can also occur during eustatic rise if sediment input exceeds sea level rise. Progradation was then terminated by a rise in relative sea level associated with regional subsidence and/or eustatic rise, and resulted in the rapid westward displacement of the local strandline. Transgression during relative sea level rise caused deposition of the coarse lag deposits which cap four of the five shoaling-upward sequences.

The Bootlegger Member in the Great Falls study area is made up of five regressive/transgressive couplets. Each couplet indicated the temporal variation of local sea level and its influence on the position of the local strandline. However, since the Bootlegger Member was deposited in approximately 2 (± 1) million years, one must appeal to an agent which would have resulted in very rapid and recurring change in relative sea level position. In close proximity to the Great Falls study area is the palaeostructure the Sweetgrass Arch. Since throughout Bootlegger Member time the local strandline was within or at least near to the study area, even small vertical movements of the Sweetgrass Arch would have had a profound effect on the rise or fall of relative sea level, strandline position and ultimately the depositional sedimentary sequence.

# THE SWEETGRASS ARCH

The Sweetgrass Arch of northwestern Montana represents a north-northwest-trending antiformal structure which loses its identity beneath the Alberta Plains (Stebinger, 1916; Collier, 1929; Romaine, 1929). However, several studies have indicated that the northeast-trending Bow Island Arch of southern Alberta (Fig. 4) may represent its northern extension (Dowling, 1917; Michener, 1934; Tovell, 1958; Herbaly, 1974). Peterson (1966) notes that in the northwestern United States the Sweetgrass Arch is only one of several positive relief features forming a linear band running northwestward from the Transcontinental Arch. These features include the Chadron-Cambridge High, The Black Hills, Central Montana Uplift and finally the Sweetgrass Arch.

In north-central Montana the Sweetgrass Arch is made up of two antiformal structures; (1) the South Arch, and, (2) the Kevin-Sunburst Dome, which are separated along the Marias River Saddle (coincident with the Pendroy Fault Zone)(Fig. 4). With a complex and long-lived history of uplift the Sweetgrass Arch has had a dramatic influence on local and regional sedimentary patterns dating back to the late Cambrian or possibly late Precambrian (Peterson, 1966; Lorenz, 1982).

Thrust loading during Cordilleran mountain-building resulted in downwarping of the eastward cratonic margin and the development of an elongate, asymmetric trough. Recently, various authors (Beaumont, 1981; Jordan, 1981; Lorenz, 1982) have attempted to model the effects of thrust plate loading on a lithosphere exhibiting different mechanical flexure behaviours. The major difference between each model lies in the history of events after the induced flexure. The choice of different flexural behaviours is an attempt by these authors to best account for the sedimentary history in the foreland basin. In all the models, however, subsidence of the lithosphere caused uplift of the forebulge which was always located a specified distance to the east. Lorenz (1982) and Elliot (1977 in Jordan, 1981) have respectively suggested that the Sweetgrass and Moxa arches represent flexure related forebulges, although in the case of the Sweetgrass Arch the location of the forebulge and its interpreted stationary position through mountain-building time may reflect continued exploitation of a pre-existing crustal feature (Lorenz, 1982).

During Bootlegger Member time, late Albian to early Cenomanian, the area stretching from Idaho to southern Alberta was characterised by widespread igneous intrusion and volcanic eruption (McGookey *et al.*, 1972). Evidence includes the bentonitic rich lithologies of the Vaughn Member, abundant Bootlegger Member bentonites, contemporary activity of the Crowsnest volcanics and intrusion of the Coast Plutonic and Idaho Batholith complexes. If as suggested by Kauffman (1977, 1985) and Harrison (1985) that periods of active Cordilleran volcanism correlated closely with episodes of accelerated thrust faulting, then there would have been a concomitant increase in the number of lithospheric flexure episodes and associated forebulge uplifts. Accelerated thrusting would have also led to intense Cordilleran erosion with the transport and delivery of large volumes of clastic sediment into the eastward lying sedimentary basin. Even with the short lag time expected between thrusting and sediment influx into the basin, the effect of forebulge uplift and increased sediment supply is interpreted to have caused the vertical aggradation and eastward progradation of the local shoreline.

## DISCUSSION

The Bootlegger Member in the Great Falls, Montana area consists of five regressive and five intervening transgressive sequences. Although it should be noted that the

Vaughn/Bootlegger contact, representing the initial transgression of the Greenhorn Sea into the area, represents a sixth transgressive surface but is not considered part of the five aforementioned sequences. Each regressive deposit is characterised by a thick (10 - 35 m) shoaling-upward sequence which indicated eastward progradation of the local shoreline. Shale-rich lithologies at the base of each regressive deposit crop-out sharply above the coarse-grained transgressive lag of the underlying Bootlegger sequence. The uppermost sand-rich lithologies of each sequence are in turn sharply overlain by its own transgressive lag. Transgressive lag deposits are typically thin (< 1.5 m thick), sharply based and anomalously coarse-grained compared to the underlying regressive portion of the couplet. Lag deposits of sequences 1, 3 and 5 are characterised by black chert granule and/or pebble deposits. Abundant fish bones and scales are also associated with the Sequence 5 transgressive lag. In certain localities Sequence 1 lag deposits are more feldspathic and possess a higher magnetic susceptibility, commonly an order of magnitude higher than the underlying regressive sediments. Collectively these transgressive lag deposit characteristics suggest erosion and reworking of the top of the underlying regressive portion of each sequence during the subsequent marine transgression. Continued transgression led to the deposition of the shale-rich base of the overlying sequence.

The repetitive regressive/transgressive sequences making up the Bootlegger Member are thought to reflect recurrent uplift and subsidence of the Sweetgrass Arch (Arnott, 1987). As noted above, the proximity of the arch to the study area and the position of the local strandline either close to or within the study area throughout Bootlegger Member time would enable even small vertical movements of the arch to have a dramatic effect on the nature of local sedimentation. Uplift of the Sweetgrass Arch was most likely related to periods of Cordilleran thrust faulting and consequent lithospheric flexure. Each episode of uplift and associated drop of relative sea level is suggested by the eastward displacement of the strandline and development of each of the five shoaling-upward Bootlegger sequences.

Regressive depositional conditions were also augmented because of the large influx of clastic sediment from the recent Cordilleran thrust episode. During thrusting quiescence, on the other hand, the arch subsided under the influence of sediment loading and elastic lithospheric relaxation. Subsidence resulted in a rise in relative sea level, the development of local transgressive conditions and the rapid westward migration of the strandline. Transgression led to the deposition of a thin, coarse-grained transgressive lag, the composition of which depended on the extent of strandline progradation during the regressive portion of the regressive/transgressive couplet.

## PROBLEMS WITH THE MODEL

The most glaring problem with the use of the Sweetgrass Arch as a mechanism for the development of the Bootlegger sequences is that of time. Since the Bootlegger Member was deposited in approximately 2 (~± 1) my, this model invokes five episodes of Sweetgrass Arch uplift and subsidence. Consequently, lithospheric flexure and associated arch uplift followed by lithospheric relaxation and arch subsidence must have occurred on a short time scale. Therefore, would it have been possible for the lithosphere to mechanically react in a similar fashion five times and for all this to have occurred in the span of approximately 2 (~± 1) my ? However, the strict use of a sediment supply mechanism related to events in the source area, the Cordillera, which varied through time would seem incompatible. For such a mechanism is also constrained by time, and in addition the consistent nature of the Bootlegger sequences would seem to suggest a recurring mechanism which throughout Bootlegger Member time was not radically different. The explanation of the Bootlegger sequences as being the result of a localized sedimentary phenomenon such as channel avulsion or delta lobe switching would also appear inappropriate. Evidence for this includes the cropping-out of Bootlegger sequences similar to those in the Great Falls area located 200 km to the north in the Sweetgrass Hills (Arnott and Hein, in preparation). Another possible causitive agent for the development of the Bootlegger sequences could be related to Milankovitch Cycles (Heckel, 1986; Fisher *et al.*, 1985). However, the non-rhythmic nature of time-equivalent strata of the Vaughn Member in the Sun River Canyon area to the west (Mudge, 1972), the Bootlegger stratal sequences near Great Falls and the Mowry shales to the east (Reeside and Cobban, 1960) suggest that the observed style of Bootlegger cyclicity is inconsistent with a time varying mechanism related to Milankovitch cyclicity.

Evidence supporting the involvement of the Sweetgrass Arch lies in the Bootlegger Member sedimentary record itself. In the western part of the Great Falls study area, near to the crest of the Sweetgrass Arch, Bootlegger sequences are typically incomplete and often show conglomeratic transgressive lags overlying shale-rich lithologies. However in the eastern Great Falls study area, further from the arch crest, transgressive lags invariably overlie the sand-rich upper portion of a more complete shoaling-upward sedimentary sequence. The typical lack of sand-rich strata in the western study area suggests two possibilities, and both could be related to Sweetgrass Arch uplift. Firstly, sand-rich strata were never deposited or only very thinly due to the rapid eastward displacement of the local shoreline in response to a relative sea level drop caused by arch uplift. Eastward displacement of the strandline was terminated once a new equilibrium position was established, a balance between sediment input and relative sea level drop. From this point in time until the next transgression, progradation under still-stand conditions resulted in the development of the more complete shoaling-upward regressive sequences observed in the eastern Great Falls study area. A second possibility may be that sand-rich strata in the upper portion of the shoaling-upward sequences observed in the western study area were removed by terrestrial erosion during strandline progradation and/or marine erosion during transgression. Uplift of the arch could have caused a relative sea level drop, eastward displacement of the local shoreline and elevation of local stream gradients. The latter would have served to increase terrestrial erosion and the supply of sediment to the shoreline. However, the complete removal of all the sand-rich strata as suggested by the second possibility would seem inappropriate, and therefore a condition of non-deposition as suggested by the first possibility would appear to be a more plausible explanation.

From the above discussion it is postulated that the development of the Bootlegger sequences was primarily a result of the episodic uplift and subsidence of the Sweetgrass Arch and its ultimate control over relative sea level. Other sedimentary influences including sediment influx into the basin and the influence of local sedimentary features may have been of great importance during development of the Bootlegger sequences, but were however subordinate to the influence of the arch.

Several other features related to the Bootlegger Member must be taken into account. Firstly, the Bootlegger Member was deposited during a global sea level rise and on a local scale Bootlegger Member strata indicated regressive depositional episodes. Also, this period of the late Lower Cretaceous to early Upper Cretaceous was chartacterised by intense volcanic and intrusive activity. If the link between these latter events and Cordilleran thrusting episodes is indeed correct, then this would have also been a time of abundant lithospheric flexure episodes and consequent forebulge uplift. Therefore, if as suggested earlier that the Sweetgrass Arch had acted as a forebulge then it would have been a very active feature during this period of the Cretaceous.

## CONCLUSIONS

The upper Albian to lower Cenomanian Bootlegger Member in the Great Falls area is characterised by five vertically stacked regressive/transgressive couplets or Bootlegger sequences. Stratigraphically-upward strata making up the regressive portion of each couplet indicated shoaling-upward depositional characteristics. Each regressive sequence is sharply overlain by a thin, more coarsely-grained transgressive lag deposit.

The cyclic nature of Bootlegger deposition is thought to be related to the episodic activity of the Sweetgrass Arch (South Arch) whose crest lies close to the Great Falls study area. During periodic Cordilleran thrusting events uplift of the arch, which at this time may have acted as a forebulge, resulted in the drop of relative sea level, rapid eastward displacement of the local shoreline. Establishment of a new equilibrium strandline position some distance to the east allowed for still-stand progradation and development of the thick shoaling-upward sequences typically observed in the eastern Great Falls study area. Subsequent reduced Cordilleran thrust activity caused the arch to subside in response to sediment loading and elastic lithospheric relaxation. Subsidence caused a relative sea level rise, a consequent transgression and the development of the observed transgressive lag deposits.

# REFERENCES

Arnott, R.W., 1987. Stratigraphy of the Lower Cretaceous Bootlegger Member near Great Falls, Montana and its relationship with the ancestral Sweetgrass Arch. Geological Association of Canada, Program with Abstracts, p. 22.

Beaumont, C., 1981. Foreland basins. Geophysical Journal of the Royal Astronomy Society, v. 65, pp. 291-329.

Cannon, J.L., 1966. Outcrop examination and interpretation of paleocurrent patterns of the Blackleaf Formation near, Great Falls, Montana. Billings Geologic Society Guidebook, 17th annual field conference, pp. 71-111.

Cant, D.J., Hein, F.J., 1986. Depositional sequences in ancient shelf sediments: Some contrasts in style. *In* Knight, R.J., McLean, J.R., eds., Shelf Sands and Sandstones.Canadian Society of Petroleum Geologists Memoir No. 11, pp. 303-312.

Cobban, W.A., 1951. Colorado Shale of central and northwestern Montana and equivalent rocks of Black Hills. American Association of Petroleum Geologists Bulletin, v. 35. pp. 2170-2198.

Cobban, W.A., Erdmann, C.E., Lemke, R.W., Maughn, E.K., 1959. Revision of Colorado Group on Sweetgrass Arch, Montana. American Association of Petroleum Bulletin Geologists, v. 43, pp. 2786-2796.

--------, 1976. Type sections and stratigraphy of the members of the Blackleaf and Marias River Formations (Cretaceous) of the Sweetgrass Arch, Montana. U.S.G.S. Professional Paper 974, 66 p.

Collier, A.J., 1929. The Kevin-Sunburst oil field and other possibilities of oil and gas in the Sweetgrass Arch, Montana. U.S.G.S. Bulletin 812-B, pp. 57-87.

Dowling, D.B., 1917. The southern plains of Alberta. Geologic Survey of Canada Memoir 93, 200 p.

Fisher, A.G., Herbert, T., Silva, I.P., 1985. Carbonate bedding cycles in Cretaceous pelagic and hemipelagic sequences. *In* Pratt, L.M., Kauffman, E.G., Zelt, F.B., eds., Fine-grained deposits and biofacies of the Cretaceous Western Interior Seaway: Evidence of cyclic sedimentary processes, Society of Economic Paleontologists and Mineralogists field guidebook No. 4, pp. 1-10.

Folinsbee, R.E., Baadsgaard, H., Cumming, G.L., 1963. Dating of volcanic ash beds (bentonites) by the K-Ar method. National Academy of Science, National Research Council, Washington D.C., Nuclear Sciences Series, Report No. 38, pp. 70-82.

Harrison, C.G.A., 1985. Modelling fluctuations in water depth during the Cretaceous. *In* Pratt, L.M., Kauffman, E.G., Zelt, F.B., eds., Fine-grained deposits and biofacies of the Cretaceous Western Interior Seaway: Evidence of cyclic sedimentary processes, Society of Economic Paleontologists and Mineralogists field guidebook No. 4, pp. 11-15.

Heckel, P.H., 1986. Sea-level curve for the Pennsylvanian eustatic marine transgressive-regressivedepositional cycle along midcontinental outcrop belt, North America. Geology, v. 14, pp. 330-334.

Hattin, D.E., 1964. Cyclic sedimentation in the Colorado Group of west-central Kansas. *In* Merriam, D.F., ed., Symposium on cyclic sedimentation, Kansas Geological Survey Bulletin, pp. 205-217.

Herbaly, E.L., 1974. Petroleum geology of Sweetgrass Arch. American Association of Petroleum Geologists Bulletin, v. 58, pp. 2227-2244.

Jordan, T.E., 1981. Thrust loads and Foreland Basin evolution, Cretaceous, western United States. American Association of Petroleum Geologists Bulletin, v. 65, pp. 2506-2520.

Kauffman, E.G., 1977. Geological and biological overview: Western Interior Cretaceous Basin. Mountain Geologist, v. 14, pp. 75-99.

-------, 1985. Cretaceous evolution of the Western Interior Basin of the United States. *In* Pratt, L.M., Kauffman, E.G., Zelt, F.B., eds., Fine-grained deposits and biofacies of the Cretaceous Western Interior Seaway: Evidence of cyclic sedimentary processes, Society of Economic Paleontologists and Mineralogists field guidebook No. 4, pp. IV-XIII.

-------, Cobban, W.A., Eicher, D.L., 1977. Albian through lower Coniacian strata, biostratigraphy and principals events, Western Interior United States. *In*

Evenements de la Partie Moyenne du Cretace (Mid-Cretaceous events), Uppsala-Nice symposia, 1975-1976: Annales du Museum d'Historie Naturelle de Nice, v. 4, pp. XXIII1-XXIII24.

Lorenz, J.C., 1982. Lithospheric flexure and the history of the SweetgrassArch, northwestern Montana. *In* Rocky Mountain Association of Geologists - 1982 Symposium, Geologic studies of the Cordilleran Thrust Belt, Vol. 1, pp. 77-89.

McGookey, D.P., Haun, J.D., Hale, L.A., Goodell, H.G., McCubbin, D.G., Weimer, R.J., Wulf, G.R., 1972. Cretaceous System. *In* : Rocky Mountain Association of Geologists, Geologic atlas of the Rocky Mountain region, United States of America, pp. 190-228.

Merewether, E.A., Cobban, W.A., 1986. Biostratigraphic units and tectonism in the Mid-Cretaceous foreland of Wyoming, Colorado and adjoining areas. *In* Peterson, J.A., ed., Paleotectonics and sedimentation in the Rocky Mountain region, United States, American Association of Petroleum Geologists, Memoir 41, pp. 443-468.

Michener, C.E., 1934. The northward extension of the Sweetgrass Arch. Journal of Geology, v. 42, pp. 45-61.

Mudge, M.R., 1972. Pre-Quaternary rocks in the Sun River Canyon area, northwestern Montana. U.S.G.S. Professional Paper 663-A, 138 p.

Peterson, J.A., 1966. Sedimentary history of the Sweetgrass Arch. Billings Geologic Society Guidebook, 17th annual field conference, pp. 112-134.

Price, R.A., 1973. Large-scale gravitational flow of supracrustal rocks, southern Canadian Rockies. *In* DeJong, K.A., Scholten, R., eds., Gravity and Tectonics, New York, Interscience, John Wiley and Sons, pp. 491-502.

Reeside, J.B., Cobban, W.A., 1960. Studies of the Mowry Shale (Cretaceous) and contemperaneous formations in the United States and Canada. U.S.G.S. Professional Paper 355, 121 p.

Romaine, T.B., 1929. Oil fields and structure of Sweetgrass Arch, Montana. American Association of Petroleum Geologists Bulletin, v. 13, pp. 779-797.

Rubey, W.W., 1929. Origin of the siliceous Mowry Shale of the Black Hills region. U.S.G.S. Professional Paper 154, pp. 153-170.

------, 1930. Lithologic studies of fine-grained Upper Cretaceous sedimentary rocks of the Black Hills region. U.S.G.S. Professional Paper 165, pp. 1-54.

Stebinger, E., 1916. Possibilities of oil and gas in north-central Montana. U.S.G.S. Bulletin 641, pp. 49-91.

Stelck, C.R., Armstrong, J., 1981. Neogastroplites from southern Alberta. Bulletin of Canadian Petroleum Geology, v. 29, pp. 399-407.

Tovell, W.M., 1958. The development of the Sweetgrass Arch, southern Alberta. Geologic Association of Canada Proceedings, v. 10, pp. 19-30.

Vail, P. R., Mitchum, R.M., Thompson, S., 1977. Seismic stratigraphy and global changes of sea level, Part 4: Global cycles of relative changes of sea level. *In* Payton, C.E., ed., Seismic stratigraphy - applications to hydrocarbon exploration, American Association of Petroleum Geologists Memoir 26, pp. 83-97.

Weimer, R.J., 1984. Relation of unconformities, tectonics, and sea-level changes, Cretaceous of Western Interior, United States. *In* Schlee, J.S., ed., Interregional unconformities and hydrocarbon accumulation, American Association of Petroleum Geologists Memoir 36, pp. 7-35.

FIGURE II-1: Location map of the area near Great Falls in north-central Montana

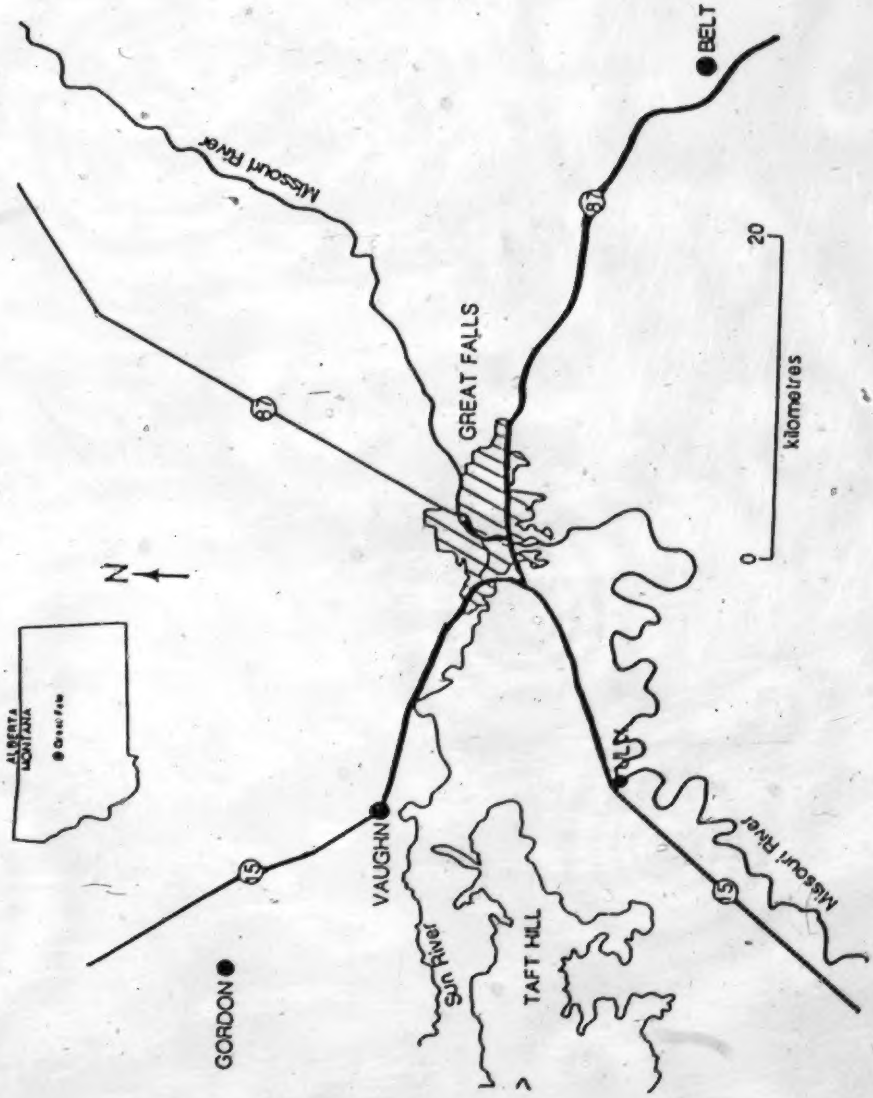
GREAT FALLS
Missouri River
Missouri River
BELT
VAUGHN
GORDON
Sun River
TAFT HILL
87
87
15
15
N
0
20
kilometres
ALBERTA
MONTANA
Great Falls

FIGURE II-2: Correlation chart of Upper and Lower Cretaceous strata in northwestern United States and south-central Alberta (modified after Stelck and Armstrong, 1981)

| | NORTHWEST WYOMING | SWEETGRASS ARCH, MONTANA | | LETHBRIDGE, ALBERTA | |
|---|---|---|---|---|---|
| UPPER CRETACEOUS | NIOBRARA | MARIAS RIVER SHALES | KEVIN MBR. | UPPER COLORADO | 1st white specs |
| | CARLILE | | FERDIG MBR. | | |
| | GREENHORN | | CONE MBR. | BLACKLEAP MBR. OF COLORADO SHALE | 2nd white specs |
| | BELLE FOURCHE | | FLOWEREE MBR.<br>▥ | | |
| LOWER CRETACEOUS | MOWRY | BLACKLEAP FORMATION | BOOTLEGGER MBR. | | fish scales |
| | SHELL CREEK | | VAUGHN MBR. | | red specs<br>BOW ISLAND SANDS |
| | NEWCASTLE | | TAFT HILL MBR. | | |
| | SKULL CREEK | | | | JOLI FOU EQUIV. |
| | FALL RIVER | | FLOOD MBR. | | BASAL SS. |
| | ▥ | ▥ | ▥ | ▥ | ▥ |
| | CLOVERLY | KOOTENAI | | BLAIRMORE | |

FIGURE II-3: Generalized section of the Bootlegger Sequences east and west of Great Falls:

Eastern area represents sections near Belt;

Western area represents sections near Gordon and on Taft Hill

(the symbol "F" means the presence of abundant fish scales and fish bones).

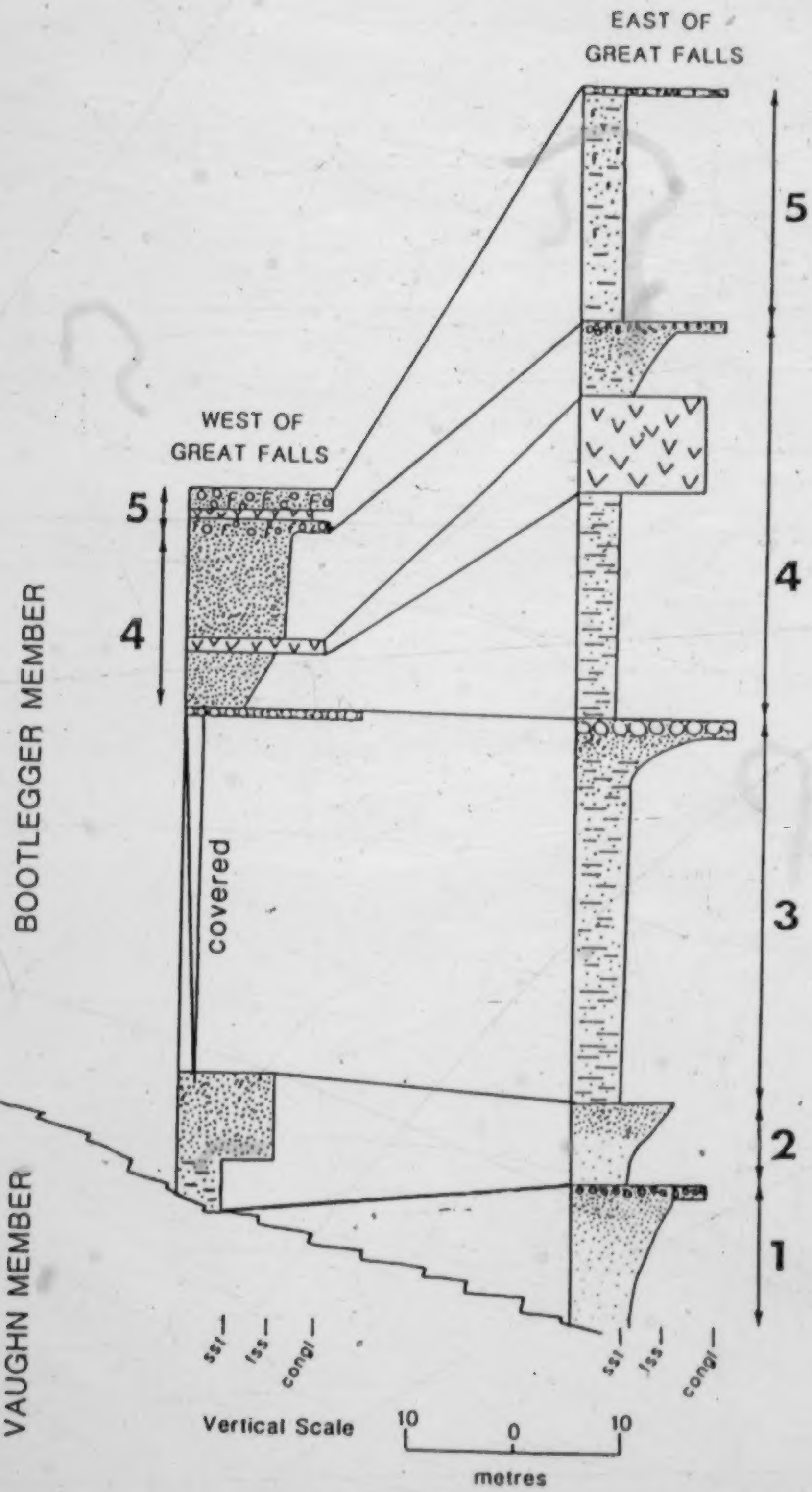
EAST OF GREAT FALLS
WEST OF GREAT FALLS
BOOTLEGGER MEMBER
VAUGHN MEMBER
covered
5
4
5
4
3
2
1
ssl
lss
congl
ssl
lss
congl
Vertical Scale
10
0
10
metres

FIGURE II-4: Location map of the constituent elements making up the Sweetgrass Arch in north-central Montana and southern portion of the Bow Island Arch of southern Alberta.

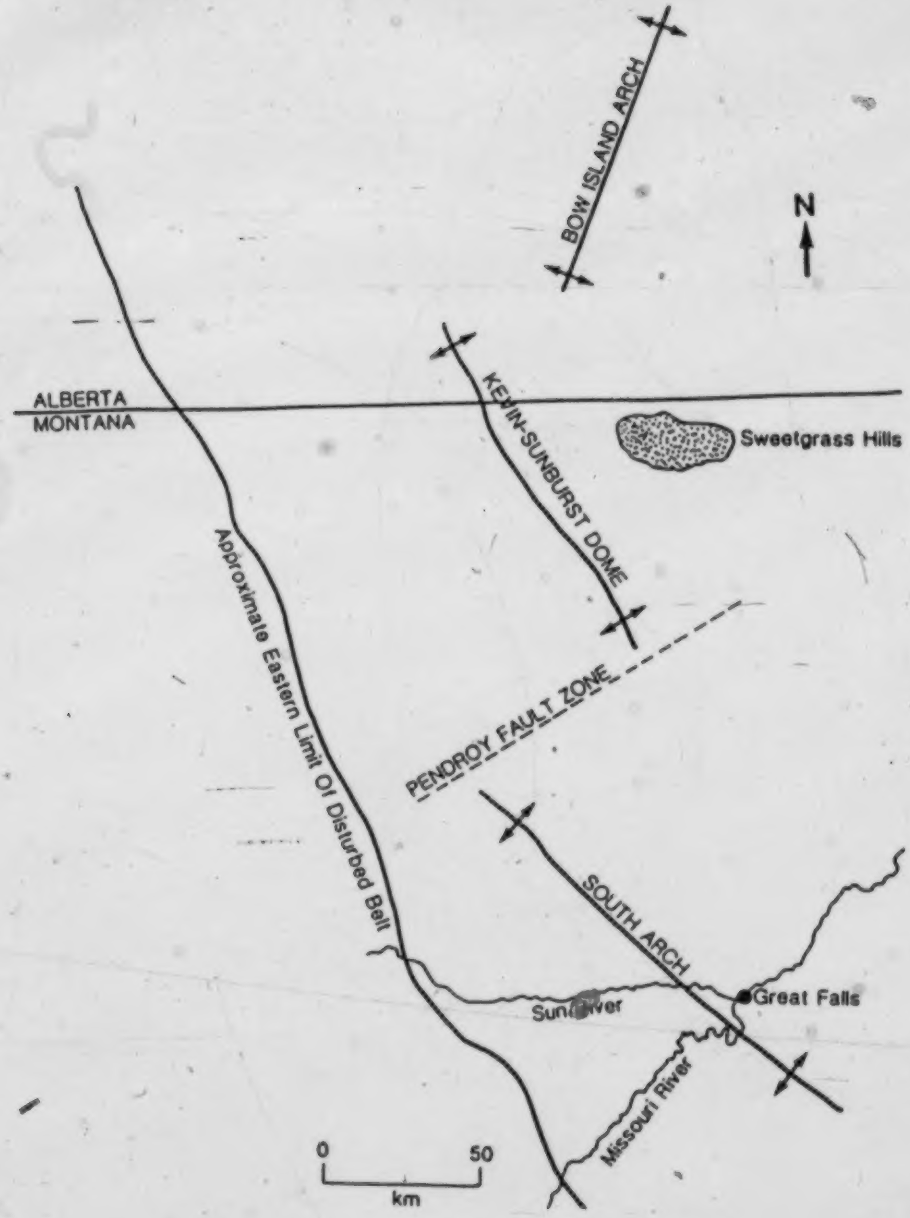
BOW ISLAND ARCH
N
ALBERTA
MONTANA
KEVIN-SUNBURST DOME
Sweetgrass Hills
Approximate Eastern Limit Of Disturbed Belt
PENDROY FAULT ZONE
SOUTH ARCH
Great Falls
Sun River
Missouri River
0
50
km

# SEDIMENTOLOGY OF A CRETACEOUS STORM-DOMINATED, NEARSHORE SEQUENCE AND ORIGIN OF GUP LAMINATION

## INTRODUCTION

During late Jurassic and Creteceous time the Western Interior Basin of North America was an elongate trough bounded on the west by the rising Western Cordillera and on the east by the North American craton. Lithospheric flexure associated with the eastward migration of the Cordilleran Fold and Thrust Belt (Price, 1973; Beaumont, 1981; Jordan. 1981) resulted in the development of this asymmetric trough. At its maximum development during the early Turonian - middle Santonian, the Western Interior Seaway of North America extended over 4800 km from north to south and 1600 km from east to west (Kauffman. 1977). During Cordilleran mountain building large amounts of clastic detritus were shed from the western mountains and deposited in the adjacent sedimentary basin to the east. Superimposed on this was the temporal variability of both intra- and extrabasinal sea level and its effect on the depositional patterns and environments developed within the basin. The most common sedimentary pattern are the typical fining-upward and coarsening-upward sequences respectively associated with transgressions and regressions.

This paper deals with the development of a prograding, storm-dominated shoreline associated with the initial transgressive phase of the basin-wide Greenhorn Cyclothem (Hattin, 1964). This shoreline, composed of shallow-offshore shelf, shoreface and beachface strata, is exposed at the Ulm Pishkun, approximately 16 km west of the city of Great Falls, Montana (Fig. 1). Details of the trace fossil assemblages will not be discussed. but will be the subject of subsequent papers by Arnott, Pemberton and Mattison (in preparation). Of particular interest in this study is the presence of a problematic sedimentary structure which exhibits gently undulating parallel lamination. This paper will describe and consider the origin of this structure and its relationship to other sedimentary structures characterising this ancient storm-dominated shoreline. The abundant occurrence of gently undulating parallel lamination in Bootlegger Member strata, though never reported elsewhere, only serves to illustrate our limited knowledge of both modern and ancient storm-dominated, nearshore sedimentary environments.

## LOCAL GEOLOGY

The Bootlegger Member is the uppermost of four members making up the late Lower Cretaceous Blackleaf Formation in north-central Montana (Fig. 1). It overlies terrestrial deposits of the Vaughn Member and in turn is overlain by deep-marine black shales of the early Upper Cretaceous Marias River shales (Cobban *et al.* 1959, 1976; Cannon, 1966) (Fig. 2). The Bootlegger Member, of latest Albian to earliest Cenomanian age (*Neogastroplites americanus* zone of Reeside and Cobban, 1960), represents the intial transgressive stage of the Greenhorn Cyclothem into north-central Montana (Kauffman *et al.*, 1977; Vuke, 1984). Representatives of the ammonite genera *Neogastroplites* and *Epengonoceras* in the Bootlegger Member indicate that the Greenhorn Sea had by this time linked the southern and northern arms of the Western Interior Seaway (C.R. Stelck, per. comm. 1987). West of Great Falls, Bootlegger Member strata onlap the terrestrial Vaughn Member while merging eastward with the deep-marine Mowry shales of east-central Montana and the Black Hills (Cobban *et al.*, 1959, 1976; Stelck and Armstrong, 1981).

In the Great Falls area the Bootlegger Member has been informally subdivided into five sedimentary sequences (Arnott and Hein, in review ), each made up of a thick regressive unit overlain by a thin transgressive unit. The regressive portion records eastward migration of the local strandline whereas the transgressive unit indicates its subsequent westward migration. The repetitive regressive-transgressive sequences within the Bootlegger Member are thought to reflect episodic uplift and subsequent subsidence of the South Arch, a segment of the Sweetgrass Arch whose axis is close to the city of Great Falls (Arnott, 1987; Arnott and Hein, in review). Periods of uplift probably coincided with episodes of accelerated Cordilleran thrusting inasmuch as the arch had acted as a forebulge associated with lithospheric flexure during Bootlegger time. On the other hand, subsidence likely recorded thrusting quiescence and lithospheric foundering due to sediment loading and elastic flexure relaxation (Arnott, 1987; Arnott and Hein, in review ).

The Ulm Pishkun (Pishkun being the Indian word for buffalo jump), is exposed on the south face of a large mesa called Taft Hill, 16 km west of Great Falls (Fig. 1). This outcrop stretches uninterrupted for approximately 2 km from east to west and is typically about 10 metres high. The entire outcrop dips very gently (about $1^{o}$ - $2^{o}$) to the west, probably a result of its location on the western limb of the South Arch. Bed-by-bed analysis of 14 vertical transects measured along a distance of 1250 metres permitted subdivision of the outcrop into five distinct lithologic units. The following is a description and interpretation of the lithologic components making up each of these units. Each unit is named after the dominant constituent lithofacies.

## LITHOLOGIC UNITS OF THE ULM PISHKUN

### Unit 1: Interbedded Grey-Black Shale And Siltstone

This recessively-weathered unit is composed of interbedded grey-black, non-calcareous bentonitic shale and siltstone. It crops out at the base and at the top of the Ulm Pishkun. The lower contact of Unit 1 strata at the base of the Ulm Pishkun with the underlying terrestrial deposits of the Vaughn Member is exposed in only one location. Here, the dark shales of the Bootlegger Member sharply overlie the regionally extensive, carbonaceous/red-specks horizon which occurs at the top of the Vaughn Member (Cobban *et al.*, 1959, 1976). The upper contact of lowermost Unit 1 strata with the more resistant sandstones of Unit 2 is rarely exposed. However, when exposed it forms a cliff-like overhang which on a small scale is bioturbated and load-casted (Fig.3A). The uppermost package of Unit 1 strata lies sharply on the upper surface of the Ulm Pishkun outcrop, but because of its high shale content is rarely exposed.

Unit 1 is dominated by very crumbly weathering grey-black bentonitic shales with abundant siltstone interbeds (Fig. 3B). Interbeds are typically < 2.5 cm thick and pinch and swell along strike. Basal bed contacts are sharp and load-casted, becoming boudinaged in cases of extreme loading. Where bioturbation and soft-sediment deformation have not obliterated primary sedimentary structures, ripple cross-stratification is commonly preserved.

Interpretation:

The fine-grained nature, characteristic sedimentary structures and association with overlying Unit 2 strata (discussed below) is interpreted to indicate a shallow-offshore shelf environment for Unit 1. The interbedded nature plus the sharp, loaded contacts of siltstone beds reflects their episodic emplacement into an otherwise mud-dominated environment. The occurrence of siltstone beds in this environment has been attributed to the transport and deposition of shoreward-derived sediments from bottom currents associated with storm wind-forcing and coastal set-up (Hobday and Reading, 1972; Hamblin and Walker, 1979; Kreisa, 1981; Morton, 1981; Dott and Bourgeois, 1982; Swift *et al.*, 1983; Walker, 1984; Hein *et al.*, 1986). Hummocky cross-stratification (HCS) has commonly been observed in ancient shallow-offshore shelf environments (Harms *et al.*., 1975; Dott and Bourgeois, 1982; Hamblin and Walker, 1979; Leckie and Walker, 1982; Walker *et al.*, 1983; Duke, 1985). Its paucity in Unit 1 at the Ulm Pishkun may be a consequence of limited exposure, since HCS is abundant in equivalent strata east of Great Falls. The more shaley nature and occurrence of very thin siltstone interbeds in Unit 1 cropping out on the top of the Ulm Pishkun may reflect a more distal environment than exemplified by the lowermost exposure.

### Unit 2: Gently Undulating Parallel Laminated Sandstone

Unit 2 is dominated by beds possessing a peculiar type of stratification which I call "gently undulating parallel lamination" (GUP lamination) (Fig. 4A). Acetate peels prepared from GUP laminated beds revealed that sand grains were typically spherical and consequently could not provide an indication of preferred axial orientation. In addition magnetic susceptibility of these strata is typically low ($<10^{-5}$ SI units), and equipment available to the author could not reliably determine a directional anisotropy of magnetic susceptibility (AMS) in most cases. However, examples of statistically reliable AMS orientation indicated a gentle ($< 10^{o}$) dip of the grains' AB planes toward the west, indicating eastward sediment transport.

Unit 2 crops out abruptly above Unit 1 and grades westward and upward into cross-bedded strata of Unit 3. Unit 2 is dominated by fine-grained sandstone beds exhibiting a thick (0.05 to 0.5 m) basal portion of GUP lamination overlain by a thin 1-3 cm cap of three-dimensional current ripples or less commonly climbing-ripple cross-stratification (Fig. 4B). Ripples usually indicate south-southeast-flowing palaeocurrents. Basal contacts are always sharp, wavy (metre-scale) and replete with bioturbation casts. Scoured contacts are common, and the soles of many beds exhibit flutes, grooves, prod marks and rare gutter casts. Shale occurs as rip-up clasts typically confined to the lower portion of the bed or as a < 1 cm veneer capping the bed. Other lithologies making up Unit 2 typically occur as 20-50 cm thick packages of interbedded sandstone and shale. Sandstones are usually 1-5 cm thick and are commonly massive with an undulating basal and upper contact or are current ripple cross-stratified (Fig. 4C).

The dominant lithology of Unit 2 is gently undulating parallel lamination (GUP lamination). Spacing of the undulation ranges from decimetres to several metres, even along a single lamina. Heights of the undulations rarely exceed 3.0 cm, and in most instances range between 1- 1.5 cm. Consequently, the spacing-to-height ratio exhibited by GUP laminated sandstones is typically in the order of 50 -100 or more. Laminae are laterally continuous, although rare low-angle truncation surfaces (< $5^{0}$) between laminae and common basal truncations are observed (Fig. 4D). Exposed bedding plane surfaces invariably show parting lineation.

Rare examples of hummocky cross-stratified (HCS) sandstone occur near the basal contact with Unit 1 (Fig. 4E). Hummocky cross-stratification resembles GUP lamination, but the form-sets of the HCS beds are characterised by hummocks and swales exhibiting several to a few tens of centimetres of relief. The typical low spacing-to-height values characterising HCS deposits (~ 10) differentiates them from the consistently higher values observed in beds with GUP lamination.

Commonly in the upper portion of Unit 2 are deep scours incised into the tops of many GUP laminated beds (Fig. 8C). Scours are usually tens of centimetres deep and their surfaces are typically ripple-covered.

Interpretation:

Beds containing GUP lamination are interpreted to have been deposited by unidirectionally-dominated combined flow. A complete discussion of this structure and its possible origin is given later in the paper. Bottom currents were capable of developing upper-flow-regime, plane bed conditions in the fine sand which led to the generation of GUP lamination.

Thin, massive sandstones with undulating upper and lower contacts are interpreted as symmetric wave ripples. Komar *et al.* (1972) reported that the influence of large surface waves can be detected at depths of over 125 metres, a depth which is far in excess of that suggested for Unit 2. Ripples showing onshore palaeocurrent directions are also probably related to surface gravity waves (Fig. 6B). However, these waves imparted a preferred direction of sediment transport at the seabed, a condition developed beneath shoaling surface gravity waves. Current-rippled sandstones exhibiting offshore palaeocurrent directions are probably deposited from storm-generated bottom currents, although these currents are markedly less competent than those depositing beds containing GUP lamination (Fig. 6B).

The deep scours in the upper portion of Unit 2 may represent storm rip channels. These channels were active during high energy events and funnelled sediment offshore. With the abatement of storm conditions the exposed scoured surfaces were then reworked and rippled by fairweather waves.

The dominance of beds exhibiting GUP lamination and the occurrence of interbedded symmetrical/unidirectional rippled sandstone and shale are taken to indicate a lower-shoreface depositional environment for beds making up Unit 2. The lower shoreface is then abruptly overlain by lithologies of Unit 3 (Fig. 4F).

### Unit 3: Medium-Scale Cross-Stratified Sandstone

Unit 3 consists of fine-grained sandstone exhibiting trough and less commonly planar tabular cross-stratification (Fig. 5A). Shale rip-up clasts are common. Basal contacts are always scoured and bioturbated. Laminae of many trough cross-stratified beds dip at angles typically $< 20^{\circ}$, suggesting that only the toeset remnant of an originally large-scale bedform has been preserved. The occurrence of back-flow ripples along some of these low-angle laminae attests to the one-time existence of a relatively high bedform which enabled flow separation and the development of strong reverse-flow eddies. Palaeoflow directions of both planar tabular cross-sets and trough axes invariably indicate sediment transport toward the northwest (Fig. 6B).

Interbedded with the medium-scale cross-stratified sandstones are beds with GUP lamination. These beds are much less common than in Unit 2, and are capped on their upper surface by ripples showing northwest palaeocurrent directions. Rare, thin (1-2 cm) interbeds of rippled sandstone/shale are also observed.

Interpretation:

Beds of Unit 3 are assigned to an upper-shoreface depositional environment. This portion of the shoreface is characterised by wave buildup prior to breaking. Wave buildup and the development of a steadily increasing asymmetry is caused by shoaling water depth and the impingement of wave orbitals on the sea bed. At the bed wave shoaling results in the unidirectional transport of sediment in the direction of wave propagation (Clifton *et al.*, 1971; Komar, 1976; Swift *et al.*, 1983) and commonly the development of large-scale, transverse-to-flow bedforms (Clifton *et al.*, 1971). The abundant medium-scale cross-stratified sandstones characterising Unit 3 are thought to have formed in this way. The general northwest-trend of the cross-stratification suggests typically northwest-moving shoaling waves, which ultimately reflects the pervasive northwesterly trend of fair-weather winds.

Interbeds of GUP laminated sandstones suggest the periodic emplacement of these beds during storm events. The reestablishment of fair-weather processes resulted in the development of large-scale, transverse-to-flow bedforms above the GUP laminated beds. Interbedded rippled sandstone/shale suggest periods of very subdued wave energy in this otherwise active depositional environment. The common occurrence of shale rip-up clasts in the cross-bedded sandstones may indicate erosion and incorporation of these locally deposited shales.

## Unit 4: Heterogenous Bedform Unit

Beds making up Unit 4 lie sharply above the cross-bedded sandstones of Unit 3 and in turn are sharply overlain by strata of Unit 5 (discussed below). The basal contact of Unit 4 is identified by the marked decrease in the abundance of cross-stratified sandstones, although matched with an increase in GUP laminated beds. Typically Unit 4 is made up of approximately 30 : 70 of these two lithofacies, respectively. Shale occurs rarely as thin interbeds (< 1cm) and more commonly as rip-up clasts occurring along the toeset portion of cross-bedded sandstones or along laminae in GUP laminated sandstone beds. Cross-stratified sandstones typically indicate northwest sediment transport, although southeastward palaeoflow directions have been recorded (Fig. 6B). Reactivation surfaces are commonly observed in cross-stratified sandstones.

Interpretation:

Most of sedimentary characteristics of Unit 4 strata indicate a depositional environment characterised by relatively high energy. However, the occurrence of thin shale interbeds indicate periods of suspension deposition. The position of Unit 4 above the interpreted upper shoreface and beneath the foreshore (discussed in Unit 5) would suggest deposition within the surf zone.

The surf zone is a physically active part of the nearshore. At its seaward edge the surf zone is characterised by wave breaking, and from this point landward by waves of translation. Development of planar laminated sandstone by upper-flow-regime currents is common in this environment (Clifton *et al.*, 1971). Medium-scale, transverse-to-flow bedforms are also common and are the result of longshore currents generated within the surf zone (Clifton *et al.*, 1971). However, the occurrence of interbedded shale, shale rip-up clasts and the common occurrence of cross-stratified sandstones exhibiting offshore palaeocurrent directions present a problem for a strict surf-zone interpretation. Therefore, Unit 4 is interpreted to have been deposited within the surf zone, but deposition occurred within a feature (rip channel ?) channellized into the surf-zone environment. This channel feature enabled development of a micro-depositional environment which at certain times was capable of suspension deposition. Consequently, the abundant shale rip-up clasts observed in Unit 4 sandstone beds were probably locally derived. Onshore migrating, medium-scale bedforms may be related to the landward-migrating wave bore, although those showing offshore palaeocurrents indicate transport by offshore-flowing currents within this channel. Deposition of GUP laminated beds, discussed in detail below, was probably the result of offshore currents which were capable of upper-flow-regime, plane-bed conditions.

### Unit 5: Thin Slabby Sandstone

Unit 5 is composed of fine-grained sandstone with rare scattered chert granules. Beds tend to be massive, but parallel lamination can sometimes be observed. Cross-bedding is rare. Unit 5 can be subdivided into two distinct packages. In the lower package beds are typically massive, 1-10 cm thick, laterally pinch and swell and exhibit wavy basal contacts. Thin beds (1-3 cm) are characterised by lower and upper bedding surfaces which undulate in-phase. Thicker beds (4-10 cm) are capped with a wavy bed-top, although it undulates on a much shorter wavelength than that characterising the wavy basal contact.

The upper package of Unit 5 is characterised by thin slab-like strata which make up numerous 5-10 cm thick sets. Each set dips gently ($5^o$ -$10^o$) typically toward the east and is separated from adjacent and subjacent sets by a low angle truncation surface (Fig. 5B). Westward dipping sets are also commonly observed. Less common medium-scale cross-bedded sandstones are also observed.

Interpretation:

Unit 5 is interpreted as a foreshore depositional environment. Rarity of cross-stratified bedforms in this unit suggests either the maintenance of high energy conditions or erosion of the bedforms during storms. The lower portion of Unit 5 is interpreted as the lower part of the foreshore environment. The common occurrence of wave ripples (thin 1-3 cm beds) suggests periods of subdued wave energy. Thicker (4-10 cm) beds were probably deposited under upper-flow-regime conditions during periods of more intense wave energy. Abatement of these conditions caused wave rippling of the bed tops. The upper portion of Unit 5 with its shallow dipping sets is interpreted as the swash-backwash portion of the foreshore. Here constant high-energy conditions produced the characteristic eastward (seaward) dipping swash lamination observed in both modern and ancient foreshore settings. The less common westward (landward) dipping lamination may represent sand deposition on the backshore beach berm. High-angle cross-stratified sandstones are probably landward migrating ridges associated with ridge-and-runnel systems formed during low-energy periods.

## PALAEOENVIRONMENTAL SUMMARY OF THE ULM PISHKUN

Exposure along the Ulm Pishkun is believed to represent the development and eastward progradation of a storm-dominated shoreline associated with the initial transgressive stage of the Greenhorn Cyclothem into the Great Falls area (Fig. 6A, 6B). Stratigraphically-upward the depositional environments included: the shallow-offshore shelf, lower shoreface, upper shoreface, chanellized surf zone and foreshore. Evidence supporting a storm-dominated interpretation includes the common alternating or interbedding of lower-flow-regime and upper-flow-regime sedimentary structures observed in almost all the depositional environments. Fluctuating hydrodynamic conditions in this ancient nearshore environment were probably the result of alternating storm and and less severe (~fair-weather) atmospheric conditions. Trace-fossil characteristics support a storm-dominated interpretation (S.G. Pemberton, pers. comm. 1987), and are the subject of a later paper.

The abrupt deposition of lower shoreface strata (Unit 2) above shallow-offshore shelf deposits (Unit 1) indicates rapid shoreface progradation. McCrory and Walker (1986) suggested that rapid shoreline progradation and the abrupt transition from shallow-offshore shelf to lower shoreface deposits is a characteristic feature of ancient storm-dominated shoreface sequences. Comparable abruptness of this contact observed at the Ulm Pishkun is, however, thought to be related to activity of the ancestral Sweetgrass Arch. In the Great Falls study area the Bootlegger Member is comprised of five regionally extensive shoaling-upward sequences, the Ulm Pishkun section representing part of the second sequence. Rapid shoreline progradation and the development of the five shoaling-upward sequences is possibly related to uplift of the South Arch, the southern element of the ancestral Sweetgrass Arch whose crest lies near the Great Falls study study area (Arnott, 1987)(Fig. 7). During the Cordilleran orogeny the Sweetgrass Arch may have acted as a forebulge associated with flexural subsidence of the lithosphere beneath the rising and eastward-migrating Cordilleran Fold and Thrust Belt (Lorenz, 1982; Arnott, 1987; Arnott and Hein, in review). Forebulge uplift during Cordilleran thrust episodes caused the rapid eastward migration of the strandline and development of shoaling-upward depositional conditions. As a result, the abrupt transition from shallow-offshore shelf to lower shoreface observed at the Ulm Pishkun is thought to reflect uplift of the Sweetgrass Arch and, is not, as suggested by McCrory and Walker (1986), to be a depositional condition related to the hydrodynamic nature of a storm-dominated shoreface. During periods of Cordilleran thrust quiescence, however, the arch subsided under the effect of sediment loading and elastic lithospheric relaxation. This resulted in the westward displacement of the strandline by the ensuing marine transgression. Reworking of an indeterminate amount of the regressive sequence during transgression resulted in the development of a planar transgressive surface over which shallow-offshore shelf deposits observed at the top of the Ulm Pishkun were eventually deposited.

Palaeocurrent information suggests that the shoreline exposed at the Ulm Pishkun was oriented north-northwest/south-southeast, an orientation which roughly parallels the axial trend of the South Arch. Prevailing fairweather winds probably blew from the southeast. This would have given rise to northwest-travelling surface gravity waves which in turn accounted for the abundance of northwest palaeocurrents observed in upper shoreface strata. However, storm events were most likely associated with winds from the east-northeast. Winds from this direction would enable maximum coastal set-up and the generation of high velocity, offshore-flowing bottom currents.

## DEVELOPMENT OF GENTLY UNDULATING PARALLEL LAMINATION (GUP LAMINATION)

On storm-dominated shorelines intense onshore storms result in the development of a coastal set-up with a concomitant offshore bottom current. On modern continental shelves these currents are known to have attained velocities of 1.6 m/s or more (Murray, 1970; Forristall *et al.*, 1977). However, on ancient continental shelves to what extent did such bottom currents control the transport and deposition of sediment seen in the geologic record ?

Sedimentary models concerned with the offshore transport and deposition of sediments on storm-dominated continental shelves are from two basic schools of thought. The first is the Swift model based primarily on observation in the modern oceans. This model relates sediment transport and deposition to an incremental process driven by strong offshore-flowing bottom currents generated during atmospheric storm events (Swift and Rice, 1984). Bottom currents flow offshore and are influenced by the Coriolis force, which in the northern hemisphere causes a right-handed deviation of the flow. With a gradual balancing of forces the bottom current is eventually forced to assume a nearly parallel-to-isobath orientation. The incremental movement of sediment indicated by the Swift model requires the episodic remobilization and redeposition of sediment further offshore or along an isobath until finally reaching its final depositional area. The second model, based mostly on observations from the rock record, is the Walker shelf turbidity current model of (Hamblin and Walker, 1979; Walker, 1984). This model suggests a single-event episode with the seaward transport and deposition of sediment from a turbulent suspension. Because of its inertia this current unlike the that in the Swift model is capable of flowing for great distances at a high angle to the isobaths. These two continental shelf sediment transport models would appear to represent end-member conditions, and differ in two fundamental respects; (1) the Walker model relates transport and final sediment deposition to a single-event process, compared with the multi-event history of the Swift model, and (2) transport of sediment in the Swift model is eventually parallel to the isobaths, but is primarily normal to the isobaths in the Walker model. Evidence from the Ulm Pishkun study area , particularly structures associated with gently undulating parallel lamination, would seem to suggest that sediment deposition (and possibly sediment transport) in this ancient nearshore sedimentary environment was predominantly from single-event currents, and that these currents showed characterisitics being intermediate with respect to the two end members.

Gently undulating parallel lamination (GUP lamination) is a very common lithofacies at the Ulm Pishkun study area, particularly in the lower shoreface. This sedimentary structure is characterised by a very subdued undulation in what otherwise appears to be upper-flow-regime, plane-bed lamination. Several lines of evidence suggest the development of GUP lamination under upper-flow-regime, unidirectionally-dominated flow. These include:

(1) common occurrence of flutes, grooves, prod marks and rare gutter casts;
(2) directional filling of basal scours;
(3) abundance of parting lineation on exposed bedding planes;
(4) development of parallel-to-flow grain fabric;
(5) surficial cap of ripples typically showing southeast palaeoflow directions;
(6) occurrence of ripple, washed-out dune or high-angle dune bedforms beneath GUP laminated beds;

Flutes, grooves, prod marks and gutter cast are erosive features commonly observed on the soles of deep-marine turbidite beds. In turbidites their association with the overlying Bouma "A" or "B" divisions or a conglomerate indicates their erosive development under upper-flow-regime conditions. Similarly, their development on the soles of GUP laminated beds is thought to suggest equivalent hydrodynamic conditions. The east-southeast trend of flute marks and the west-northwest / east-southeast orientation of groove structures indicates their development by east-southeast-flowing unidirectional currents. The paucity of gutter casts (Fig. 8A) may only be an artifact of the two-dimensional nature of the outcrop and the consequent difficulty of observing the third dimension of these long linear structures.

Another basal feature suggesting unidirectional flow is the occurrence of basal scours showing directional sediment fill (Fig. 8B). In the fill of these scours the lowermost laminae terminate at high angles against the downstream side of the scour, with subsequent laminae gradually decreasing in dip until they reassume horizontal GUP lamination across the filled scour. Invariably, scours and their sediment fills indicate incision and subsequent sediment deposition from unidirectional flows which moved in a general easterly direction, since the outcrop only allows a two-dimensional view of the scour fill.

One of the most striking features of GUP lamination is the abundance of parting lineation on exposed bedding planes. This sedimentary structure has been attributed to turbulent bursting near the wall of a turbulent unidirectional flow during upper-plane-bed conditions (Allen, 1984a, 1984b). The existence of parting lineation on bedding surfaces of GUP laminated sandstones would suggest similar hydrodynamic conditions. Also associated with upper-plane-bed conditions is the development of a preferred parallel-to-flow grain fabric (Allen, 1964; Arnott and Hand, 1987). Grain fabric analysis of GUP lamination was accomplished using the anisotropy of magnetic susceptibility (AMS). Grain orientation invariably indicated low angles ($< 10^{0}$) of imbrication and east-southeast or southeast sediment transport. Recently, Arnott and Hand (1987) have shown that under upper-plane-bed conditions the angle of grain imbrication is related to the volumetric rate of sediment fallout. Consequently, the low imbrication angles observed in GUP lamination may suggest traction deposition from unidirectional currents characterised by a slow rate of sediment fallout. Therefore the thick basal GUP laminated portion of a GUP laminated bed deposited during a single sedimentation event may have accumulated over a relatively long period of time, possibly many hours or days.

The initial impression one has of a bed containing GUP lamination is of a Bouma BC turbidite, although the Bouma-B-like division would account for 80-90% of the bed. Bouma-sequence turbidites are known to be deposited from unidirectional turbulent suspensions and that their characteristic vertical succession of divisions is suggested to reflect waning flow conditions (Middleton and Hampton, 1976; Blatt *et al.*, 1980). A similar scenario is believed to account for deposition of GUP laminated beds. Fine sand probably eroded from the beachface was transported seaward and initially deposited under upper-flow-regime plane bed conditions developed under a unidirectionally-dominated current. Although with time this current waned and upper-plane-bed was replaced by current ripple development. In the lower shoreface bed-top ripples overlying GUP lamination commonly indicate southeast palaeoflow directions, suggesting development during the waning stages of the offshore-flowing, unidirectional current. However, bed-top ripples capping GUP lamination in the upper shoreface and the surf zone channel commonly show northwest palaeocurrent directions, suggesting post-depositional reworking by fairweather currents.

In the aforegoing discussion of GUP lamination a number of points should be reemphasised. Firstly, many aspects of GUP lamination indicate transport and deposition of sediment under upper-plane-bed conditions. These conditions were developed under a unidirectionally-dominated current which flowed offshore. Secondly, the great thickness of GUP lamination in each GUP laminated bed indicates the prolonged maintenance of upper-plane-bed conditions at the sea bed. In addition the low imbrication angles of parallel-to-flow sand grains in GUP laminated sandstones indicate predominantly sediment fallout with traction by currents which flowed for a relatively long period of time. Thirdly, basal scour features plus some GUP lamination grain imbrication data indicate east-southeast palaeoflows. On the other hand, bed-top current ripples of lower shoreface strata invariably show southeast palaeocurrents. Therefore there is a slight but consistent right-handed deviation of palaeocurrent directions between the base and top of many beds. This deviation may reflect the more noticeable influence of the Coriolis force during the waning stages of the offshore-flowing, unidirectionally-dominated current.

Occasionally ripples, washed-out dunes and less commonly toeset remnants of high-angle dune bedforms are observed to be erosively overlain by GUP lamination.

Unfortunately due to the nature of the Ulm Pishkun outcrop an accurate determination of the palaeocurrent direction of the ripple and dune bedforms could not be ascertained other than that they are oriented in a general offshore direction. Therefore, the occurrence of GUP lamination above the ripple or dune bedforms may be taken to suggest a waxing (increasing) of unidirectional flow and caused a transformation from lower-flow-regime to upper-flow-regime conditions. At the Ulm Pishkun, during atmospheric storm events most if not all of the depositional environments would have been effected by surface gravity waves. If, as most of the sedimentary structures suggest, there was a unidirectional flow present, then transport / deposition of sediment was under a combined flow regime. Recently Southard and others (pers. comm. 1987) have shown that under combined flow even weak unidirectional currents are capable of generating unidirectional ripple and dune bedforms which under purely unidirectional flow would have required a much stronger unidirectional current. Consequently, the transformation from ripple or dune bedforms into GUP lamination, even though indicative of waxing flow, may not have required a dramatic increase in the unidirectional flow component.

In the above discussion of GUP lamination and associated structures it could be argued that many of the observed features could indicate a turbidity current or bottom-flow interpretation. Erosive basal scouring features, palaeocurrents oriented at a high angle to the shoreline, and the single-event generation and deposition of these strata may suggest a turbidity current interpretation. On the other hand, the right-handed deviation of bed-top ripples, the waxing sequence of sedimentary structures observed in some GUP laminated beds, plus the thickness of GUP lamination compared with the thin accumulation of bed-top ripples in GUP laminated sandstones implies the importance of bottom currents associated with coastal set-up. Considered as a whole, all these features may indicate the existence of a current which showed characterisitics common to both sediment transporting mechanisms; a set-up related bottom current and a current flowing downstream in response to an excess downstream density gradient. A possible scenario for the interaction of these two processes may be as follows: during atmospheric storms surface gravity waves may have provided enough suspended sediment to develop the required density differential for a density current. Development of fluid turbulence required by the turbidity current was provided by two sources (1) gravitational force acting on the density contrast sitting on a sloping shoreface, and, (2) possible input of energy from the unidirectional, offshore-flowing bottom current associated with coastal set-up. Therefore during the storm event sediment may have been transported from a current characterised by both turbidity current and bottom flow processes. Deposition from this intermediate current resulted in beds exhibiting features indicating the influence of both processes.

The most obvious, and unfortunately the most poorly understood trait of GUP lamination is the gentle undulation of the parallel lamination. The undulation has variable spacing, ranging from a few decimetres to many metres (even along individual lamina), which may or may not conform to the profile of the basal bed contact. Height rarely exceeds 3 cm, but is more typically between 1 - 1.5 cm. Together these two features indicate a spacing-to-height ratio for GUP lamination in the order of 50-100 or more. In addition to the undulating nature of the parallel lamination, the most enigmatic feature of the undulation is that it shows no sign of horizontal migration. Therefore, not only is the flow being forced to deposit undulating laminae, but the bedform being deposited was quasi-standing at least on the scale of the outcrop. At the present time no mechanism(s) known to the author can explain this structure; however, some possibilities may include:

(1) near-bed development of standing waves, possibly generated in a zone of density gradient within the unidirectionally-dominated combined flow;

(2) the generation of a ridge-and-trough structure caused by quasi-regularly spaced secondary flow cells generated within the main unidirectionally-dominated flow;

(3) may be an equilibrium structure developed under a unidirectionally-dominated combined flow, although this would be inconsistent with the standing nature of the bedform.

# REFERENCES

Allen, J.R.L., 1964. Primary current lineation in the Lower Old Red Sandstone (Devonian) Anglo-Welsh Basin. Sedimentology, v. 3, pp. 89-108.

------, 1984a. Sedimentary structures their character and physical basis. In: Developments in Sedimentology 30 (volumes I, II) , Elsevier Science Publishers, Amsterdam, 1256 p.

------, 1984b. Parallel lamination developed from upper-stage plane beds: a model based on the larger coherent structures of the turbulent boundary layer. Sedimentary Geology, v. 39, pp. 227-242.

Arnott, R.W., 1987. Stratigraphy of the Lower Cretaceous Bootlegger Member near Great Falls, Montana and its relationship with the ancestral Sweetgrass Arch. Geological Association of Canada, Program with Abstracts, p. 22.

-------, Hand, B.M., 1987. Inluence of suspended sediment rain on bedforms and sand fabric. Geological Association of America , Prog with Abstr., p.

Beaumont, C., 1981. Foreland basins. Geophysical Journal of the Royal Astronomy Society, v 65, pp. 291-329.

Blatt, H., Middleton, G., Murray, R., 1982. Origin of sedimentary rocks. 2nd Edition. New Yersey : Prentice-Hall Inc., 782 p.

Cannon, J.L., 1966. Outcrop examination and interpretation of paleocurrent patterns of the Blackleaf Formation near, Great Falls, Montana. Billings Geologic Society Guidebook, 17th annual field conference, pp. 71-111.

Clifton, H.E., Hunter, R.E., Phillips, R.L., 1971. Depositional structures and processes in the non-barred high-energy nearshore, Journal of Sedimentary Petrology, v. 41, pp. 651-670.

Cobban, W.A., Erdmann, C.E., Lemke, R.W., Maughn, E.K., 1959. Revision of Colorado Group on Sweetgrass Arch, Montana. American Association of Petroleum Bulletin Geologists, v.43, pp. 2786-2796.

-------, 1976. Type sections and stratigraphy of the members of the Blackleaf and Marias River Formations (Cretaceous) of the Sweetgrass Arch, Montana. U.S.G.S. Professional Paper 974, 66p.

Dott, R.H., (Jr.), Bourgeois, J., 1982. Hummocky stratification: significance of its variable bedding sequences. Bulletin of the Geologic Society of America, v. 93, pp. 663-680.

Duke, W.L., 1985. Hummocky cross-stratification, tropical hurricanes, and intense winter storms. Sedimentology, v. 32, pp. 167-194.

Forristall, G.Z., Hamilton, R.C., Cardone, V.J., 1977. Continental shelf currents in Tropical Storm Delia, observations and theory. Journal of Physical Oceanography, v. 7, pp. 532-546.

Hamblin, A.P., Walker, R.G., 1979. Storm-dominated shallow marine deposits: the Fernie-Kootenay (Jurassic) transition, southern Rocky Mountains. Canadian Journal of Earth Science, v. 16, pp. 1673-1690.

Harms, J.C., Southard, J.B., Spearing, D.R., Walker, R.G., 1975. Depositional environments as interpreted from primary structures and stratification sequences. Sociey of Economic Paleontologists and Mineralogists, Tulsa, Short Course No. 2, 161p.

Hattin, D.E., 1964. Cyclic sedimentation in the Colorado Group of west-central Kansas. *In* Merriam, D.F., ed., Symposium on cyclic sedimentation, Kansas Geological Survey Bulletin, pp. 205-217.

Hein, F.J., Dean, M.E., Delure, A.M., Grant, S.K., Robb, G.A., Longstaffe, F.J., 1986. The Viking Formation in the Caroline, Garrington and Harmatten Fields, western south-central Alberta: sedimentology and paleogeography. Bulletin of Canadian Petroleum Geology, v. 34, pp. 91-110.

Hobday, D.K., Reading, H.G., 1972. Fair weather versus storm processes in shallow marine sandbar sequences in the late Precambrian of Finnmark, north Norway, Journal of Sedimentary Petrology, v. 42, pp. 318-324.

Jordan, T.E., 1981. Thrust loads and Foreland Basin evolution, Cretaceous, western United States. American Association of Petroleum Geologists Bulletin, v. 65, pp.2506-2520.

Kauffman, E.G., 1977. Geological and biological overview: Western Interior Cretaceous Basin. Mountain Geologist, v. 14, pp. 75-99.

-------, Cobban, W.A., Eicher, D.L., 1977. Albian through lower Coniacian strata, biostratigraphy and principals events, Western Interior United States. *In* Evenements de la Partie Moyenne du Cretace (Mid-Cretaceous events), Uppsala-Nice symposia, 1975-1976: Annales du Museum d'Historie Naturelle de Nice, v. 4, pp. XXIII1-XXIII24.

Komar, P.D., Neudeck, R.H., Miller, M.C., 1972. Observation and significance of deep-water oscillatory ripple marks on the Oregon Continental Shelf. *In* Swift, D.J.P., Duane, D.B., Pilkey, O.H., eds., Shelf Sediment Transport, Stroudsberg, Pa.: Dowden, Hutchinson and Ross, pp. 601-619.

Komar, P.D., 1976. The transport of cohesionless sediments on continental shelves. *In* Stanley, D.J., Swift, D.J.P., eds., Marine Sediment Transport and Environmental Management, New York, Interscience, Wiley and Sons, pp. 107-125.

Kreisa, R.D., 1981. Storm-generated sedimentary structures in subtidal marine facies with examples from the Middle and Upper Ordovician of southwestern Virginia. Journal of Sedimentary Petrology, v. 51, pp. 823-848.

Leckie, D.A., Walker, R.G., 1982. Storm- and tide-dominated shorelines in the Cretaceous Moosebar-Gates interval - outcrop equivalents of Deep Basin gas trap in western Canada. Bulletin of the American Association of Petroleum Geologists, v. 66, pp. 138-157.

Lorenz, J.C., 1982. Lithospheric flexure and the history of the Sweetgrass Arch, northwestern Montana. *In* Rocky Mountain Association of Geologists - 1982 Symposium, Geologic studies of the Cordilleran Thrust Belt, Vol. 1, pp. 77-89.

McCrory, V. L.C., Walker, R.G., 1986. A storm and tidally-influenced prograding shoreline -- Upper Cretaceous Milk River Formation of southern Alberta, Canada. Sedimentology, v. 33, pp. 47-60.

Middleton, G.V., Hampton, M.A., 1976. Subaqueous sediment transport and deposition by sediment gravity flows. *In* Stanley, D.J., Swift, D.J.P., eds., Marine sediment transport and environmental management, New York, Interscience, Wiley and Sons, pp. 197-218.

Morton, R.A., 1981. Formation of storm deposits by wind-forced currents in the currents in the Gulf of Mexico and the North Sea. *In* Nio, S.D., *et al.*, eds., Holocene marine sedimentation in the North Sea Basin. International Association of Sedimentologists, Special Publication 5, pp. 385-396.

Murray, S.P., 1970. Bottom currents near the coast during Hurricane Camille. Journal of Geophysical Research, v. 75, pp. 4579-4582.

Peterson, J.A. 1966. Sedimentary history of the Sweetgrass Arch. Billings Geologic Society Guidebook, 17th annual field conference, pp. 112-134.

Price, R.A., 1973. Large-scale gravitational flow of supracrustal rocks, southern Canadian Rockies. *In* DeJong, K.A., Scholten, R., eds., Gravity and Tectonics. New York. Interscience, John Wiley and Sons, pp. 491-502.

Reeside, J.B., Cobban, W.A., 1960. Studies of the Mowry Shale (Cretaceous) and contemperaneous formations in the United States and Canada. U.S.G.S. Professional Paper 355, 121 p.

Stelck, C.R., Armstrong, J., 1981. Neogastroplites from southern Alberta. Bulletin of Canadian Petroleum Geology, v. 29, pp.399-407.

Swift, D.J.P., Figueiredo, A.G. (Jr.), Freeland, G.L., Oertel, G.F., 1983. Hummocky cross-stratification and megaripples: a geological double standard. Journal of Sedimentary Petrology, v. 53, pp. 1295-1317.

Swift, D.J.P., Rice, D.D., 1984. Sand-bodies on muddy shelves: A model for sedimentation in the Western Interior Cretaceous Seaway, North America. *In* Tillman, R.W., Siemers, C.T., eds., Siliciclastic Shelf Sediments. Sociey of Economic Paleontologists and Mineralogists Special Publication No. 34, pp. 43-62.

Vuke, S.M., 1984. Depositional environments of the Early Cretaceous Western Interior Seaway in southwestern Montana and the northern United States. *In* Stott, D.F., Glass, D.J., eds., The Mesozoic of middle North America. Canadian Society of Petroleum Geologists Memoir 9, pp. 127-144.

Walker, R.G., 1984. Shelf and shallow marine sands. *In* Walker, R.G., ed. Facies models. Geoscience Canada, Reprint series 1, second edition, pp. 141-170.

-----, Duke, W.L., Leckie, D.A., 1983. Hummocky stratification: Significance of its variable bedding sequences: Discussion and reply. Geological Society of America Bulletin, v. 94, pp. 1245-1251.

FIGURE III-1: Location map of the Ulm Pishkun and surrounding area near Great Falls, Montana.

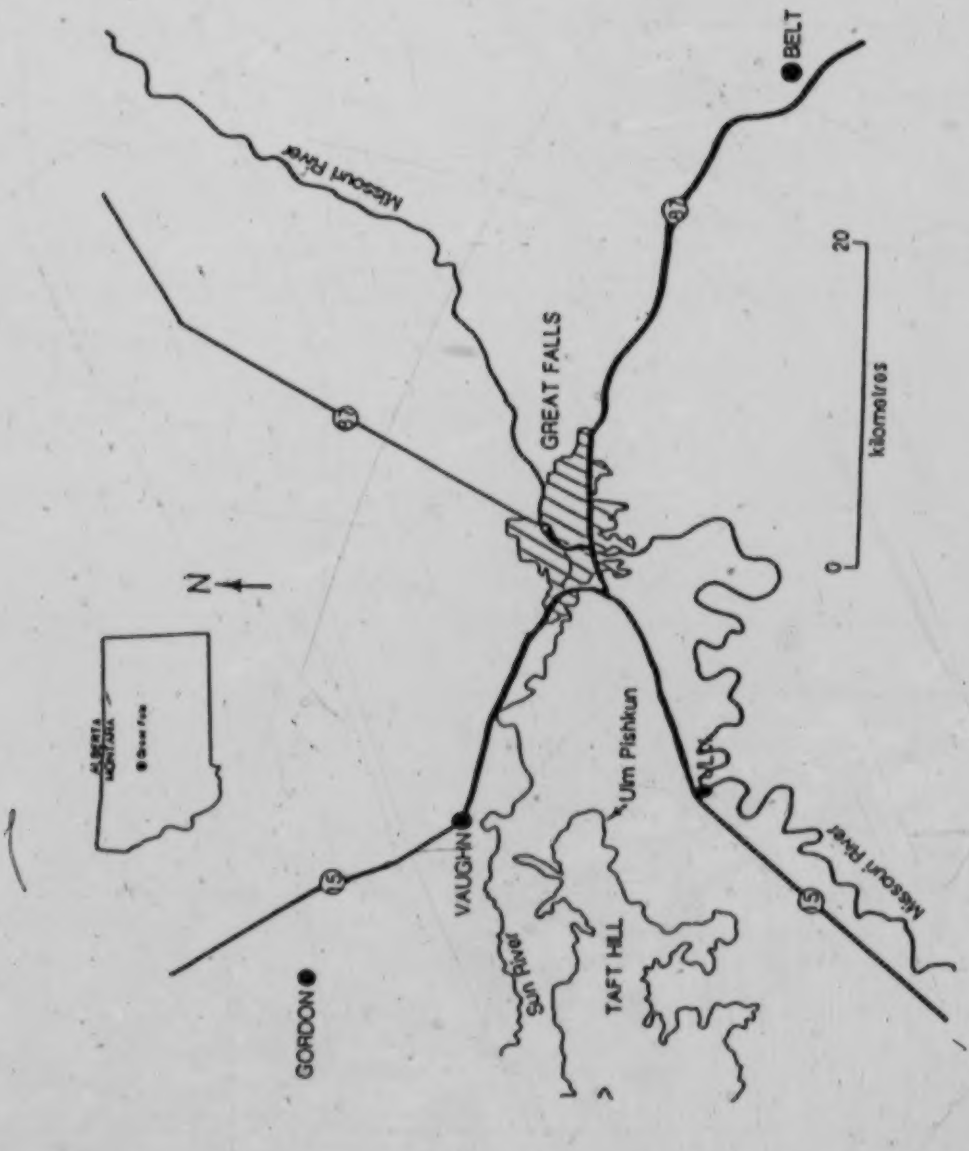
GREAT FALLS
Missouri River
Missouri River
BELT
VAUGHN
GORDON
Sun River
TAFT HILL
Ulm Pishkun
87
87
15
15
N
ALBERTA
MONTANA
Great Falls
0
20
kilometres

FIGURE III-2: Correlation chart of Upper and Lower Cretaceous strata in northwestern United States and south-central Alberta (modified after Stelck and Armstrong, 1981).

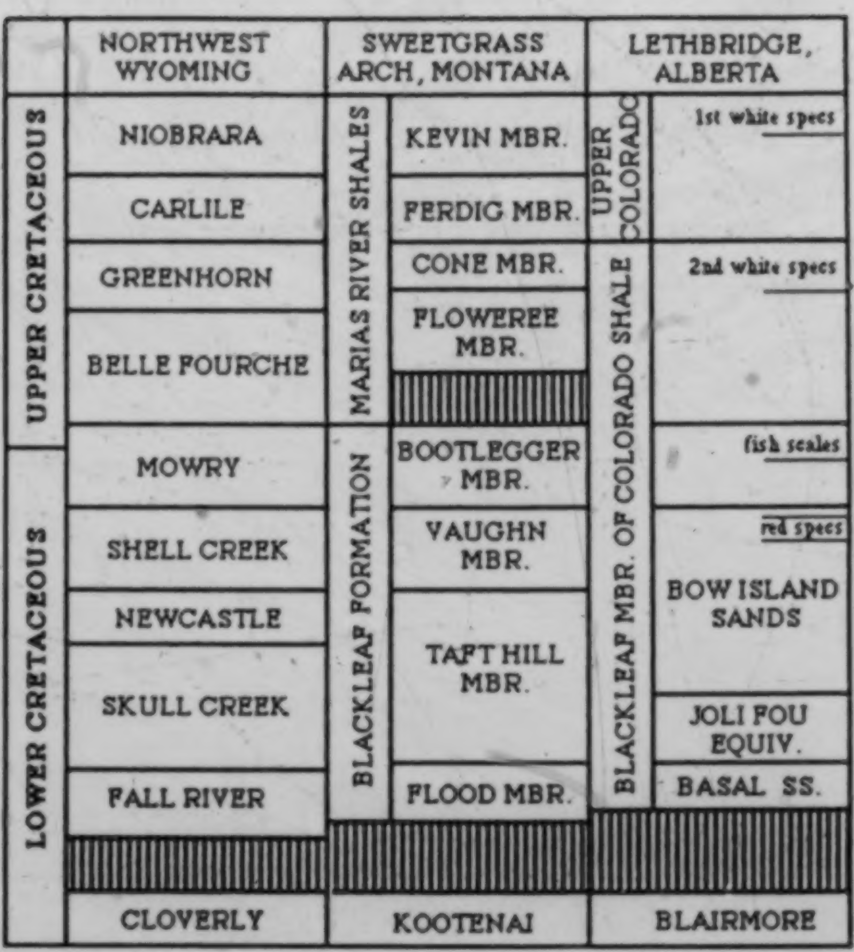

| | NORTHWEST WYOMING | SWEETGRASS ARCH, MONTANA | | LETHBRIDGE, ALBERTA | |
|---|---|---|---|---|---|
| UPPER CRETACEOUS | NIOBRARA | MARIAS RIVER SHALES | KEVIN MBR. | UPPER COLORADO | 1st white specs |
| | CARLILE | | FERDIG MBR. | | |
| | GREENHORN | | CONE MBR. | BLACKLEAF MBR. OF COLORADO SHALE | 2nd white specs |
| | BELLE FOURCHE | | FLOWEREE MBR.<br>▥ | | |
| LOWER CRETACEOUS | MOWRY | BLACKLEAF FORMATION | BOOTLEGGER MBR. | | fish scales |
| | SHELL CREEK | | VAUGHN MBR. | | red specs<br>BOW ISLAND SANDS |
| | NEWCASTLE | | TAFT HILL MBR. | | |
| | SKULL CREEK | | | | JOLI FOU EQUIV. |
| | FALL RIVER | | FLOOD MBR. | | BASAL SS. |
| | ▥ | ▥ | ▥ | ▥ | ▥ |
| | CLOVERLY | KOOTENAI | | BLAIRMORE | |

FIGURE III-3(A): Sharp contact between Unit 1 and Unit 2 (staff is 1.5 m long).

FIGURE III-3(B): Interbedded bentonitic shale and siltstone (Unit 1).

B
A

FIGURE III-4(A): Gently-undulating, parallel laminated sandstones (GUP lamination) of Unit 2 (outcrop is approximately 10 m high).

FIGURE III-4(B): Asymmetric ripple cap above GUP laminated sandstone bed.

FIGURE III-4(C): Interbedded wave and current rippled sandstone and shale sandwiched between two GUP laminated beds (scale bar is 10 cm long).

FIGURE III-4(D): Low-angle truncation surfaces within and between individual GUP laminated beds.

FIGURE III-4(E): HCS at the base of Unit 2 (beneath hammer), over and underlain by GUP laminated sandstones.

FIGURE III-4(F): Sharp contact between Unit 2 and Unit 3 (just above person's head).

A
B
C
D
E
F

FIGURE III-5(A): Medium-scale cross-stratified sandstones of Unit 3.

FIGURE III-5(B): Thin slabby sandstones (swash lamination) of Unit 5. Note low angle truncation surfaces (width of photo approximately 1.5 m).

B
A

FIGURE III-6(A): Cross-sectional palaeo-reconstruction of the Ulm Pishkun study area.

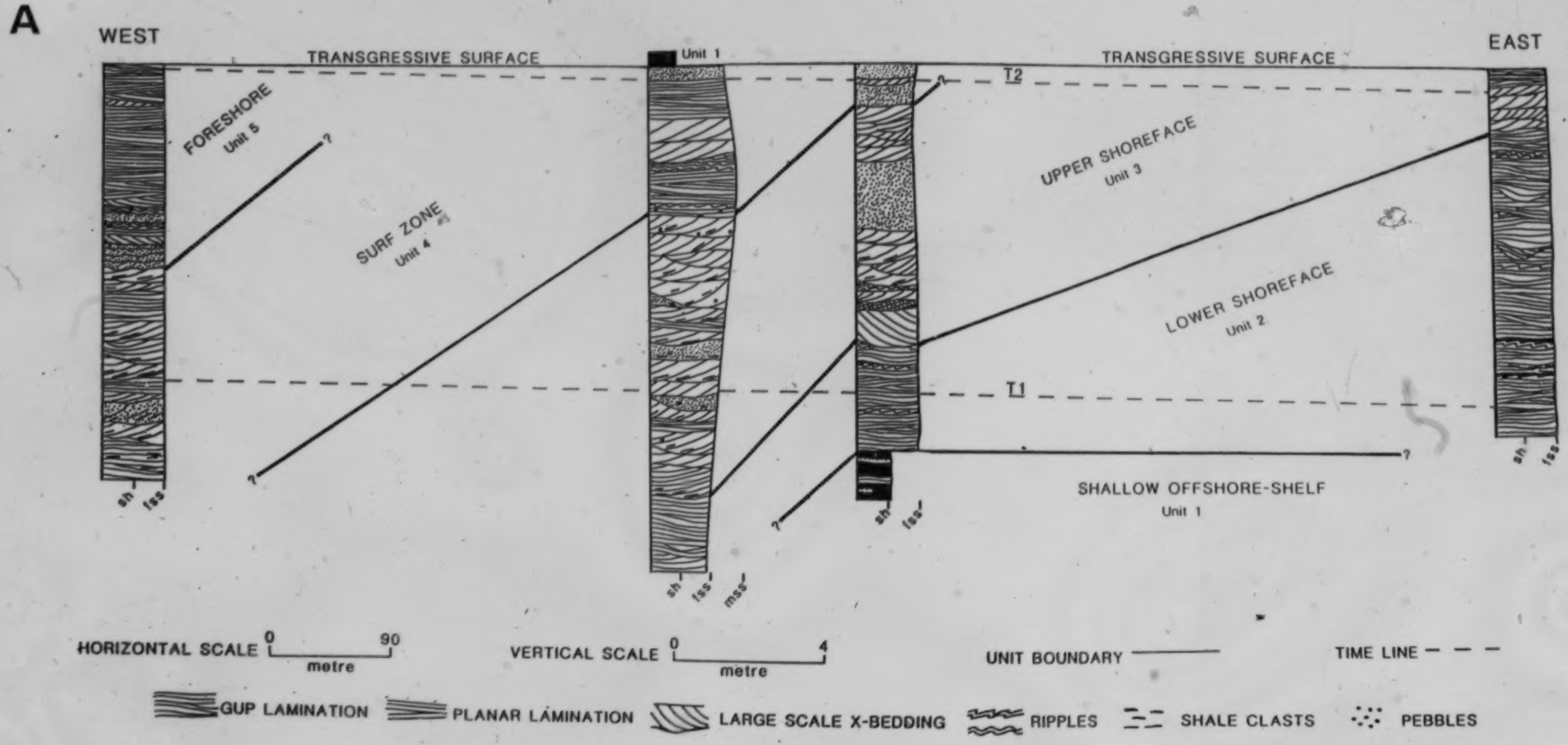
A
WEST
EAST
TRANSGRESSIVE SURFACE
Unit 1
TRANSGRESSIVE SURFACE
T2
FORESHORE
Unit 5
SURF ZONE
Unit 4
UPPER SHOREFACE
Unit 3
LOWER SHOREFACE
Unit 2
T1
SHALLOW OFFSHORE-SHELF
Unit 1
?
sh
fss
mss
HORIZONTAL SCALE 0 90 metre
VERTICAL SCALE 0 4 metre
UNIT BOUNDARY
TIME LINE
GUP LAMINATION
PLANAR LAMINATION
LARGE SCALE X-BEDDING
RIPPLES
SHALE CLASTS
PEBBLES

FIGURE III-6(B): Palaeocurrent rose diagrams for each depositional environment (Cosets = medium-scale, 3-D bedform (dune) coset measurements).

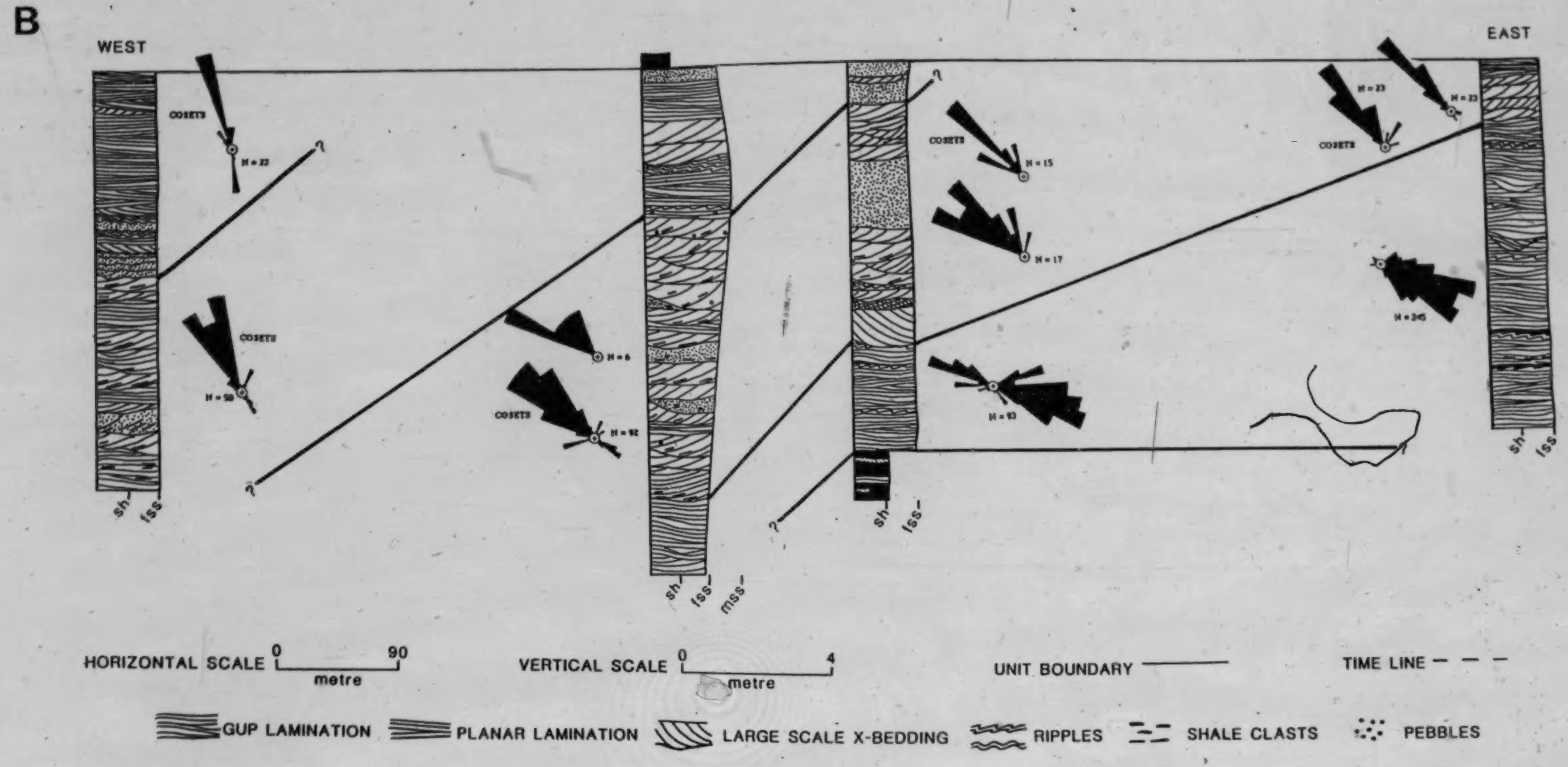
B
WEST
EAST
COSETS
N = 22
COSETS
N = 50
N = 6
COSETS
N = 92
COSETS
N = 15
N = 17
N = 13
COSETS
N = 23
N = 23
N = 245
?
sh
fss
mss
HORIZONTAL SCALE 0 90 metre
VERTICAL SCALE 0 4 metre
UNIT BOUNDARY
TIME LINE
GUP LAMINATION
PLANAR LAMINATION
LARGE SCALE X-BEDDING
RIPPLES
SHALE CLASTS
PEBBLES

FIGURE III-7: The axial trace of the South Arch through the Great Falls study area (Inset shows the constituent elements (South Arch and Kevin-Sunburst Dome) of the ancestral Sweetgrass Arch plus the Bow Island Arch of south-central Alberta.

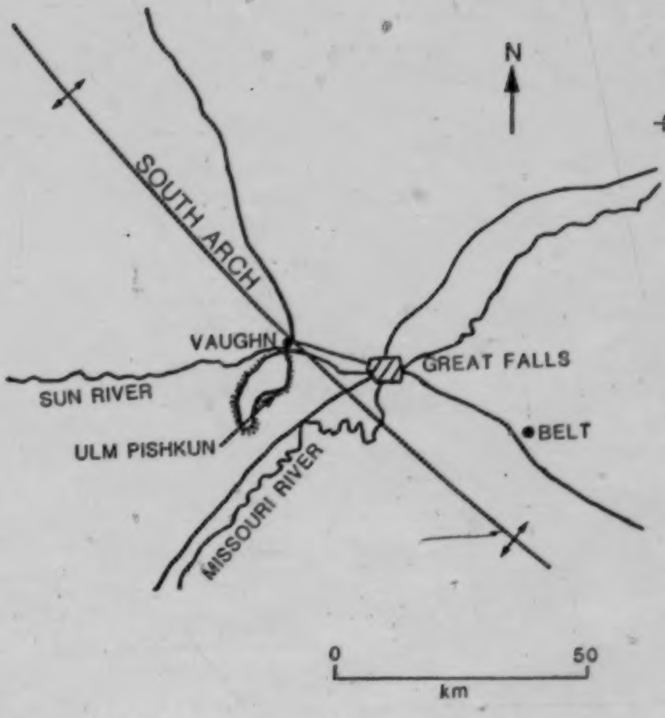
N
SOUTH ARCH
VAUGHN
GREAT FALLS
SUN RIVER
ULM PISHKUN
BELT
MISSOURI RIVER
0
50
km

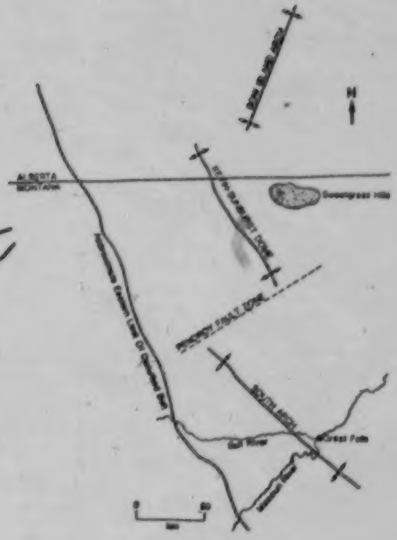
N
ALBERTA
MONTANA
Sweetgrass Hills
SOUTH ARCH
Sun River
Great Falls

FIGURE III-8(A): Gutter cast and numerous flute marks on the sole of a GUP laminated bed.

FIGURE III-8(B): Directional scour fill (current flowed from left to right).

FIGURE III-8(C): Deep, rippled scoured surfaces incised into the top of GUP laminated beds.

D
A
C

# PALAEOSHORELINE AND LITHOLOGIC UNIT MAPPING OF THE BOOTLEGGER MEMBER, NORTH-CENTRAL MONTANA

## INTRODUCTION

Many Mesozoic lithologic sequences of the Western Interior of North America show a vertical pattern marked by a coarsening-upward grain size, amalgamation of sandstone and/or conglomerate beds and a change in the nature of bioturbation structures. Such sequences are capped by finer-grained, commonly bioturbated, sandstone and shale. These trends have traditionally been interpreted as representing shoaling conditions associated with regression followed by a rapid deepening associated with transgression. Many coarsening-upward sequences are reported to represent offshore-tapering wedges of regressive shoreline-attached sandstone. The regressive pulses are separated by transgressions, and as such represent stacked ancient "graded shelf" (Johnson, 1919) sequences. Other coarsening-upward sequences are stratigraphically more discrete, occurring as numerous, isolated sand bodies, with a more patchy distribution. These include the stratigraphically isolated reservoir sandstones of the Cardium and Viking formations of south-central Alberta. These latter sequences were deposited under low-stands of sea level, followed by a sea level rise, and represent isolated deposits of a regressive-transgressive pulse (Cant and Hein, 1986). Whether the styles of shelf sedimentation are patchy or more widespread, the lateral distribution and continuity of facies patterns in such coarsening-upward sequences have not been well documented (Atkinson *et al.*, 1986; Cant, 1984; Leckie and Walker, 1984; Plint and Walker, 1987; Rice, 1984; Walker, 1983). This is particularly true for the more amalgamated, storm and shoal deposits at the top of many of these sequences.

The present study concerns a detailed lithologic analysis of shallow, marine coarsening-upward sequences in the vicinity of Great Falls and at Mt. Lebanon in the Sweetrass Hills of north-central Montana. These sequences are superbly exposed in long buttes and afford ample opportunity for detailed lithologic analysis. Of particular interesting is the ability to delineate the temporal sedimentary history and position of shorelines and shoreline-attached clastic wedges. The purpose of this paper is to outline, in both time and space, the lithologic development of the many sandstone units making up the Bootleger Member of the Blackleaf Formation in north-central Montana.

## REGIONAL GEOLOGY

In the vicinity of Great Falls, and within the Sweetgrass Hills of north-central Montana, late Aptian to early Cenomanian clastic strata are exposed (Fig. 1). Since the beginning of the century several studies have been conducted on these Lower Cretaceous and early Upper Cretaceous strata (Fisher, 1907; Steginger, 1918; Collier, 1929; Cobban, 1951; Cobban *et al.*, 1959, 1976; Cannon, 1966). However, since the work of Cobban *et al.* (1959, 1976) these strata have been formally subdivided into the; Kootenai, Blackleaf and Marias River formations (Fig. 2). The Kootenai Formation, equivalent to the upper portion of the Mannville and Blairmore groups of Alberta, is regionally extensive and is easily recognised in the field by its reddish colouration. Numerous features of these strata indicate terrestrial deposition (Cobban *et al.*, 1959, 1976; Cannon, 1966; Hopkins, 1985). Unconformably overlying the Kootenai is the Blackleaf Formation (Cobban *et al.*, 1976; Cannon, 1966). This formation was originally called the Blackleaf Sandy Member by Stebinger (1918) because of its anomalous sandstone content compared with equivalent strata in eastern Montana. Later work by Cobban and others elevated this member to formational status and in north-central Montana subdivided it into four members. These are from bottom to top: Flood, Taft Hill, Vaughn and Bootlegger members. At the top of the uppermost

Bootlegger Member there outcrops a regionally extensive unit characterised by an anomalous abundance of fish remains. This unit has been termed the Base of the Fish Scales by petroleum geologists in Canada and it represents a synchronous marker extending for more than 1100 km from north to south (Stelck and Armstrong, 1981; Arnott and Hein, in review). The fish scale unit represents an unconformity separating the Bootlegger Member and the early Upper Cretaceous Floweree Member of the Marias River shales.

Recently, Vuke (1984) developed a regional depositional model for Lower Cretaceous strata in this part of the northwestern United States; this model resembles others constructed for equivalent strata in the Western Interior Seaway (Weimer, 1984; Merewether and Cobban, 1986). These models relate sedimentation episodes, represented by individual formations and members, to transgressive and regressive events. Such events occur on two different scales; (1) a mega-scale, where depositional patterns within the entire seaway are affected; being similar to the supercycles of Vail *et al.* (1977) ; and (2) a micro-scale, where the effect is only locally illustrated. Two basin-wide transgressions which occurred between upper Albian to lower Turonian time have been recognised in Cretaceous strata of the western United States (Kauffman, 1977, 1985). The older of these events has been called the Kiowa-Skull Creek Cyclothem (Kauffman *et al.*, 1977) and the younger, the Greenhorn Cyclothem (Hattin, 1964). It should also be noted that these two events have been documented on a global scale (Vail *et al.*, 1977).

In north-central Montana these two major, basin-wide events are recorded in strata making up the Blackleaf Formation. The initial development of marine conditions associated with the early transgressive stage of the Kiowa-Skull Creek Cyclothem is identified by marine deposits of the Flood Member which unconformably overlie terrestrial deposits of the Kootenai Formation. The subsequent regressive stage is first evidenced by the restricted marine conditions of the glauconitic Taft Hill Member (Cobban, 1951; Vuke, 1984). Continued regression eventually culminated in development of the terrestrial deposits of the bentonitic Vaughn Member. Transgression associated with the early stages of the Greenhorn Cyclothem resulted in the return of marine conditions to north-central Montana and the deposition of the marine Bootlegger Member. Continued transgression into the early Upper Cretaceous lead to the deposition of deep basinal shales composing the Floweree Member of the Marias River shales (Vuke, 1984). Superimposed on these large-scale events are smaller transgressive/regressive episodes observed in each of the members making up the Blackleaf Formation. These smaller-scale events suggest a local control on sediment deposition, and with specific reference to the Bootlegger Member is the topic of this paper.

## THE BOOTLEGGER MEMBER

Near Great Falls, the Bootlegger Member crops out along low-relief buttes, usually forming its cap rock. Strata are typically undisturbed; where the only major structural feature in this area is the South Arch, the southern element of the Sweetgrass Arch. This broad, gently northwestward plunging antiform is characterised by dips on its limbs of less than one degree (Cobban *et al.*, 1976) and consequently poses no problem in lateral stratigraphic correlations. In the Sweetgrass Hills, on the other hand, the Bootlegger Member, along with the entire Blackleaf Formation, is exposed in a river valley incised into the axis of a steep, northward plunging anticline which crops out on the northwest side of Mt. Lebanon (the easternmost peak in the Sweetgrass Hills). Structural deformation of Bootlegger Member strata in the Sweetgrass Hills and isolated areas near Great Falls was the result of uplift by post-depositional Tertiary intrusions.

By definition the Bootlegger Member is strictly marine (Cobban *et al.*, 1959, 1976) and represents the initial transgressive stage of the Greenhorn Cyclothem into this area of the western Cretaceous Seaway. To the west the Bootlegger Member onlaps terrestrial deposits of the Vaughn Member and merges to the east with deep basinal shales of the Mowry Member (Cobban *et al.*, 1959, 1976; Stelck and Armstrong, 1981). The occurrence of *Neogastroplites americanus* (Reeside and Cobban, 1960) dated at approximately 96 Ma (Folinsbee *et al.*, 1963), and the Clay Spur Bentonite which crops out at the top of the Mowry Shale Member in eastern Montana (Rubey, 1929, 1930) and dated 94 Ma (Folinsbee *et al.*, 1963), indicate a depositional period of approximately 2 (~± 1)million years for the Bootlegger Member.

In both the Great Falls and Sweetgrass Hills study areas the Bootlegger Member is characterised by stacked depositional sequences. In the Great Falls area there are five sequences compared with four in the Sweetgrass Hills (Fig. 3). Each sequence is composed of a thick basal unit indicating shoaling-upward depositional conditions. These are then bounded above and below by an erosional transgressive surface. Shoaling-up sedimentary conditions are the result of shoreline progradation usually caused by a sea level still-stand or drop, although similar conditions can develop during base-level rise when sediment influx is sufficiently large. Shoaling-upward deposition was terminated by a rise in relative sea level, its associated marine transgression and deposition of a transgressive lag deposit.

The cyclic nature of Bootlegger deposition has been suggested to be the result of episodic reactivation of the ancestral Sweetgrass Arch. In the Great Falls study area the crest of the southern element of the Sweetgrass Arch, the South Arch, lies immediately to the southwest while the crest of the northern element, the Kevin-Sunburst Dome, lies to the west of the Sweetgrass Hills study area (Fig. 4). Periodic uplift and subsidence of the arch, thought to be respectively associated with episodes of active and reduced Cordilleran thrusting, is interpreted to be the underlying cause of cyclic sedimentation characterising the Bootlegger Member (Arnott, 1987). Relative sea level drop and the associated shoreline progradation is interpreted to be contemporaneous with arch uplift, whereas a relative sea level rise and its transgression reflect subsequent arch subsidence. In addition, throughout

Bootlegger time the strandline was either within or close to the Great Falls area. Because of this fact, the closeness of the crest of the Sweetgrass Arch precluded the necessity for large vertical movements in order to produce marked changes in the pattern of local sedimentation.

## SEDIMENTARY ANALYSIS OF THE BOOTLEGGER SEQUENCES

Bootlegger sequences are characterised by a thick regressive sequence commonly bound above and below by typically planar transgressive surfaces and associated thin transgressive lags. Sequences range from several metres to a few tens of metres thick, and in the Great Falls area consistently thicken northeastward . Also in the Great Falls area, the undisturbed nature of the strata enables one to follow many of these sequences laterally for many tens of kilometres. In the idealised sequence (Fig. 5) the regressive portion of each sequence reflects the eastward progradation of the strandline and the vertical stacking of shallow-offshore shelf to shoreface to beachface deposits. However, this sequence is rarely observed in its entirety for two possible reasons:

(1) progradation of the shoreline did not extend across the entire area, resulting in an incomplete sequence; and/or

(2) the upper portion of the regressive sequence was removed erosively during progradation and/or the subsequent transgression.

Nonetheless, the lithologic and biogenic characteristics of each sedimentary unit composing the idealised Booltlegger sequence, in ascending order, are discussed below. Each unit is named after the dominant constituent lithofacies.

## UNIT 1: Interbedded grey-black shale and siltstone

Unit 1 is made up of grey-black bentonitic shale and thin siltstone interbeds (Fig. 6A), and because of its recessive weathering is rarely exposed. Siltstone interbeds are typically 2.5-5.0 cm thick, although they become thicker (10-15 cm), coarser (fine sandstone) and more abundant with stratigraphic height. Current ripple cross-stratification is the most abundant sedimentary structure in these beds, but oscillation ripples, gently undulating parallel lamination (Arnott, in preparation) and hummocky cross-stratification (Harms *et al.*, 1975)(Fig. 6B) are common. Palaeoflow directions are typically toward the southeast in the Great Falls area and toward the northeast in the Sweetgrass Hills, although southwest directions are common at both localities.

Biogenic structures also show a demonstrable change stratigraphically-upward, reflecting changes in the nature of the substrate. In the lower, shale-rich portion of Unit 1 *Teichichnus, Planolites montanus* and *Chrondrites* are dominant. However, with increasing stratigraphic height sand-inhabiting structures show a progressive increase in abundance and diversity, including: *Palaeophycus, Thalassinoides, Skolithos, Cylindrichnus, Bergauria, Ophiomorpha* and *Asterosoma* .

Interpretation:

Unit 1 is interpreted to be deposited in a shallow-offshore shelf environment. This environment is characterised by quiet depositional conditions which are, however, episodically interrupted by brief, high-energy events. Deposition of bentonitic shales dominated during the pervasive low-energy conditions, whereas the interbeds of siltstone and sandstone reflect deposition from the high-energy events. Thickening, coarsening and increasing abundance of siltstone and particularly sandstone interbeds stratigraphically-upward indicates shoaling conditions with a progressive increase of physical energy. Similarly, the upward change from shale-dominant to sand-dominant biogenic structures indicates a progressive enrichment of the sand content.

Siltstone/sandstone interbeds are common features of shallow-offshore shelf environments, and as pointed out above, are deposited during episodic high-energy events. These events are thought to be associated with surface storms capable of producing large surface gravity waves and coastal set-up. Kulm *et al.* (1975) point out that the influence of large surface waves can be detected at depths of over 200 metres, and are probably responsible for the generation of the symmetric oscillation ripples observed in Unit 1. Also observed are asymmetric ripples showing offshore and less commonly onshore transport. Onshore-migrating ripples may represent asymmetric wave ripples developed under shoaling surface waves with the preferred landward transport of bottom sediments, however, offshore-migrating ripples, on the other hand, require a different mechanism (see below).

Hummocky cross-stratification (HCS) has commonly been reported from ancient shallow-offshore shelf deposits (Harms *et al.*, 1975; Hamblin and Walker, 1979; Dott and Bourgeois, 1982; Leckie and Walker, 1982; Hein *et al.*, 1986) and is thought to have been produced by combined flow associated with intense storm events (Hunter and Clifton, 1981; Swift *et al.*, 1983; Duke, 1985). Gently undulating parallel lamination (GUP lamination) has been suggested to have been deposited from unidirectionally-dominated combined flow associated high nenergy storm events (Arnott, in review). Stratigraphically-upward, the loss of HCS and the concomitant appearance of GUP lamination is interpreted to indicate the shoaling-upward increase in the unidirectional flow component during storm events. This observation ultimately reflects shoaling-upward conditions, or more appropriately, the approach of the prograding palaeoshoreline.

## UNIT 2: Gently undulating parallel laminated sandstone

Normally Unit 2 lies gradationally above deposits of Unit 1, although in one instance (the Ulm Pishkun) this contact is knife-sharp, forming a distinct overhang (Fig. 6C). Beds of Unit 2 are composed of fine-grained sandstone dominated by gently undulating parallel lamination (GUP lamination) (Fig. 6D), a feature which is discussed in detail in Arnott (in review). These beds are typically 5-60 cm thick, commonly interbedded with 5-30 cm of interbedded rippled sandstone and shale. Beds composed of GUP lamination are characterised by a thick basal portion of gently undualting parallel lamination capped with a thin < 1-3 cm cap of current ripple cross-stratification or wave ripples. Basal contacts are always wavy with metre-spacing and minor (1-3 cm) amplitude. GUP lamination is characterised by a subdued undulation of what may appear to be upper-plane-bed lamination. Spacing of the undulation is variable, ranging from decimetres to several metres, even along the same lamina, and amplitudes which rarely exceed 3 cm (typically 1-1.5 cm). Ripple cross-stratification capping these beds is usually directed toward the southeast (offshore), however, southwest directions are also commonly observed. Basal scour features include: basal scours, flutes, grooves prod marks and rare gutter casts. Parting lineation is also a common feature on exposed bedding planes of GUP lamination.

Strata of Unit 2 contain the most abundant and diverse trace fossil assemblage. Most trace fossils indicate the pervasively sandy nature of these strata, although *Teichichnus* and *Planolites montanus* can be found in the interbedded rippled sandstone and shale units. The common biogenic structures of Unit 2 include: *Thalassinoides, Ophiomorpha, Skolithos, Cylindrichnus, Arenicolites, Diplocraterion, Asterosoma, Bergauria, Lockeia, Palaeophycus, Polycladichnus, Planolites* and Escape Structures.

Interpretation:

The characteristic physical and biogenic sedimentary structures of Unit 2 are interpreted to reflect a lower-shoreface depositional environment. As discussed above GUP lamination is thought to reflect deposition from a offshore-flowing, unidirectionally-dominated combined flow generated during high-energy storm events. Parting lineation and the parallel lamination suggest that these flows were capable of generating upper-plane-bed conditions in the fine-grained sand, although the origin of the undulation is not understood (Arnott, in preparation). Ripple cross-stratification capping the GUP lamination and exhibiting southeast palaeoflow directions implies deposition during the waning stages of this offshore-flowing current. Consequently, beds containing GUP lamination would appear to resemble a Bouma BC turbidite (Bouma, 1962)). Asymmetric ripples which exhibit southwest palaeocurrent directions plus symmetric oscillation ripples are probably the product of surface gravity waves, however, the former implies the generation of unidirectional onshore sediment transport by shoaling waves.

## UNIT 3: Medium-scale, cross-stratified sandstone

Unit 3 rests sharply above Unit 2 and is dominated by medium-scale cross-stratified fine- and less commonly medium-grained sandstone (Fig. 6E). Trough cross-stratification is by far the most common; planar-tabular cross-stratification is rare. Trough cross beds typically dip < $20^{\circ}$-$25^{\circ}$, but this is probably the result of the removal of the upper portion of the bedform by post-depositional reworking. The common occurrence of back-flow ripples along trough crossbed toe-sets indicates the original existence of a relatively high bedform which enabled the development of flow separation. Also making up this unit, although much less abundant than the medium-scale cross-stratified sandstones, are beds characterised by

GUP lamination with ripple caps. Palaeocurrents from both medium-scale cross-stratification and ripples indicate a pervasive northwest sediment transport. Rare interbeds of interbedded rippled sandstone and shale plus dispersed chert pebbles and granules are commonly observed.

Biogenic structures are markedly less abundant and diverse compared with strata of Unit 2. Once again, however, trace fossils indicate a pervasive sandy substrate and include: *Palaeophycus, Planolites, Ophiomorpha, Thalassinoides, Skolithos, Bergauria* and *Lockeia*.

Interpretation:

Unit 3 is interpreted to have been deposited in an upper-shoreface environment. The dominant source of physical energy in this portion of the shoreface is provided by shoaling waves (Clifton *et al*., 1971; Clifton, 1981). This process preferentially transports sediment in the direction of wave propogation and in the case of Unit 3 beds was of sufficient strength to produce medium-scale, transverse-to-flow bedforms. Similar structures have been reported from other ancient upper shoreface sequences (Vos and Hobday, 1977; Clifton, 1981; Dupre, 1984). Interbeds of GUP lamination suggest episodes of even higher energy probably associated with storms during when upper-plane-bed conditions temporally interrupted the development of shoreward-migrating, large-scale bedforms.

UNIT 4: Massive and planar-laminated sandstone

Unit 4 is observed only at the top of the Ulm Pishkun , Little Belt Creek and Willow Creek sections. This unit rests sharply above Unit 3 and is composed of massive or planar-laminated fine-grained sandstone (Fig. 6F). Bioturbation is rare and is dominated by *Planolites montanus*. At the Ulm Pishkun section a thick unit of Unit 4 indicates that the laminated sandstones are arranged in a number of sets showing low-angle, erosive contacts with adjacent and subjacent sets. At most localites Unit 4 is capped by a planar surface overlain by Unit 1 or Unit 5 lithologies.

Interpretation:

The association of Unit 4 with the underlying deposits of the upper shoreface (Unit 3) suggests a foreshore depositional environment for these strata. Sets of planar-laminated sandstone are indicative of swash lamination (Clifton *et al.*, 1971) , a common feature in both ancient (Dupre, 1984; DeCelles, 1987) and modern foreshore settings (Clifton *et al.*, 1971; Howard and Reineck, 1981). Its upper planar contact with Unit 1 lithologies, or the planar or wavy contact with coarse-grained Unit 5 strata is interpreted as a transgressive surface. This surface represents the erosive planation and possible removal of part of the upper portion of the regressive sequence during a rise of relative sea level. Lithologic contacts of this nature have been discussed by Goodwin and Anderson (1985), and is one of the main components of their punctuated aggradational cycles.

## UNIT 5: Anomalous deposits

Exposures of Unit 5 abruptly outcrop above any of the other lithologic units, thereby interrupting the idealised Unit 1 to Unit 4 shoaling-upward sequence. Its contact with strata of the underlying unit is commonly planar, although rare wavy and channelled contacts are observed. Deposits of Unit 5 are very distinctive, exhibiting anomalous lithologic characterisitics which differentiate them from the underlying strata of the shoaling-upward sequence. In the uppermost deposits of the Bootlegger Member, Unit 5 strata are characterised by anomalous concentrations of fish remains, typically fish scales and bones. Also associated with this unit are many of the hard-body fossils observed in the entire Bootlegger Member, including *Neogastroplites americanus* , *Posidonia nahwasi nahwasi* and *Epengonoceras* (Dr. C.R. Stelck, pers. comm. 1987). In two of the Bootlegger sequences Unit 5 deposits are anomolously coarse-grained, particularly in Sequence 3 where deposits of Unit 5 are composed of black chert pebbles. This conglomerate is characterised by a crudely graded clast- or matrix-supported framework and typically crops out above a symmetrical, wavy surface molded into the top of the underlying fine-grained sandstones of Unit 3. These wavy features are characterised by an average wavelength and amplitude of 1 metre and 7 cm respectively and a crestline typically oriented north-south (Fig. 7A). Most Bootlegger Member strata atr typically quartzose, although some Unit 5 lithologies are highly feldspathic.

Interpretation:

Deposits of Unit 5 are thought to reflect deposition during the transgressive events which bring to an end the regressive (progradational) portion of each Bootlegger sequences. Transgression usually led to the erosive removal of an unknown amount of the underlying regressive sequence and to the deposition of the anomalous deposits characterising Unit 5.

In Bootlegger sequences 3 and 5, transgressive deposits of Unit 5 are anomalously coarse-grained and lie directly above an erosive transgressive surface. Chert pebbles and chert-granule sandstone characterise each, respectively. Coarse-grained deposits are common features of transgressive events and are termed transgressive lags. Commonly lag deposits show crude normal grading, particularly with respect to the coarsest-grained clasts, which are invariably concentrated on the underlying transgressive surface. Typically transgressive surfaces are planar, although at some locations this surface is characterised by a wave-like feature molded into the underlying fine-grained sandstones of the regressive sequence (Fig. 7A). This latter feature, characterised by straight-crested symmetrical waves with 1 metre wavelength and 7 cm amplitude, is thought to represent an erosive transgressive surface molded by large-scale oscillatory waves. Crestlines of these symmetric waves are oriented generally north-south, an orientation which is approximately parallel to the palaeoshoreline. Once developed, this surface was mantled by the chert pebbles and thus was isolated from further erosion. Larger pebbles are concentrated on the seaward (eastward) side of each of the wave crests, and most pebbles are oriented with their longest-axis parallel to the wave crestline.

Highly feldspathic, coarse-grained Unit 5 strata are observed at the Black Horse Lake section. This two metre thick, typically massive arkose, although faint medium-scale cross bedding can be commonly seen, outcrops as a channel-fill incised into Unit 1 strata (Fig. 7B). However, the high feldspar content and coarseness of the channel-fill are lithologic characterisitics of terrestrial Vaughn Member strata west of the Great Falls study area. Consequently, these channel-filling strata may represent deposition of terrestrial, fluvial deposits associated with shoreline progradation, and thus differ from other Unit 5 strata which are associated with transgression. This channel-fill deposit may provide an estimate of the minimum distance of shoreline progradation associated with the regression.

The uppermost strata of the Bootlegger Member are characterised by an anomalous concentration of fish remains, usually fish bones and scales, and contain virtually all of the observed hard-body fossils. Similar anomalous fish bone concentrations make up the "White Specks" horizons observed in Upper Cretaceous strata of western Canada. These fish scale horizons are thought to reflect depositional hiatuses which resulted in long-term reworking and concentrating of fish and hard-body fossil remains.

## RECONSTRUCTION OF THE BOOTLEGGER SEQUENCES

The Bootlegger Member is made up of a number of sedimentary sequences. Each sequence is composed of a thick regresive or shoaling-up unit which is overlain by a transgressive surface and/or lag deposit. The regional nature of the Bootlegger sequences, observed in the two study areas separated by approximately 200 km, would suggest that the shoaling-upward portion of each sequence is primarily related to shoreline progradation and only secondarily influenced by local sediment source controls (*eg*. delta lobe switching, channel avulsion *etc*.). Each regressive event, probably associated with a still-stand or fall in relative sea level, resulted in the eastward progradation of the local strandline. Progradation was then terminated by a relative sea level rise which caused a westward migration of the local shoreline. The repetitive nature of Bootlegger sedimentation is thought to indicate episodic uplift and subsidence of the Sweetgrass Arch and its effect on relative sea level.

Reconstruction of the palaeoshoreline positions associated with each of the Bootlegger sequences depends on several pieces of evidence:

(1) completeness of the regressive sequence;
(2) nature of the transgressive surface;
(3) characteristics of the transgressive lag deposit (if present);
(4) nature of the deposits overlying each sequence.

Using these features an approximate determination of the minimum limit of eastward strandline progradation during each Bootlegger sequence has been made. Unfortunately, in the Sweetgrass Hills the shallowest-water deposits characterising the regressive portion of each Bootlegger Sequence are those describing the lower shoreface (Unit 2). Directly overlying these deposits are strata of Unit 1, indicating the return of shallow-offshore shelf deposition. Consequently, in the Sweetgrass Hills area the shoreline was located to the west throughout Bootlegger time, although it did show at least three periods of eastward progradation. In the Great Falls area, on the other hand, Bootlegger strata indicate that the shoreline often migrated significant distances across many parts of the study area. The following is a summary of the reconstructed positions of the palaeoshorelines in the Great Falls study area throughout Bootlegger Member time.

## SEQUENCE 1:

Sequence 1, or what can be more appropriately termed "basal Bootlegger", represents the initial incursion of marine conditions associated with the Greenhorn Cyclothem into this area of the western Cretaceous Seaway. Outcrops of this sequence can be observed at Black Horse Lake (1) and Belt Butte (2) and isolated areas east of Belt Butte (3) (Fig. 8A). At each of these areas (presented below by the number given above) strata are characterised by:

(1): Unit 1 strata overlain by a coarse-grained, arkosic channel fill which in turn is overlain by Unit 1 strata;

(2): Unit 1 to Unit 3 which is overlain by a thin veneer of Unit 5 pebbles which is overlain by Unit 1 deposits;

(3): Unit 1 to Unit 2 overlain by Unit 1 strata.

The occurrence of Unit 1 strata above the Vaughn Member throughout the study area would indicate that at the beginning of Sequence 1 the Bootlegger shoreline was located some distance to the west. However, during Sequence 1 the strandline migrated eastward depositing the shoaling-upward deposits observed at all three study localities. Progradation was terminated by the westward displacement of the shoreline at the close of Sequence 1, and deposition of Unit 1 strata over the entire study area (Fig. 8A, 8B).

The coarse-grained, arkosic channel-fill at Black Horse Lake may represent terrestrial fluvial deposition associated with shoreline progradation. If this is correct then this would provide a minimum distance of eastward shoreline progradation during the regression.

## SEQUENCE 2:

Sequence 2 crops out at the Ulm Pishkun (1), Belt Butte (2), Little Belt Creek (3) and Black Horse Lake (4) (Fig. 8C) and at each location is characterised by:

(1): complete Unit 1 to Unit 4 sequence which is truncated by a planar surface

(2) Unit 1 strata overlain by a thin deposit of Unit 2 beds;

(3) only Unit 1 deposits;

(4) only Unit 1 deposits;

and at all locations Sequence 2 strata are overlain by Unit 1 deposits.

The occurrence of Unit 1 at the base of Sequence 2 at all localities suggests that at the onset of Sequence 2 time the shoreline was some distance to the west of the Great Falls area. The complete Unit 1 to Unit 4 sequence observed at the Ulm Pishkun, although indicates that during this time the shoreline prograded at least that far east. The deposition of Unit 1 strata over the entire area indicates that at the close of Sequence 2 time the shoreline was once again west of the Great Falls area.

## SEQUENCE 3:

Strata of Sequence 3 are well exposed in much of the Great Falls study areas. Excellent exposures are present along the Missouri River canyon near Carter (1) and as the lower resistant ridge exposed on many hillsides in the area near Belt (2). Other areas of exposure include North Willow Creek (3) and Gordon (4) (Fig. 8E).

(1) shoaling-upward sequence of Unit 1 to Unit 3 which is sharply overlain by Unit 1;

(2) complete sequence of Unit 1 to Unit 4 sharply overlain by a wavy contact and chert pebble conglomerate capped with Unit 1 strata;

(3) and (4) Unit 1 sharply overlain by chert pebble conglomerate which in turn is overlain by Unit 1 deposits.

The occurrence of Unit 1 deposits at the base of Sequence 3 over the entire area suggests that at the beginning of Sequence 3 the strandline was located to the west of the study area (Fig. 8E, 8F). The presence of chert pebble conglomerates as far east as Belt and the occurrence of Unit 3 beds at Carter would imply that during Sequence 3 the strandline migrated almost across the entire Great Falls study area (Fig. 8F). The regionally extensive chert pebble conglomerate bed is probably the result of transgressive reworking of beach or possibly fluvial gravels initially deposited during the regressive portion of Sequence 3. The occurrence of the chert pebble conglomerate unit above Unit 1 deposits at North Willow Creek and Gordon would suggest that prior to conglomerate deposition extreme erosion had resulted in the complete removal of all previously deposited shoreface and stratigraphically higher deposits. The timing of this erosion is uncertain, but it may imply possible terrestrial down-cutting during progradation and/or erosive removal during marine transgression. Nonetheless, the occurrence of Unit 1 above Unit 5 conglomerates across the entire study area indicates a rise in relative sea level, transgression and the eventual positioning of the strandline beyond the study's western boundary.

## SEQUENCE 4:

Sequence 4 crops out extensively in the Great Falls area. Thick, vertical outcrops of this sequence are well exposed along the Missouri River canyon near Carter (1), at Gordon (2) and Highwood (3) (Fig. 8G). In the area near Belt (4), strata of Sequence 4 outcrops as a long linear ridge lying above and parallelling the resistant regressive portion of Sequence 3.

(1) Unit 1 to Unit 3 overlain by black-chert-granule sandstone which is in turn overlain by

shale-rich Unit 1 strata with fish scales and bones;

(2) Unit 1 overlain by chert-granule sandstone beds with abundant fish scales overlain by Unit 1 shale-rich strata;

(3) Unit 1 strata overlain by shale-rich Unit 1 strata with fish bones and scales;

(4) Unit 1 to Unit 2 strata overlain by shale-rich Unit 1 strata with fish scales and bones.

Reconstruction of palaeoshoreline positions during Sequence 4 are not as straight forward as in Sequences 1, 2 and 3. Much of the uncertainty stems from the possible erosive bevelling associated with the Base of Fish Scales unit and the development of a condensed stratigraphic section (discussed in more detail in Sequence 5). Nonetheless, the presence of Unit 1 strata at the base of Sequence 4 across the entire study area indicates that at least at the onset of Sequence 4 the strandline was some distance to the west (Fig. 9A, 9B). During Sequence 4, however, the strandline migrated east. The occurrence of Unit 3 and chert-granule sandstone at the Carter and Belt area sections suggests that the shoreline may have prograded close to or beyond these areas, with the chert-granule sandstone representing a Unit 5 transgressive lag deposit (Fig. 9B). However, the lack of the chert-granule sandstone at Highwood and the presence of only Unit 1 strata may indicate the existence of a deep basin between the Carter and Belt areas throughout Sequence 4 time (Fig. 9A).

Interestingly, the Unit 5 chert-granule sandstone cropping out at Gordon is composed of abundant fish scales and bones, a characteristic not exhibited by the other granule sandstones observed at the top of Sequence 4. In addition, the Unit 1 strata overlying the Unit 5 deposits at Gordon are devoid of fish scales and bones, a condition which is not observed at the other study locations. As will be pointed out in the Sequence 5 discussion, Unit 5 chert-granule sandstone strata at Gordon are equivalent to fish-bearing, chert-granule sandstones which in the eastern portion of the Great Falls study area crops out above Sequence 4. Consequently, the Gordon section represents a condensed stratigraphic section, possibly related to post-depositional erosion. The lack of fish remains in Unit 1 shales overlying the Unit 5 sandstone at Gordon is characteristic of the Floweree Member shales. The presence of fish scales in Unit 1 strata elsewhere suggests that these latter strata are "Bootlegger" but the former are not, thereby supporting the interpretation of a condensed section .

## SEQUENCE 5:

Sequence 5 rarely crops out in the Great Falls study area, a feature which may be the result of an erosional unconformity separating the Bootlegger Member and the overlying Floweree Member of the Marias River Formation. At the Willow Creek Ranch Section (1), large allochthonous pieces of chert-granule sandstone with abundant fish remains (Unit 5 strata) can be found on the grassy slopes above Sequence 4. Cannon (1966), reports that these strata crop out approximately 30 metres above the "E" sand (equivalent to Sequence 4), although they were never found in place in this study. Outcrops of Sequence 5 are observed at the Missouri River section near Carter (2) and Highwood (Fig. 9C, 9D). At both areas strata are poorly exposed, but when visible are dominated by Unit 1 strata with abundant bentonite interbeds. The lack of the fish-bearing, chert-granule sandstones may only be a consequence of the limited vertical extent of these latter exposures.

The occurrence of Unit 1 strata above Sequence 4 would imply that at the onset of Sequence 5 the strandline needed to be west of the Great Falls area. On the other hand, the presence of the chert-granule sandstone at the top of Sequence 5 suggests that with time the strandline migrated east. The presence of the deep basinal, non-fish-bearing shales of the Floweree Member capping Sequence 5 strata over the entire Great Falls study area indicates a dramatic depositional deeping and an associated westward displacement of the local shoreline.

The fish-bearing, chert-granule sandstone at the top of Sequence 5 forms the Base of the Fish Scales unit in the Great Falls study area, and as mentioned earlier may represent an unconformity. The occurrence of these Unit 5 strata 30 metres above Sequence 4 strata in the eastern portion of the Great Falls areas, and their occurrence above an abbreviated Sequence 4 section in the western study area, may support this interpretation. Consequently, the lack of section in the west may reflect a greater erosive bevelling of pre-existing strata and the development of a more condensed stratigraphic section compared with that characterising the stratigraphic record in the east. The observed stratigraphic height variation exhibited along the Base of the fish Scales marker within the Great Falls study area suggests that ~~its~~ use as a stratigraphic datum, particularly for small-contour isopach or structure maps may be a poor choice.

## CONCLUSIONS

The Bootlegger Member represents the initial development of marine conditions associated with the early transgressive stages of the Greenhorn Cyclothem into north-central Montana. Initially transgression resulted in the drowning of the underlying terrestrial deposits of the bentonite-rich Vaughn Member and deposition of the Bootlegger Member. However, with time transgression eventually culminated in deposition of the deep basinal shales of the Upper Cretaceous Floweree Member of the Marias River Formation.

In both the Great Falls and Sweetgrass Hills study areas, the Bootlegger Member is characterised by a number (five and four respectively ) of shoaling-upward sedimentary sequences, all sharply truncated on their upper surface. Shoaling-upward deposition was associated with eastward strandline progradation during a still-stand or fall in relative sea level. These conditions were terminated by a rise in relative sea level and the westward migration of the local shoreline. The recurring nature of Bootlegger deposition is thought to be related to uplift/subsidence of the ancestral Sweetgrass Arch and its controlling influence on relative sea level.

Lithologic and biogenic analysis of Bootlegger Member strata enabled it to be sub-divided into five sedimentary units, interpreted to represent five depositional environments. Analysis of the vertical and lateral relationships existing among these units indicates that in the Great Falls study area the Bootlegger Member is composed of five distinct shoaling-upward sequences. Detailed analysis of the strata making up each Bootlegger sequence enabled the delineation of shoreline position at the beginning and end of each sequence, as well as its approximate progradational limit.

The marked difference in stratal thickness between the western and eastern portions of the Great Falls study area may be a consequence of erosive bevelling associated with an unconformity responsible for the development of the Base of the Fish Scales unit. Consequently, the use of this marker unit as a stratigraphic datum, particularly for small-contour isopach and structure maps, may be in error. Deposition following this unconformity resulted in the regional emplacement of deep basinal shales composing the early Upper Cretaceous Floweree Member of the Marias River Formation.

# REFERENCES

Arnott, R.W., 1987. Stratigraphy of the Lower Cretaceous Bootlegger Member near Great Falls, Montana and its relationship with the ancestral Sweetgrass Arch. Geological Association of Canada, Program with Abstracts, p. 22.

Atkinson, C.D., Goesten, M,J,B,G., Speksnijder, A., van der Vlugt, W., 1986. Storm-generated sandstones in the Miocene Miri Formation, Seria Field, Brunei (N.W. Borneo). *In* Knight, R.J., McLean, J.R., eds., Shelf Sands and Sandstones. Canadian Society of Petroleum Geologists Memoir No. 11, pp. 213-240.

Bouma, A.H., 1962. Sedimentology of some flysch deposits. Elsevier, Amsterdam, 168 p.

Cannon, J.L., 1966. Outcrop examination and interpretation of paleocurrent patterns of the Blackleaf Formation near, Great Falls, Montana. Billings Geologic Society Guidebook, 17th annual field conference, pp. 71-111.

Cant, D.J., 1984. Development of shoreline-shelf sand bodies in a Cretaceous epeiric sea deposit, Journal of Sedimentary Petrology, v. 54, pp. 541-556.

Cant, D.J., Hein, F.J., 1986. Depositional sequences in ancient shelf sediments: Some contrasts in style. *In* Knight, R.J., McLean, J.R., eds., Shelf Sands and Sandstones. Canadian Society of Petroleum Geologists Memoir No. 11, pp. 303-312.

Clifton, H.E., 1976. Wave-formed sedimentary structures - a conceptual model. *In* Davies, R.A., Jr., Ethington, R.L., eds., Beach and Nearshore Sedimentation. Society of Economic Paleontologists and Mineralogists Special Publication No. 24, pp. 126-148.

------, 1981. Prograding sequences in Miocene shoreline deposits, southeastern Caliente Range, California. Journal of Sedimentary Petrology, v. 51, pp. 165-184.

Clifton, H.E., Hunter, R.E., Phillips, R.L., 1971. Depositional structures and processes in the non-barred high-energy nearshore. Journal of Sedimentary Petrology, v. 41, pp. 651-670.

Cobban, W.A., 1951. Colorado Shale of central and northwestern Montana and equivalent rocks of Black Hills. American Association of Petroleum Geologists Bulletin, v. 35, pp. 2170-2198.

Cobban, W.A., Erdmann, C.E., Lemke, R.W., Maughn, E.K., 1959. Revision of Colorado Group on Sweetgrass Arch, Montana. American Association of Petroleum Bulletin Geologists, v. 43, pp. 2786-2796.

--------, 1976. Type sections and stratigraphy of the members of the Blackleaf and Marias River Formations (Cretaceous) of the Sweetgrass Arch, Montana. U.S.G.S. Professional Paper 974, 66 p.

Collier, A.J., 1929. The Kevin-Sunburst oil field and other possibilities of oil and gas in the Sweetgrass Arch, Montana. U.S.G.S. Bulletin 812-B, pp. 57-87.

DeCelles, P.G., Variable preservation of Middle Tertiary, coarse-grained, nearshore to outer-shelf storm deposits in southern California. Journal of Sedimentary Petrology, v. 57, pp. 250-264.

Dott, R.H., (Jr.), Bourgeois, J., 1982. Hummocky stratification: significance of its variable bedding sequences. Bulletin of the Geologic Society of America, v. 93, pp. 663-680.

Duke, W.L., 1985. Hummocky cross-stratification, tropical hurricanes, and intense winter storms. Sedimentology, v. 32, pp. 167-194.

Dupre, W.R., 1984. Reconstruction of paleo-wave conditions during the Late Pleistocene from marine terrace deposits, Monterey Bay, California. Marine Geology, v. 60, pp. 435-454.

Fisher, C.A., 1907. The Great Falls Coal Field. U.S.G.S. Bulletin 316-C, pp. 161-173.

Folinsbee, R.E., Baadsgaard, H., Cumming, G.L., 1963. Dating of volcanic ash beds (bentonites) by the K-Ar method. National Academy of Science, National Research Council, Washington D.C., Nuclear Sciences Series, Report No. 38, pp. 70-82.

Goodwin, P.W., Anderson, E.J., 1985. Punctuated aggradational cycles: A general hypothesis of episodic stratigraphic accumulation. Journal of Geology, v. 93, pp. 515-533.

Hamblin, A.P., Walker, R.G., 1979. Storm-dominated shallow marine deposits: the Fernie-Kootenay (Jurassic) transition, southern Rocky Mountains. Canadian Journal of Earth Science, v. 16, pp. 1673-1690.

Harms, J.C., Southard, J.B., Spearing, D.R., Walker, R.G., 1975. Depositional environments as interpreted from primary structures and stratification sequences. Sociey of Economic Paleontologists and Mineralogists, Tulsa, Short Course No. 2. 161 p.

Hattin, D.E., 1964. Cyclic sedimentation in the Colorado Group of west-central Kansas. *In* Merriam, D.F., ed., Symposium on cyclic sedimentation, Kansas Geological Survey Bulletin, pp. 205-217.

Hein, F.J., Dean, M.E., DeIure, A.M., Grant, S.K., Robb, G.A., Longstaffe, F.J., 1986. The Viking Formation in the Caroline, Garrington and Harmatten Fields, western south-central Alberta: sedimentology and paleogeography. Bulletin of Canadian Petroleum Geology, v. 34, pp. 91-110.

Hopkins, J.C., 1985. Channel-fill deposits formed by aggradation in deeply-scoured, superimposed distributaries of the Lower Kootenai Formation (Cretaceous), Journal of Sedimentary Petrology, v. 55, pp. 42-52.

Howard, J.D., Reineck, H.E., 1981. Depositional facies of a high-energy beach-to-offshore sequence: Comparison with low-energy sequence. Bulletin of the American Association of Petroleum Geologists, v. 63, pp. 807-830.

Hunter, R.E., Clifton, H.E., 1982. Cyclic deposits and hummocky cross-stratification of probable storm origins in Upper Cretaceous rocks of the Cape Sebastian area, southwestern Oregon. Journal of Sedimentary Petrology, v. 52, pp. 127-143.

Johnson, D.W., 1919. Shore processes and shoreline development. New York, John Wiley and Sons, 585 p.

Kauffman, E.G., 1977. Geological and biological overview: Western Interior Cretaceous Basin.Mountain Geologist, v. 14, pp. 75-99.

------, 1985. Cretaceous evolution of the Western Interior Basin of the United States. *In* Pratt, L.M., Kauffman, E.G., Zelt, F.B., eds., Fine-grained deposits and biofacies of the Cretaceous Western Interior Seaway: evidence of cyclic sedimentary processes, Society of Economic Paleontologists and Mineralogists field guidebook No. 4, pp. IV-XIII.

-------, Cobb[illegible]n, W.A., Eicher, D.L., 1977. Albian through lower Coniacian strata, biostratigraphy and principals events, Western Interior United States. *In* Evenements de la Partie Moyenne du Cretace (Mid-Cretaceous events), Uppsala-Nice symposia, 1975-1976: Annales duMuseum d'Historie Naturelle de Nice, v. 4, pp. XXIII1-XXIII24.

Kulm, L.D., Roush, R.C., Harlett, J.C., Neudeck, R.H., Chambers, D.M., Runge, E.J., 1975. Oregon continental shelf sedimentation: Interrelationships of facies distribution and sedimentary processes. Journal of Geology, v. 83, pp. 145-175.

Leckie, D.A., Walker, R.G., 1984. Storm- and tide-dominated shorelines in the Cretaceous Moosebar-Gates interval - outcrop equivalents of Deep Basin gas trap in western Canada. Bulletin of the American Association of Petroleum Geologists, v. 66, pp. 138-157.

Merewether, E.A., Cobban, W.A., 1986. Biostratigraphic units and tectonism in the Mid-Cretaceous foreland of Wyoming, Colorado, and Adjoining areas. *In* Peterson, J.A., ed., Paleotectonics and Sedimentation. American Association of Petroleum Geologists Memoir 41, pp. 443-468.

Niedoroda, A.W., Swift, D.J.P., Hopkins, T.S., 1985. The shoreface. *In* Davis, R.A., ed. Coastal sedimentary environments. New York: Springer-Verlag, pp. 533-624.

Plint, A.G., Walker, R.G., 1987. Cardium Formation 8. Facies and environments of the Cardium shoreline and coastal plain in the Kakwa Field and adjacent areas, northwestern Alberta. Bulletin of Canadian Petroleum Geology, v. 35, pp. 48-64.

Reeside, J.B., Cobban, W.A., 1960. Studies of the Mowry Shale (Cretaceous) and contemperaneous formations in the United States and Canada. U.S.G.S. Professional Paper 355, 121 p.

Rice, D.D., 1984. Widespread, shallow-marine, storm-generated sandstone units in the Upper Cretaceous Mosby Sandstone, central Montana. *In* Tillman, R.W., Siemers, C.T., eds., Siliciclastic Shelf Sediments. Society of Economic Paleontologists and Mineralogists Special Publication No. 34, pp. 143-161.

Rubey, W.W., 1929. Origin of the siliceous Mowry Shale of the Black Hills region. U.S.G.S. Professional Paper 154, pp. 153-170.

------, 1930. Lithologic studies of fine-grained Upper Cretaceous sedimentary rocks of the Black Hills region. U.S.G.S. Professional Paper 165, pp. 1-54.

Stebinger, E., 1916. Possibilities of oil and gas in north-central Montana. U.S.G.S. Bulletin 641, pp. 49-91.

Stelck, C.R., Armstrong, J., 1981. Neogastroplites from southern Alberta. Bulletin of Canadian Petroleum Geology, v. 29, pp. 399-407.

Swift, D.J.P., Figueiredo, A.G. (Jr.), Freeland, G.L., Oertel, G.F., 1983. Hummocky cross-stratification and megaripples: a geological double standard. Journal of Sedimentary Petrology, v. 53, pp. 1295-1317.

Vail, P. R., Mitchum, R.M., Thompson, S., 1977. Seismic stratigraphy and global changes of sea level, Part 4: Global cycles of relative changes of sea level. *In* Payton, C.E., ed., Seismic stratigraphy - applications to hydrocarbon exploration, American Association of Petroleum Geologists Memoir 26, pp. 83-97.

Vos, R.G., Hobday, D.K., 1977. Storm beach deposits in the Late Palaeozoic Ecca Group of South Africa. Sedimentary Geology, v. 19, pp. 217-232.

Vuke, S.M., 1984. Depositional environments of the Early Cretaceous Western Interior Seaway in southwestern Montana and the northern United States. *In* Stott, D.F., Glass, D.J., eds., The Mesozoic of middle North America. Canadian Society of Petroleum Geologists Memoir 9, pp. 127-144.

Walker, R.G., 1984. Shelf and shallow marine sands. *In* Walker, R.G., ed. Facies models. Geoscience Canada, Reprint series 1, second edition, pp. 141-170.

Weimer, R.J., 1984. Relation of unconformities, tectonics, and sea level changes, Cretaceous of Western Interior, United States. *In* Schlee, J.S., ed., Interregional unconformitiesand hydrocarbon accumulation, American Association of Petroleum Geologists Memoir 36, pp. 7-35.

FIGURE IV-1: Location map of the Great Falls and Sweetgrass Hills study areas in north-central Montana.

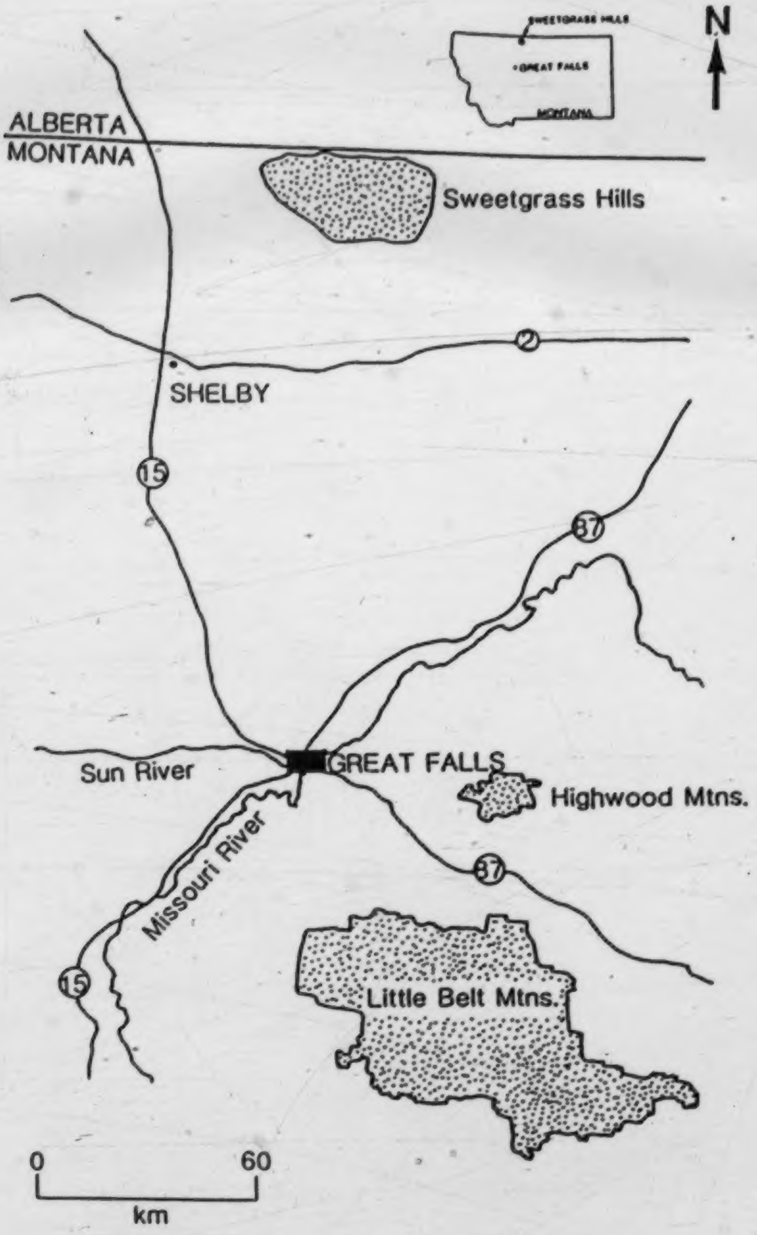
SWEETGRASS HILLS
GREAT FALLS
MONTANA
N
ALBERTA
MONTANA
Sweetgrass Hills
2
SHELBY
15
87
GREAT FALLS
Sun River
Highwood Mtns.
Missouri River
87
15
Little Belt Mtns.
0
60
km

FIGURE IV-2: Correlation chart of Upper and Lower Cretaceous strata in northwestern United States and south-central Alberta (modified after Stelck and Armstrong, 1981).

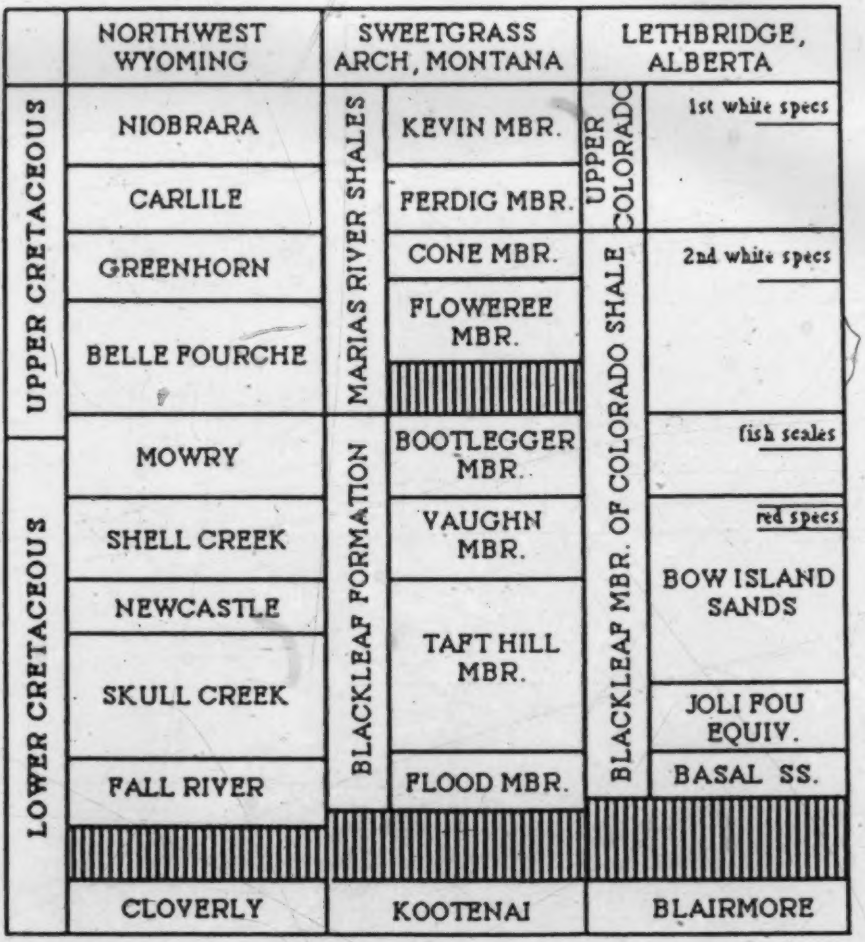
NORTHWEST WYOMING
SWEETGRASS ARCH, MONTANA
LETHBRIDGE, ALBERTA
UPPER CRETACEOUS
LOWER CRETACEOUS
NIOBRARA
CARLILE
GREENHORN
BELLE FOURCHE
MOWRY
SHELL CREEK
NEWCASTLE
SKULL CREEK
FALL RIVER
CLOVERLY
MARIAS RIVER SHALES
KEVIN MBR.
FERDIG MBR.
CONE MBR.
FLOWEREE MBR.
BLACKLEAF FORMATION
BOOTLEGGER MBR.
VAUGHN MBR.
TAFT HILL MBR.
FLOOD MBR.
KOOTENAI
UPPER COLORADO
1st white specs
2nd white specs
BLACKLEAF MBR. OF COLORADO SHALE
fish scales
red specs
BOW ISLAND SANDS
JOLI FOU EQUIV.
BASAL SS.
BLAIRMORE

FIGURE IV-3: Diagrammatic sketch of the five Bootlegger sequences in the Great Falls study area and four sequences in the Sweetgrass Hills study area.

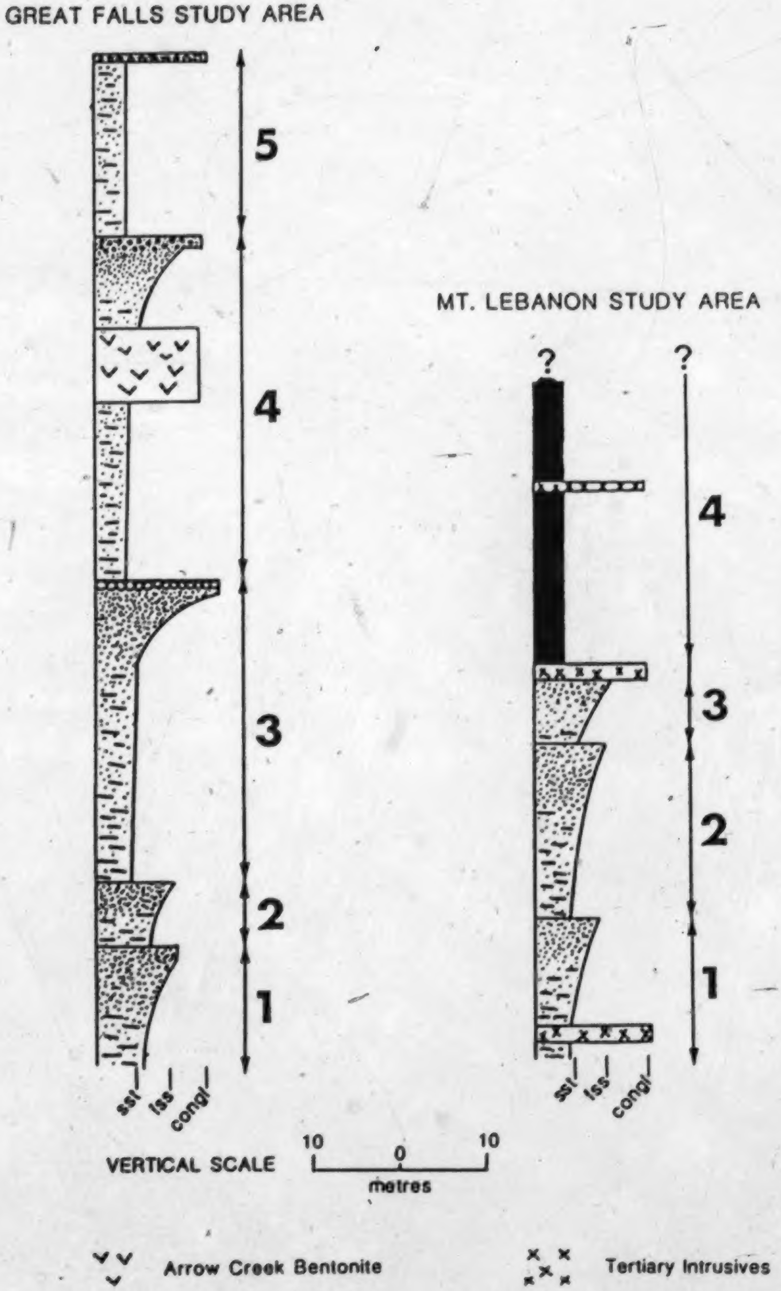
GREAT FALLS STUDY AREA
5
4
3
2
1
ssl
fss
congl
MT. LEBANON STUDY AREA
?
?
4
3
2
1
ssl
fss
congl
VERTICAL SCALE
10
0
10
metres
Arrow Creek Bentonite
Tertiary Intrusives

FIGURE IV-4: Sweetgrass Arch of north-central Montana.

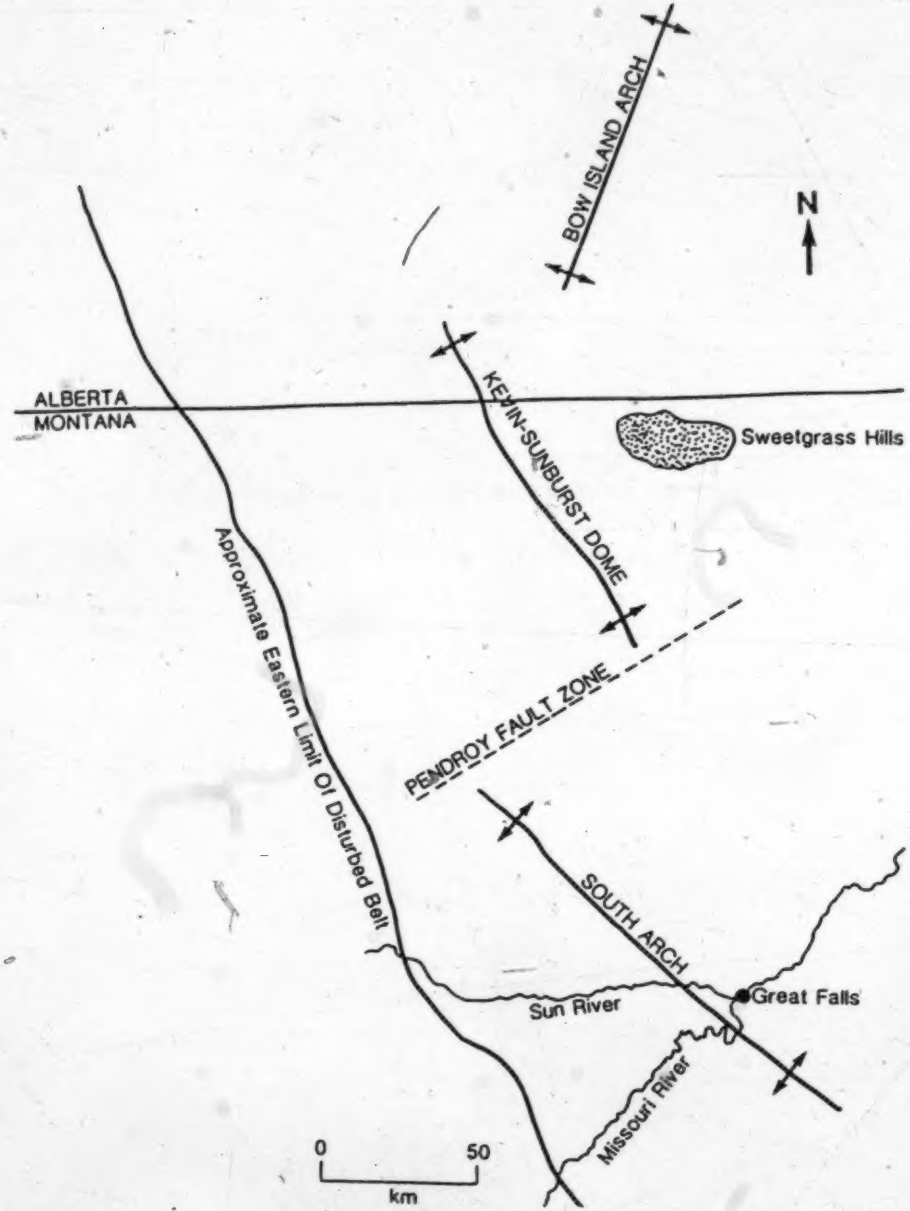
BOW ISLAND ARCH
N
ALBERTA
MONTANA
KEVIN-SUNBURST DOME
Sweetgrass Hills
Approximate Eastern Limit Of Disturbed Belt
PENDROY FAULT ZONE
SOUTH ARCH
Great Falls
Sun River
Missouri River
0
50
km

FIGURE IV-5: Idealised Bootlegger Sequence.

IDEALISED SEQUENCE

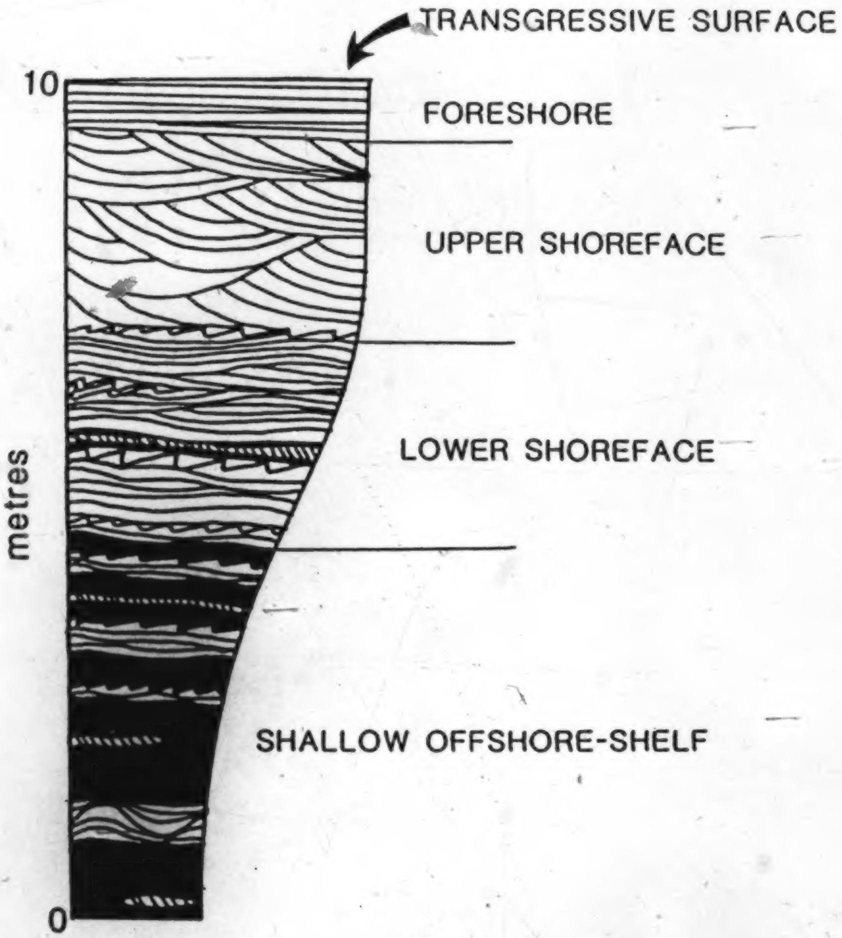
TRANSGRESSIVE SURFACE
10
FORESHORE
UPPER SHOREFACE
LOWER SHOREFACE
metres
SHALLOW OFFSHORE-SHELF
0

FIGURE IV-6(A): Interbedded siltstone/sandstone and shale of Unit 1 (scale bar is 2cm).

FIGURE IV-6(B): Hummocky cross-stratified sandstone interbedded within shale of Unit 1.

FIGURE IV-6(C): Sharp contact between Unit 1 and Unit 2 lithologies at the Ulm Pishkun (staff is 1.5 m long).

FIGURE IV-6(D): Gently-undulating, parallel lamination (GUP lamination) (note subtle undulation and low angle truncations) (scale bar is 10 cm).

FIGURE IV-6(E): Medium-scale, cross-stratified sandstones of Unit 3.

FIGURE IV-6(F): Massive (faint parallel laminated) sandstone characterising the foreshore (Unit 4) (scale bar is 20 cm).

A
C
E

FIGURE IV-7(A): Symmetric wave ripples ($\lambda$=1.0 m, amplitude=7cm) overlain with a veneer of chert pebbles capping Sequence 3 near Belt, Montana .

FIGURE IV-7(B): Coarse-grained, arkosic channel-fill overlying and incised into Unit 1 lithologies (Black Horse Lake, Montana) (scale bar is 1m).

FIGURE IV-8(A, C, E, G, I): Palaeoshoreline positions of Sequence 1, 2,3 and 4 respectively.

FIGURE IV-8(B, D, F, H, J): Stratigraphic fence diagrams of Sequences 1,2,3 and 4 respectively.

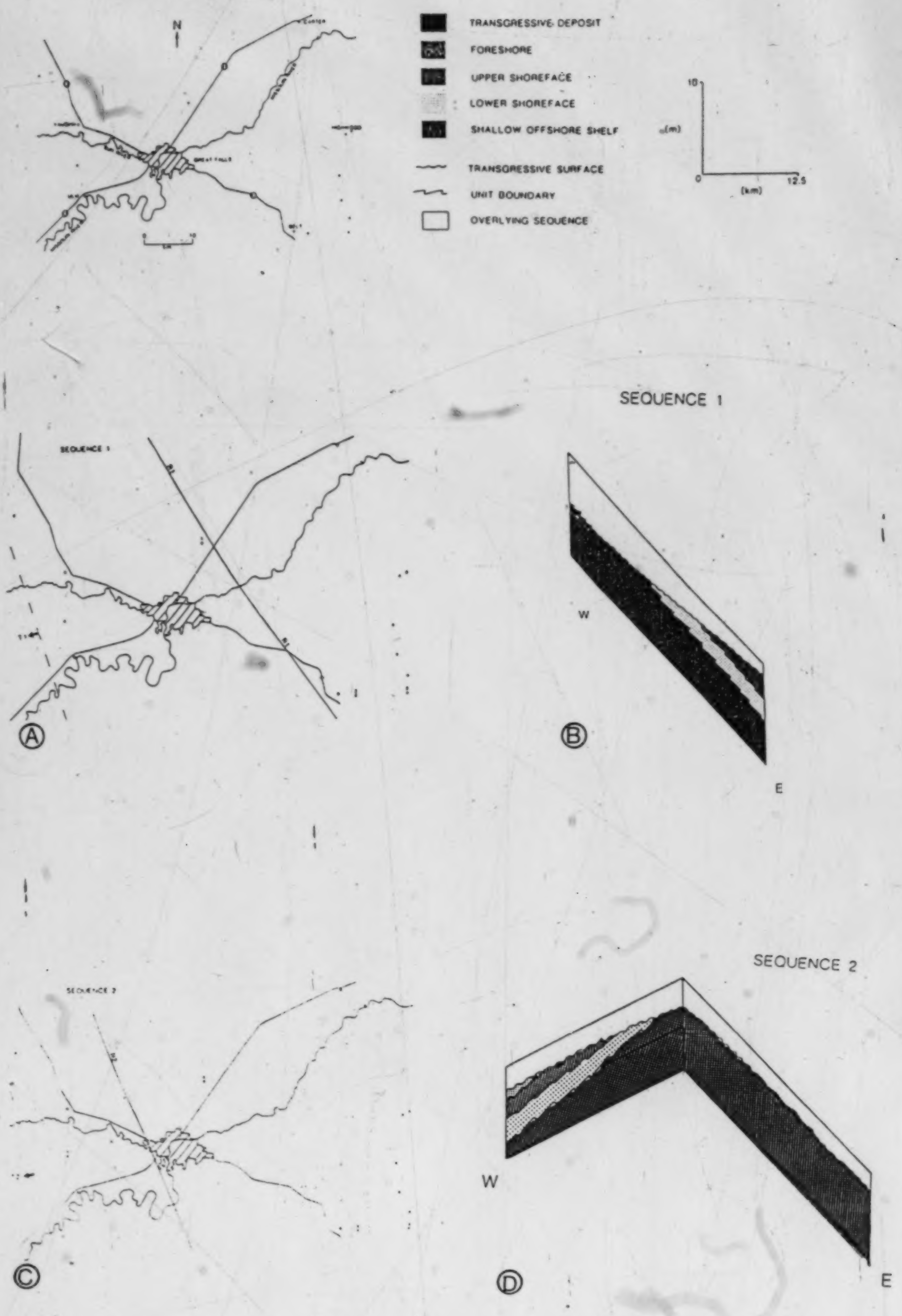
N
GREAT FALLS
0
10
km
TRANSGRESSIVE DEPOSIT
FORESHORE
UPPER SHOREFACE
LOWER SHOREFACE
SHALLOW OFFSHORE SHELF
TRANSGRESSIVE SURFACE
UNIT BOUNDARY
OVERLYING SEQUENCE
10
0
(m)
12.5
(km)
SEQUENCE 1
B1
B1
Ⓐ
SEQUENCE 1
W
E
Ⓑ
SEQUENCE 2
D2
Ⓒ
SEQUENCE 2
W
E
Ⓓ

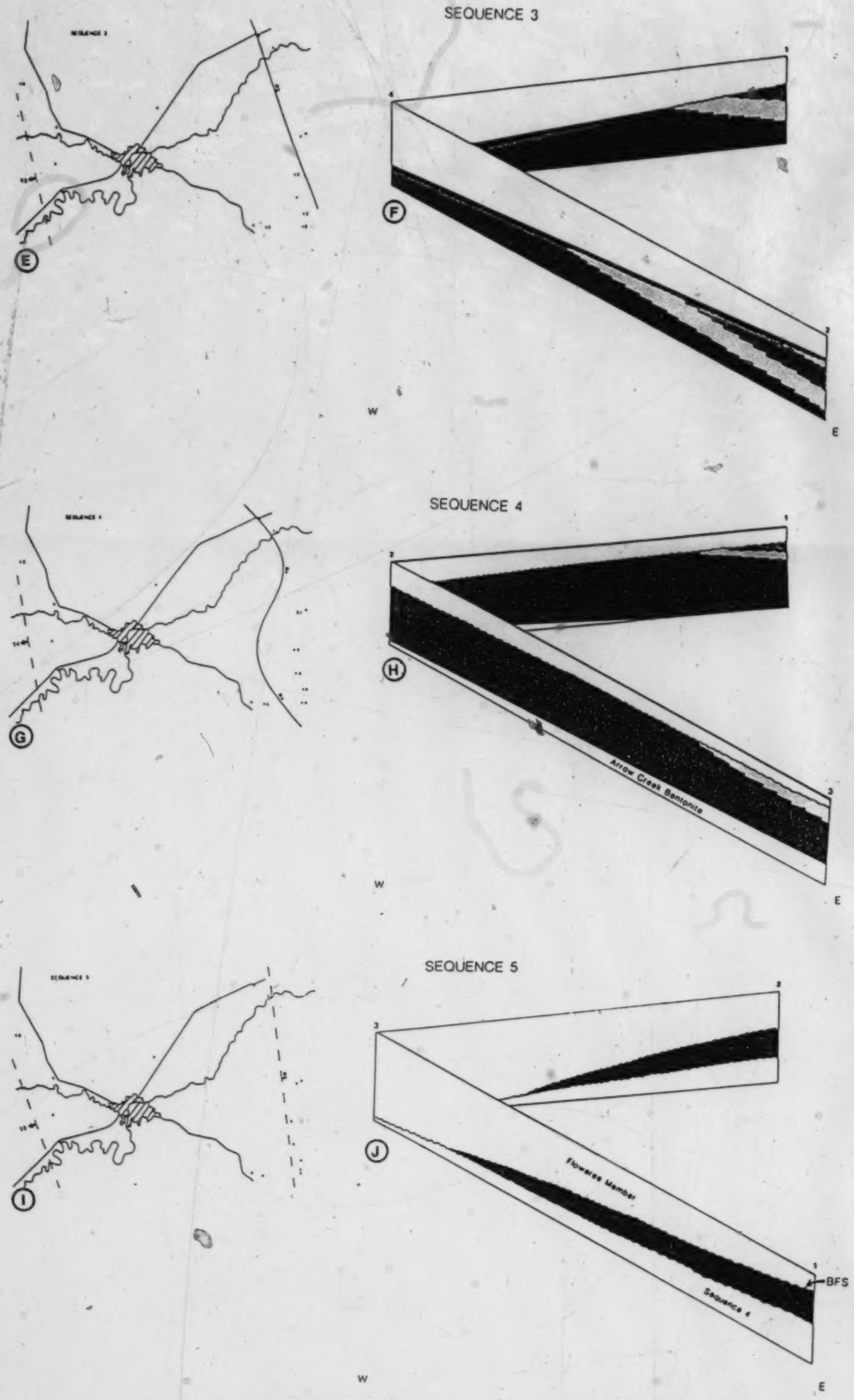
SEQUENCE 3
E
F
W
E
SEQUENCE 4
G
H
Arrow Creek Bentonite
W
E
SEQUENCE 5
I
J
Flowerss Member
BFS
Sequence 4
W
E

# AMALGAMATING PHYSICAL AND BIOGENIC SEDIMENTARY STRUCTURES: A CASE STUDY; BOOTLEGGER MEMBER

## INTRODUCTION

During the late Jurassic and Cretaceous western North America was characterised by a rising Cordillera to the west and the flat-lying craton to the east. Separating these two geologic provinces was an extensive asymmetric basin, known as the Cretaceous Interior Seaway, whose origin was related to the tectonic events which shaped the western Cordillera. Copious amounts of coarse-grained clastic sediment were shed from the rising mountains into the western margin of the basin, in contrast to the volumetrically reduced and fine-grained nature of the eastern sediment influx. Resulting from its proximity to this tectonically active area and the volume of sediment deposited, the stratal record of the western portion of the Cretaceous Interior Seaway is extremely diverse and due to the abundance of excellent exposure affords a prime laboratory for sedimentary analysis.

Until only recently most studies reconstructing the palaeogeographic and palaeohydrodynamic conditions present during the deposition of clastic sequences derived most of its substantiating evidence from primary physical sedimentary structures. These structures, for the most part, are independant of environmental setting and owe their existence and characteristic morphology solely to the state of the fluid boundary layer immediately above the sediment/water interface. However, for reconstructing palaeogeography it only seems reasonable that some type of structure that is susceptible to the physical as well as the other components characterising a particular environment may provide as much if not more information than that provided in the record of physical structures.

Recently, another set of primary structures have been utilised, greatly enhancing our ability to reconstruct the detailed palaeohistory of a sedimenary rock sequence. These primary structures are the biogenic structures, trace fossils, formed by the in-situ activity of various animals. Trace fossils reflect an adapted burrowing behaviour of an animal(s) as it strives to live under a certain set of in-situ environmental conditions. In marine environments for instance, the early work of Seilacher (1967) suggested the existence of an offshore-trending partitioning of biogenic structures. This was reasoned to arise because of the variation of food resources which was ultimately linked to water depth. However, as has been recently shown the nature of the substrate is the primary control over the nature of the adapted burrowing behaviour and ultimately the biogenic structure(s) developed (Ekdale *et al.*, 1984). In some cases the biogenic record is more demonstrative of a particular sedimentary environment than are the primary physical structures. Therefore by amalgamation both primary physical and biogenic sedimentary structures one can make an accurate account of the conditions present during the depositional history of a particular sedimentary sequence.

With reference to the late Albian to early Cenomanian Bootlegger Member of the Blackleaf Formation, this paper will illustrate the compatible amalgamation of physical and biogenic sedimentary structures observed in an ancient, storm-dominated nearshore sequence.

## GEOLOGY OF THE BOOTLEGGER MEMBER

The Bootlegger Member is the uppermost of four members composing the late Lower Cretaceous Blackleaf Formation in north-central Montana. Excellent exposures of the Bootlegger Member are found near the city of Great Falls and within the Sweetgrass Hills. This paper, however, will focus on two outcrop locations of the Bootlegger Member exposed at Taft Hill, located approximately 16 km west of Great Falls (Fig. 1).

The Bootlegger Member by definition is fully marine (Cobban *et al.*, 1959, 1976) and overlies and onlaps westward terrestrial deposits of the Vaughn Member, while merging eastward with the Mowry shales of east-central Montana (Fig. 2). Capping the Bootlegger Member is a fossiliferous unit characterised by abundant fish bones and scales plus ammonite and pelecypod hard-body fossils. This unit has been termed the "Base of the Fish Scales" by Canadian petroleum geologists and may represent an unconformity separating the Bootlegger Member from the overlying Floweree Member of the early Upper Cretaceous Marias River shales (Fig. 4 of Rice, 1984; Arnott and Hein, in review). In addition, this unit has been shown to be contemporaneous for a distance of over 1100 km in a north-south direction (Stelck and Armstrong, 1981; Arnott and Hein, in review).

The Bootlegger Member represents deposition during the incursion of marine conditions into north-central Montana associated with the initial transgressive stage of the basin-wide Greenhorn Cyclothem (Hattin, 1964). In the Great Falls area the Bootlegger Member is characterised by five vertically stacked regressive/transgressive sequences (Arnott, 1987; Arnott and Hein, in review). The regressive portion of each sequence is characterised by shoaling-upward depositional conditions associated with eastward progradation of the local strandline. Shoaling conditions are well illustrated by a progressive increase in the sand/shale ratio, increasing grain size, and the details of the preserved physical and biogenic sedimentary structures. Regressive depositional conditions are terminated by the subsequent transgression, which displaced the shoreline westward. Transgression resulted in the return of relatively deep-water conditions and the development of a markedly different suite of physical and biogenic sedimentary structures in a finer-grained, shale-rich lithology.

## THE TAFT HILL STUDY AREA

The Bootlegger Member is well exposed on the south and west faces of Taft Hill, approximately 16 km west of Great Falls. Exposure on the south face is typically 10 metres high and extends uninterrupted laterally for almost 2 km, of which 1250 metres was measured in detail. This exposure will be called the Ulm Pishkun, after the name of a state park at its easternmost limit. The study area on the west face of Taft Hill is typically less than 5.5 metres high, extends laterally for close to 1 km and is called the Missile Tower Section.

Facies analysis of the physical aspects of the strata cropping out at the Ulm Pishkun and Missile Tower sections have been interpreted to indicate deposition within a prograding, storm-dominated nearshore environment (Arnott, in review). Based on the physical sedimentary structures the outcrops were subdivided into five distinct sedimentary environments, each characterised by a unique assemblage of constituent sedimentary structures (Fig. 3). As will be shown later in the paper the biogenic evidence would seem to suggest a compatible interpretation, but it is also capable of illustrating a number of features which are lacking in the physical sedimentary structure record. Below is a brief discussion of the lithologies and physical sedimentary structures characterising each of the five sedimentary environments; a more detailed account can be found in Arnott (in review).

## PHYSICAL STRUCTURES

### SHALLOW OFFSHORE -SHELF

At the Taft Hill study area lithologies of the shallow offshore-shelf are rarely exposed, although when exposed are composed of interbedded siltstone and bentonitic shale

(Fig. 4A). Physical sedimentary structures are rarely preserved owing to the high degree of biogenic reworking, but current and oscillation ripples can be found. In Bootlegger strata in the eastern part of the Great Falls study area, on the other hand, outcrops of shallow-offshore shelf deposits are better exposed and show a stratigraphically-upward trend of increasing sand/shale ratio plus the abundance and thickness of siltstone/sandstone interbeds. Sedimentary structures exhibited in the interbeds include hummocky cross-stratification (Harms *et al.*, 1975), current and oscillation ripples plus less commonly gently undulating parallel lamination (Arnott, in review). Siltstone/sandstone interbeds indicate deposition during episodic, high-energy events most likely associated with storm events. Following these brief events normal shale deposition resumed.

## LOWER SHOREFACE

At Taft Hill the contact between strata of the shallow offshore-shelf and the lower shoreface is rarely exposed, but when exposed is knife sharp and forms a distinct overhang (Fig. 4B). This contact has been interpreted to represent rapid eastward progradation of the local strandline in response to reactivated uplift of the South Arch; the southern element of the ancestral Sweetgrass Arch (Fig. 1) (Arnott, 1987; Arnott and Hein, in review).

Strata of the lower shoreface are characterised by fine-grained sandstones dominated by gently undulating parallel lamination (Arnott, in review). This sedimentary structure is characterised by parallel lamination which undulates on decimetre to metre spacing and a height which rarely exceeds a centimetre or two. Gently undulating parallel lamination has been interpreted to be deposited from upper-flow-regime, unidirectionally-dominated comfined flow during storm events, and is discussed in detail in Arnott (in review). Intercalated with gently undulating parallel laminated beds are units of interbedded rippled sandstone and shale (Fig. 4C).

Strata making up the lower shoreface suggest fluctuating sedimentation within this depositional environment. High-energy events associated with storms resulted in the deposition of gently undulating parallel laminated sandstone, whereas the typical background sedimentation was characterised by shale and thinly-bedded, rippled sandstone deposition.

## UPPER SHOREFACE

Upper shoreface strata are dominated by medium-scale cross-stratified sandstone typically indicating oblique onshore sediment transport (Fig. 4D). These are interpreted as remnant large-scale bedforms which developed under the effect of shoaling waves in an upper shoreface environment. Reactivation surfaces are common, indicating episodic bedform migration. Interbedded with the cross-stratified strata are beds of gently undulating parallel lamination which were deposited during storm events, and rare interbedded rippled sandstone and shale deposited during very low-energy conditions

## CHANNELLIZED SURF ZONE

Strata of the channellized surf zone are differentiated from those of the underlying upper shoreface by the increased abundance of gently undualting parallel lamination and a reduction of medium-scale cross-stratification (Fig. 4E). These features suggest deposition within an environment characterised by fluctuating but consistently high physical energy and associated active sediment transport. The major source of physical energy within this channel were currents associated with surf wave bore or offshore-flowing bottom currents generated during storm events.

## FORESHORE

Foreshore deposits are made up of rippled and more commonly massive 1-2 cm thick slabs of fine-grained sandstone. Sandstone slabs typically form thicker (10 cm) units showing low-angle trunation surfaces between adjacent and subjacent units (Fig. 4F). These strata are interpreted as swash laminated sandstone and are characteristic deposits of the high-energy foreshore. The presence of rippled sandstone interbeds indicates periods of reduced physical energy thereby enabling ripple development instead of the typical upper-flow-regime swash lamination.

## BIOGENIC STRUCTURES

At both the Ulm Pishkun and Missile Tower study areas, biogenic structures and the ichnologic assemblages they define are as diagnostic of each depositional environment as are the physical structures. The following is a discussion of the biogenic structures characterising each environment, and are summarised in Figure 3. Many of the common forms are illustrated in Figures 5A to 5F and Figures 6A to 6D.

### SHALLOW OFFSHORE-SHELF

As perviously noted shallow offshore-shelf deposits are rarely observed at the Taft Hill study area, and only at the Ulm Pishkun were biogenic structures identified. Biogenic structures included *Teichichnus*, *Planolites montanus* and *Chondrites* . This biogenic assemblage indicates a dominance of feeding structures that typically resulted in the total reworking of the originally stratified sediment, and has been commonly reported from other sequences in the Cretaceous of western North America interpreted as shallow offshore-shelf (Pemberton and Frey, 1984). The low diversity of biogenic forms and abundance of *Chondrites* has been suggested to be indicative of a stressed sedimentary environment, typically oxygen-limited (Bromley and Ekdale, 1984; Ekdale *et al.*, 1984). However, at the Ulm Pishkun the paucity of other inchogenera may only be an artifact of the lack of a contrasting, coarser-grained sediment which would highlight other biogenic forms.

Shallow offshore-shelf strata at Taft Hill are shale-rich and abruptly overlain by sandstones of the lower shoreface. On the other hand, Bootlegger strata in the eastern portion of the Great Falls study area show a well developed, gradational shoaling-upward character from shale-rich to sandstone-rich strata before the appearance of lower shoreface strata. This trend is well illustrated by both the physical structures (see above) and the biogenic structures. Once again in the basal shale-rich strata *Teichichnus*, *Chondrites* and *Planolites montanus* are the common forms, but *Palaeophycus tubularis*, *Bergauria* and small *Thalassinoides* are observed on the soles of siltstone interbeds. In the upper portion (shallower) of the shallow offshore-shelf the diversity of biogenic forms increases, although most forms are horizontal and again preserved as casts on the soles of siltstone/sandstone interbeds. Observed trace fossils include: *Bergauria*, *Teichichnus*, *Gyrolithes* (rare), *Planolites montanus*, *Planolites beverlyensis*, *Palaeophycus striatus*, *Palaeophycus tubularis*, *Skolithos*, *Lockeia*, *Thalassinoides*, *Arenicolites* (rare), *Ophiomorpha nodosa*, *Monocraterion*, *Cylindrichinus* and *Asterosoma* (rare).

At Taft Hill the lack of these latter biogenic and the sandy sedimentary rock in which they are found structures may be the result of: (1) erosive removal of the upper, sandy sediments of the shallow offshore-shelf before deposition of the initial lower shoreface deposits; or (2) because of such rapid shoreline progradation the upper, sandy portion of the shallow offshore-shelf was only very thin and easily eroded, or was never deposited.

## LOWER SHOREFACE

High diversity and abundance of recognisable, well exposed trace fossils are characteristic of lower shoreface strata. Biogenic forms are dominately horizontal and found as casts on the soles of sandstone beds. Vertical forms are commonly observed, although they are usually concentrated within single laterally continuous horizons (a point to be discussed in more detail below). The observed lack of vertical forms transcending bed boundaries would indicate that bioturbation, like deposition of the bed itself, was associated with episodically-recurring events, suggesting a storm-dominated interpretation. The fact that biogenic structures of this lower shoreface are dominated by horizontal casts on sandstone soles may indicate that these traces are the remnant features of post-event bioturbation activity. Following deposition of the sandstone bed, typically exhibiting gently undulating parallel lamination developed during a high-energy storm event, opportunistic trace makers responding to the changed substrate burrow vertically down from the sediment/water interface and then along the basal bedding plane. This resulted in the common occurrence of vertical and the profusion of horizontal biogenic structures:

Horizontal forms: *Ophiomorpha nodosa, Ophiomorpha borniensis, Thalassinoides, Planolites montanus, Planolites beverlyensis, Lockeia, Bergauria, Asterosoma, Palaeophycus striatus* and *Palaeophycus tubularis* .

Vertical forms: *Polycladichnus, Monocraterion, Skolithos, Cylindrichnus, Arenicolites, Rosselia, Diplocraterion, Ophiomorpha nodosa* and Escape Structures.

Inter-storm periods are marked by the deposition of interbedded rippled sandstone and shale which buried the previous storm-emplaced sandstone bed. Loss of the sandy substrate and its associated opportunistic trace makers resulted in the return of quiet-water, mud-loving indigenous forms of this lower shoreface; *Teichichnus* and *Planolites montanus*

## UPPER SHOREFACE

At both study locations the contact of the dominately cross-stratified sandstones of the upper shoreface with the gently undulating parallel laminated sandstones of the lower shoreface is very sharp. Similarly, there is a dramatic change in the trace fossil assemblage, to one characterised by lower abundance and a markedly reduced diversity. Most trace fossils occur as horizontal casts on the soles of sandstone beds or along the basal surface of sandstone cross-bed lamination, although vertical forms are also commonly observed.

Biogenic structures include: *Thalassinoides* (commonly very large), *Skolithos*, *Planolites montanus*, *Planolites beverlyensis*, *Ophiomorpha nodosa* (horizontal and vertical), *Palaeophycus tubularis*, *Bergauria* and *Lockeia*.

The domination of horizontal forms, particularly the very large *Thalassinoides* , indicates substrate invasion after the sedimentation event. Animals burrowed vertically down through the sediment and then developed abundant biogenic structures along a particular horizon, typically the sole of a bed or along a cross-lamination. This bioturbation feature augments the physical structure evidence for suggesting an episodic sedimentation history characterising this upper-shoreface depositional environment.

## CHANNELLIZED SURF ZONE AND FORESHORE

Bioturbation within strata of the surf zone and foreshore depositional environments is limited in both abundance and diversity. Biogenic structures are always horizontal and dominated by *Planolites montanus* , although small *Thalassinoides* are observed in the channellized surf zone. This horizontally-dominated biogenic assemblage contrasts with the vertical Skolithos Ichnofacies commonly reported from high-energy beachface environments (Seilacher, 1967; McCarthy, 1979; Howard and Frey, 1984), and is discussed in more detail below. In addition, the lack of the trace fossil species *Macaronichnus segregatis* (Clifton and Thompson, 1978), a dominantly horizonal burrow observed in both modern and ancient foreshore settings, is also an intriguing anomaly. However, the lack of *Macaronichnus* may only be a consequence of the low abundance of dark minerals in the foreshore sediments and therefore the difficulty in recognising this biogenic structure.

## SPECIFIC EXAMPLES OF UTILIZING THE BIOGENIC RECORD

Within lower shoreface strata at both the Ulm Pishkun and Missile Tower study areas are laterally extensive horizons, typically one bed thick, characterised by an anomalous abundance of vertical biogenic structures (Fig. 7). These units indicate extensive post-depositional bioturbation which may have resulted from a temporary, but localised depositional hiatus. Such a condition would render the sediments near the sediment/water interface prone to extensive bioturbation, thereby contrasting them with superjacent and subjacent strata. Strict use of only the physical structures would probably result in the omission of this horizon, since the physical structures below, within and above this horizon may be very similar, and an erosional surface between the latter two may not necessarily exist.

Another example in which the biogenic record has proven useful in this study is the explanation of the marked diparity in stratal thickness between the two study areas (Fig. 8). At the Missile Tower Section the lower shoreface is only on the order of a metre thick, whereas similar strata at the Ulm Pishkun are several metres thick. On the other hand, thickness of the overlying upper shoreface strata are roughly equal (Fig. 8). Several explanations could account for this discrepancy, but the biogenic record provides the most plausible. At the Ulm Pishkun the many anomalously vertically burrowed beds are dominated by *Polycladichnus, Ophiomorpha, Skolithos* and *Cylindrichnus* and as pointed out above are thought to indicate temporary depositional hiatuses. At the Missile Tower study area, however, intense vertical bioturbation occurs along two horizons, being best developed in the stratigraphically-higher horizon cropping-out immediately beneath the contact between the lower shoreface and upper shoreface. Biogenic structures observed at the Missile Tower include: *Diplocraterion, Rosselia, Arenicolites, Skolithos, Monocraterion* and *Cylindrichnus* (Fig. 9A to 9D). The markedly different trace fossil assemblage characterising each study area indicates a difference in the nature of the original substrate present during post-depositional biogenic invasion.

At the Missile Tower area, several biogenic features observed in the vertically burrowed horizon immediately beneath the contact between the lower shoreface and upper shoreface suggest the burrowing of a substrate of unique character. Many *Diplocraterion* burrows possess scratched wall markings, while horizontal *Thalassinoides* structures possess scratch marks and *Palaeophycus* burrows commonly exhibit ropy textures (Fig. 9E to 9F). Characterisitics of the horizontal structures and particularly the abundance of *Diplocraterion* at the Missile Tower study area suggests the burrowing of a semi-consolidated substrate, a condition which was never achieved at the Ulm Pishkun. This information may then account for the thickness disparity between lower shoreface strata observed at the two study areas; summarised in Figures 10A to 10D and discussed below:

(1) The initial shallow offshore-shelf deposits of the Bootlegger Member were deposited on the drowned palaeotopography of the terrestrial Vaughn Member, since the regional red specks/coal marker horizon demarcating the top of the Vaughn Member can be observed beneath the initial Bootlegger sediments at both study areas. Vaughn palaeotopography may have possessed a topographic high in the area of the Missile Tower Section and a topographic low in the vicinity of the Ulm Pishkun.

(2) Rapid shoreline progradation associated with South Arch uplift (see above) resulted in the abrupt depostion of lower shoreface strata above shallow-offshore shelf strata, but topographic relief on the seabed was retained.

(3) Continued shoaling-upward conditions associated with shoreline progradation may have resulted in sediment by-passing in the vicinity of the topographically higher Missile Tower Section with contemporaneous deposition in the topographically lower area at the Ulm Pishkun. Non-deposition at the Missile Tower enabled the substrate to consolidate to some

degree and thereby support trace makers including *Diplocraterion* , development of scratched wall linings and ropy textured burrows. On the other hand, the Ulm Pishkun was a site of constant deposition, excluding minor hiastuses, and consequently never possessed a suitable substrate for *Diplocraterion* invasion.

(4) Elimination of differential topography during deposition of the lower shoreface resulted in a planar surface between the two study areas over which upper shoreface strata were deposited.

Within the *Diplocraterion* horizon at the Missile Tower study area several vertical ichnogenera are present, although many are indicative of burrowing behaviours adapted to substrates of markedly different consistencies (Ekdale *et al*., 1984). Consequently, the co-existence of softground burrows (*eg. Rosselia, Arenicolites*) with firmground burrows (*eg. Diplocraterion*) would suggest the temporal evolution of a lithifying sediment substrate, and would result in the superposition of temporally-related, substrate-dependent burrowing behaviours and related biogenic forms.

Another feature of the *Diplocraterion* unit which can be used for palaeogeographic reconstruction is the orientation of the individual burrows. Suspension-feeding animals producing this structure preferentially orient themselves with their intake apparatus pointed into the ambient current and their excretory apparatus downstream. Unfortunately, however, one can not differentiate the intake half of the "U-shaped" tube from the effluent half, so palaeocurrent information based on these structures can be justified to only within 180$^{o}$ of the true current direction. In most cases, however, the true orientation of the *Diplocraterion* burrow could not be discerned because of the limited exposure of combined bed-top and cross-sectional views of the same structure; consequently only three burrow orientation measurements were obtained. These measurements suggest that the *Diplocraterion* structures were tightly clustered in a southeast-northwest orientation, agreeing with the northwest (oblique onshore) palaeocurrent directions measured from asymmetric wave ripples.

A peculiarity observed at both study areas is that biogenic structures, regardless of depositional environment, are dominated by horizontal forms. However, it is a commonly accepted notion that as marine environments shallow there is a general increase in the relative abundance of vertical versus horizontal burrow forms (Seilacher, 1967; Ekdale *et al.*, 1984). Such a transformation is typically illustrated by the gradual shoaling-upward replacement of horizontal forms making up the Cruzina Ichnofacies with the vertical forms of the Skolithos Ichnofacies. However, this tranformation is not observed at either the Ulm Pishkun or the Missile Tower study area, or at any other location where Bootlegger Member strata were studied. The virtual exclusion of the Skolithos Ichnofacies and the enhancement of the Cruzina Ichnofacies into even very shallow depositional environments (*eg.* foreshore, upper shoreface) may have palaeohydrodynamic implications. The low observed abundance of vertical forms in shoreface and beachface strata at both study areas may suggest that the level of physical energy characterising this ancient nearshore system was sufficiently high, for the most part, to prevent habitation by suspension-feeding animals. Consequently, horizontal deposit-feeding burrowers living beneath the sediment/water interface were able to flourish under these conditions and thereby overwhelm the biogenic record. Therefore, the typical lack of vertical burrowing forms in these strata may suggest that the Skolithos Ichnofacies, even though representative of high-energy environments (Seilacher, 1967), is excluded from anomalously high-energy environments. Under these conditions, horizontal burrowers flourish and likewise dominate the biogenic record. Consequently, the identification of this ichnologic condition may provide insight into the palaeohydrodynamic nature of ancient shoreline sequences.

This paper illustrates the use of biogenic sedimentary structures in reconstructing an ancient storm-dominated nearshore sequence. The biogenic evidence agrees well with the physical sedimentary record, but is also capable of illustrating a number of sedimentary conditions poorly illustrated in the physical record. The main point of the paper is to illustrate the compatible amalgamation of both physical and biogenic sedimentary structures, and how together these two bodies of information can be utilised in more accurately reconstructing ancient sedimentary sequences.

# REFERENCES

Arnott, R.W., 1987. Stratigraphy of the Lower Cretaceous Bootlegger Member near Great Falls, Montana and its relationship with the ancestral Sweetgrass Arch. Geological Association of Canada, Program with Abstracts, p. 22.

Bromley, R.G., Ekdale, A.A., 1984. *Chondrites* : A trace fossil indicator of anoxia in sediments. Science, v. 224, pp. 872-874.

Clifton, H.E., Thompson, J.K., 1978. *Macaronichnus segregatis* - a feeding structure of shallow marine polychaetes. Journal of Sedimentary Petrology, v. 48, pp. 1293-1302.

Cobban, W.A., Erdmann, C.E., Lemke, R.W., Maughn, E.K., 1959. Revision of Colorado Group on Sweetgrass Arch, Montana. American Association of Petroleum Bulletin Geologists, v.43, pp. 2786-2796.

-------, 1976. Type sections and stratigraphy of the members of the Blackleaf and Marias River Formations (Cretaceous) of the Sweetgrass Arch, Montana. U.S.G.S. Professional Paper 974, 66p.

Ekdale, A.A., Bromley, R.G., Pemberton, S.G., 1984. Ichnology: The use of trace fossils in sedimentology and stratigraphy. Sociey of Economic Paleontologists and Mineralogists Short Course No. 15, 317 p.

Harms, J.C., Southard, J.B., Spearing, D.R., Walker, R.G., 1975. Depositional environments asinterpreted from primary structures and stratification sequences. Sociey of Economic Paleontologists and Mineralogists Short Course No. 2, 161p.

Hattin, D.E., 1964. Cyclic sedimentation in the Colorado Group of west-central Kansas. *In* : Merriam, D.F., ed., Symposium on cyclic sedimentation. Kansas Geological Survey Bulletin, pp. 205-217.

Howard, J.D., Frey, R.W., 1984. Characteristic trace fossils in nearshore to offshore sequences, Upper Cretaceous of east-central Utah. Canadian Journal of Earth Science, v. 21, pp. 200-219.

McCarthy, B., 1979. Trace fossils from a Permian shoreface-foreshore environment, eastern Australia. Journal of Paleontology v. 53, pp. 345-366.

Pemberton, S.G., Frey, R.W., 1984. Ichnology of storm-influenced shallow marine sequence: Cardium Formation (Upper Cretaceous) at Seebe, Alberta. *In* : Stott, D.F., Glass, D.J., eds., The Mesozoic of Middle North America. Canadian Society of Petroleum Geologists Memoir No. 9, pp. 281-304.

Rice, D.D., 1984. Widespread, shallow-marine, storm-generated sandstone units in the Upper Cretaceous Mosby Sandstone, central Montana. *In* Tillman, R.W., Siemers. C.T., eds., Siliciclastic Shelf Sediments. Society of Economic Paleontologists and Mineralogists Special Publication No. 34, pp. 143-161.

Seilacher, A., 1967. Bathymetry of trace fossils. Marine Geology, v. 5, pp. 413-428.

Stelck, C.R., Armstrong, J., 1981. Neogastroplites from southern Alberta. Bulletin of Canadian Petroleum Geology, v. 29, pp.399-407.

FIGURE V-1: Location map of the Taft Hill study area near Great Falls, Montana. (1) Ulm Pishkun study area; (2) Missile Tower study area.

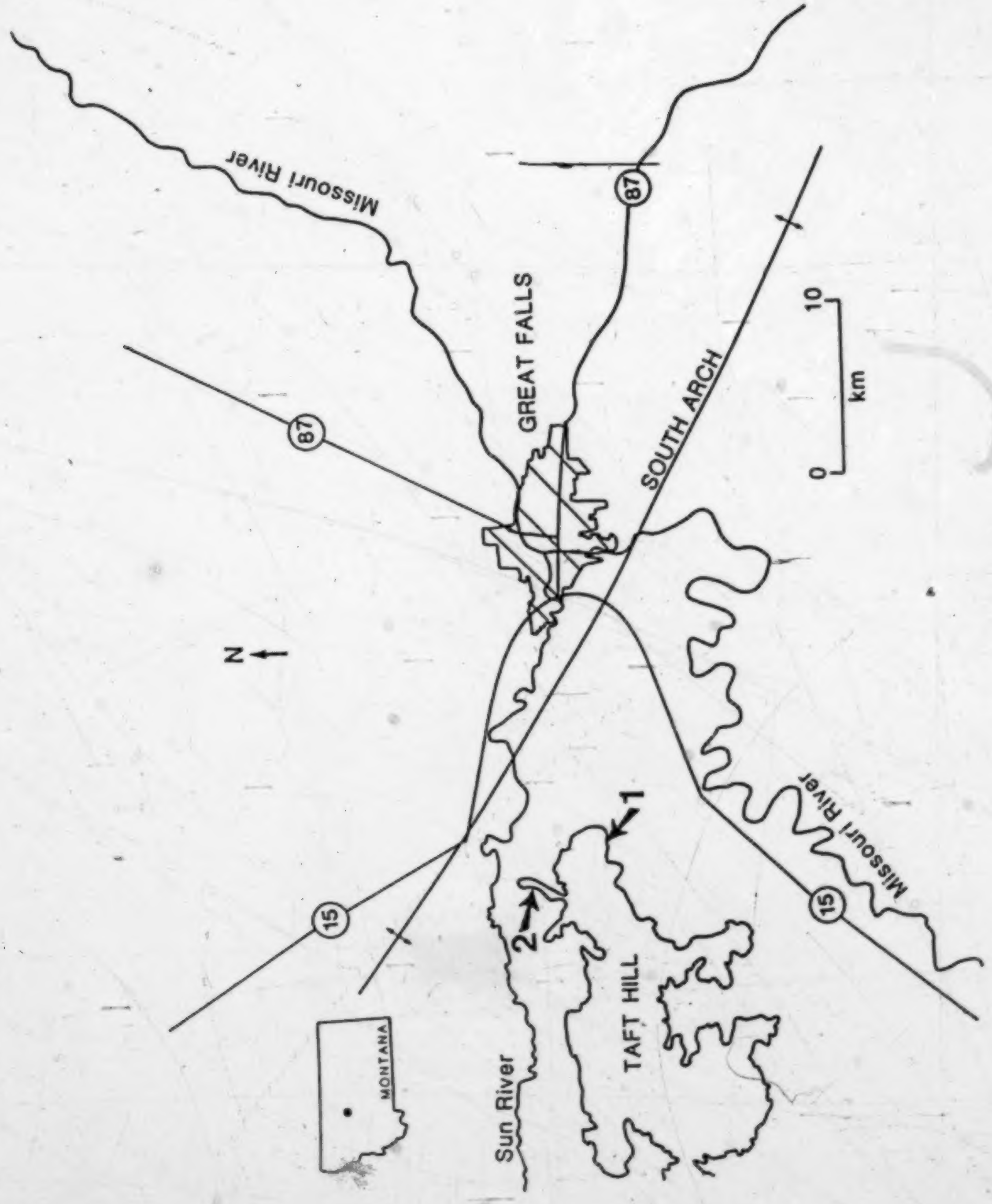
Missouri River
GREAT FALLS
87
87
SOUTH ARCH
0
10
km
N
15
15
Missouri River
1
2
TAFT HILL
Sun River
MONTANA

FIGURE V-2: Correlation chart of Upper and Lower Cretaceous strata in northwestern United States and south-central Alberta (modified after Stelck and Armstrong, 1981).

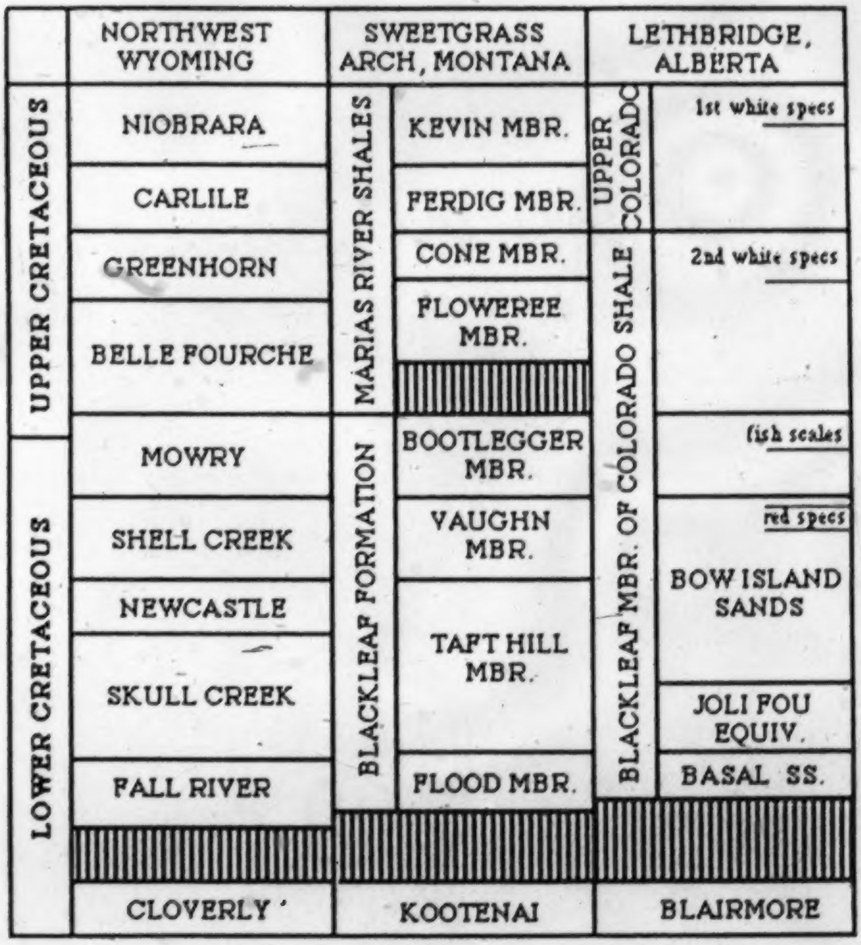
NORTHWEST WYOMING
SWEETGRASS ARCH, MONTANA
LETHBRIDGE, ALBERTA
UPPER CRETACEOUS
LOWER CRETACEOUS
NIOBRARA
CARLILE
GREENHORN
BELLE FOURCHE
MOWRY
SHELL CREEK
NEWCASTLE
SKULL CREEK
FALL RIVER
CLOVERLY
MARIAS RIVER SHALES
KEVIN MBR.
FERDIG MBR.
CONE MBR.
FLOWEREE MBR.
BLACKLEAF FORMATION
BOOTLEGGER MBR.
VAUGHN MBR.
TAFT HILL MBR.
FLOOD MBR.
KOOTENAI
UPPER COLORADO
1st white specs
2nd white specs
BLACKLEAF MBR. OF COLORADO SHALE
fish scales
red specs
BOW ISLAND SANDS
JOLI FOU EQUIV.
BASAL SS.
BLAIRMORE

FIGURE V-3: Idealised shoaling-upward lithologic sequence at the Taft Hill study area. Also included are the observed environmental ranges of some of the common biogenic structures.

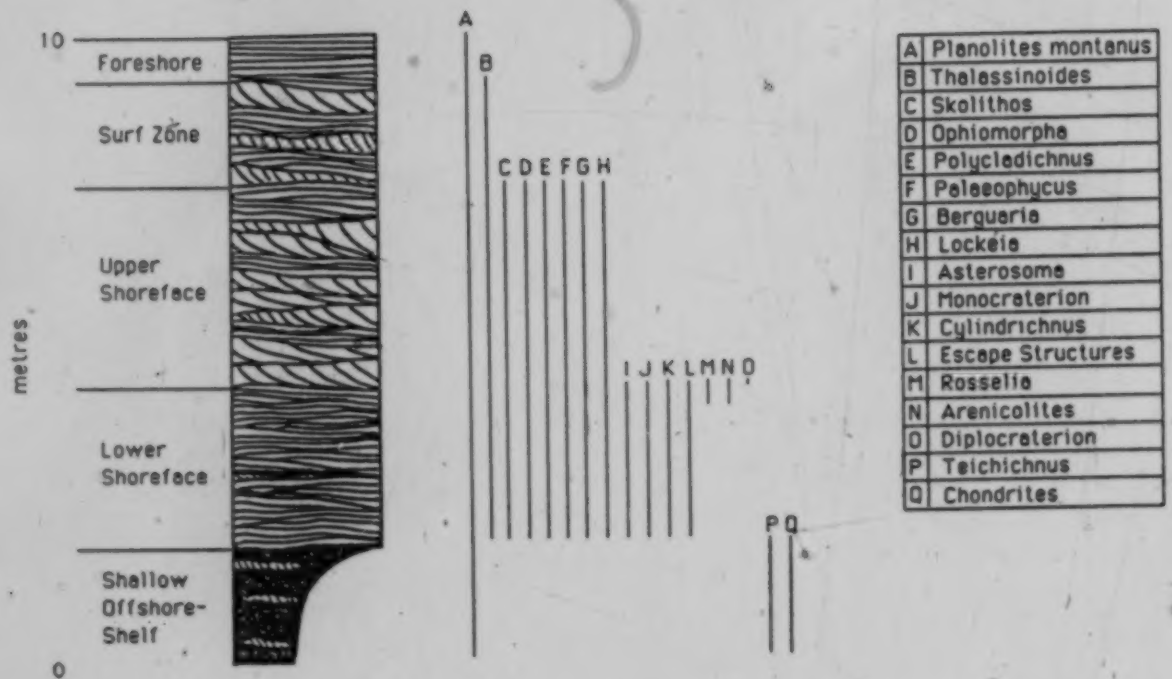
10
0
metres
Foreshore
Surf Zone
Upper Shoreface
Lower Shoreface
Shallow Offshore-Shelf
A
B
C D E F G H
I J K L M N O
P Q
A Planolites montanus
B Thalassinoides
C Skolithos
D Ophiomorpha
E Polycladichnus
F Palaeophycus
G Bergueria
H Lockeia
I Asterosoma
J Monocraterion
K Cylindrichnus
L Escape Structures
M Rosselia
N Arenicolites
O Diplocraterion
P Teichichnus
Q Chondrites

FIGURE V-4(A): Intensely bioturbated, interbedded bentonitic shale and siltstone characterising the shallow offshore-shelf (scale bar represents 7 cm).

FIGURE V-4(B): Sharp contact between the shallow offshore-shelf and the overlying lower shoreface at the Ulm Pishkun study area (scale bar is 25 cm long).

FIGURE V-4(C): Gently-undulating, parallel lamination characteristic of the lower shoreface depositonal environment. Note numerous low-angle truncations (scale bar represents 15 cm).

FIGURE V-4(D): Medium-scale, cross-bedded sandstones representing the upper shoreface.

FIGURE V-4(E): Abundant gently undulating, parallel lamination and interbedded medium-scale, cross-bedded sandstones of the surf zone (scale bar is 0.90 m long).

FIGURE V-4(F): Swash-laminated sandstones deposited in a foreshore environment (scale bar is 0.25 m long).

A
B
C
D
E
F

FIGURE V-5(A): Boxwork morphology of *Ophiomorpha nodosa* burrow (scale bar is 3.5 cm long).

FIGURE V-5(B): Branching *Thalassinoides* burrow cast (scale bar is 1.3 cm long).

FIGURE V-5(C): Abundant *Lockeia* burrow casts formed by the proposed activity of bivalves (scale bar is 0.9 cm long).

FIGURE V-5(D): Basal bedding plane view of *Cylindrichnus* burrows (top of bed is into the photo)(scale bar is 1.8 cm long).

FIGURE V-5(E): Circular *Berguaria* burrow cast formed by an ancient burrowing sea anemone (scale bar is 0.75 cm long).

FIGURE V-5(F): One very large and several smaller *Planolites beverlyensis* burrows (scale bar is 5 cm long).

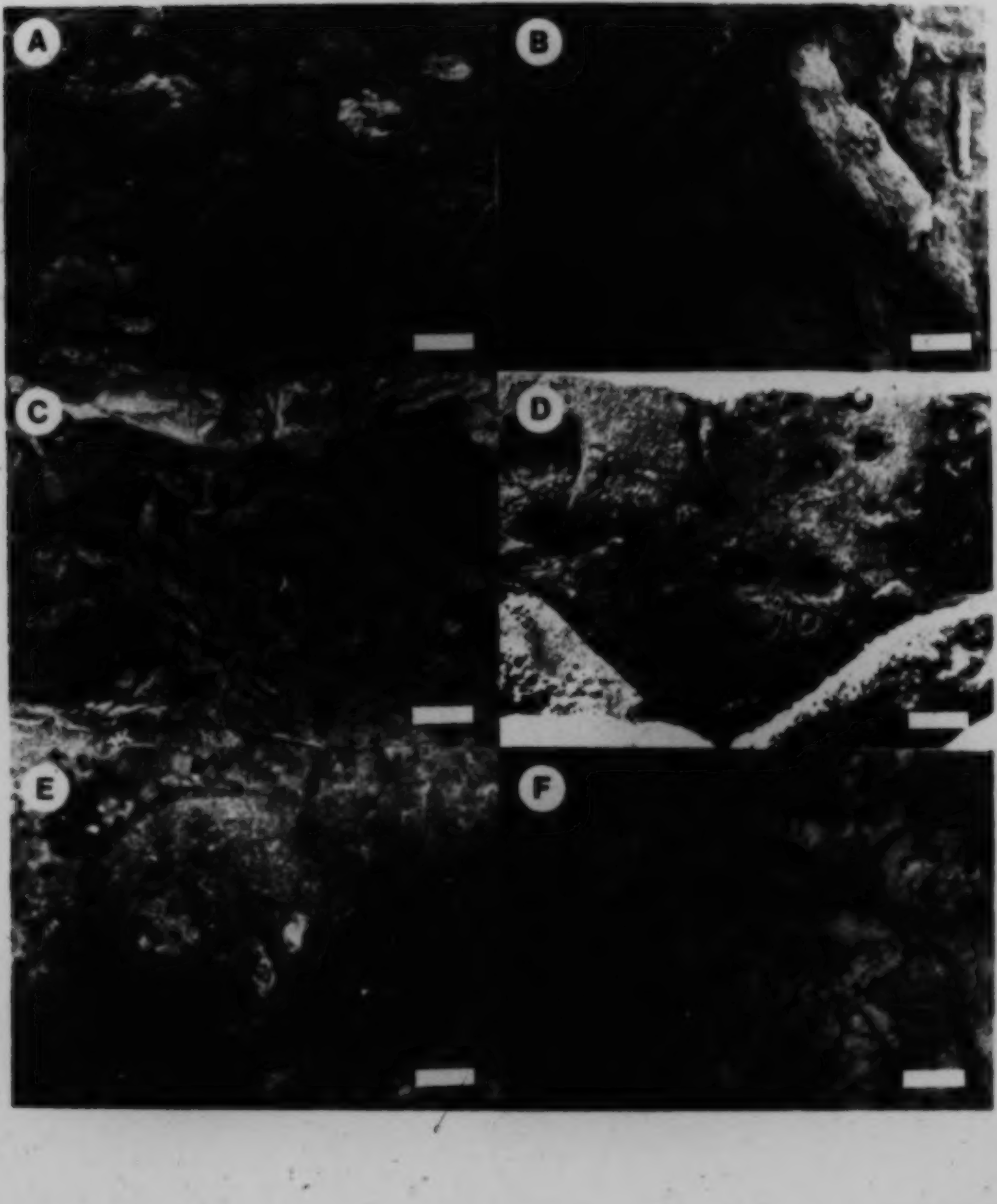
A
B
C
D
E
F

FIGURE V-6(A): Cross-sectional view of a *Polycladichnus* burrow within a gently undulating, parallel laminated bed. Note the presence of an amalgamated bed contact immediately above the *Polycladichnus* burrow (scale bar is 2.5 cm long).

FIGURE V-6(B): An escape structure created by the vertical burrowing activity of a buried animal following the rapid emplacement of the bed.

FIGURE V-6(C): Abundant *Palaeophycus* burrow casts (scale bar is 3.0 cm long).

FIGURE V-6(D): Cross-sectional view of a *Teichichnus* burrow (scale is 8.0 mm long).

A
B
C
D

FIGURE V-7: Anomalous abundance of vertical burrows, in this case *Ophiomorpha nodosa* , observed along particular laterally continuous horizons at the Ulm Pishkun study area. These horizons are interpreted to represent temporary depositonal hiatuses which rendered the bed susceptible to anomalous degrees of bioturbation (scale bar represents 4 cm).

FIGURE V-8: Diagrammatic sketch of the Ulm Pishkun and Missile Tower study areas. Note the thinner lower shoreface deposits and the occurrence of the *Diplocraterion* unit at the top of the lower shoreface at the Missile Tower study area.

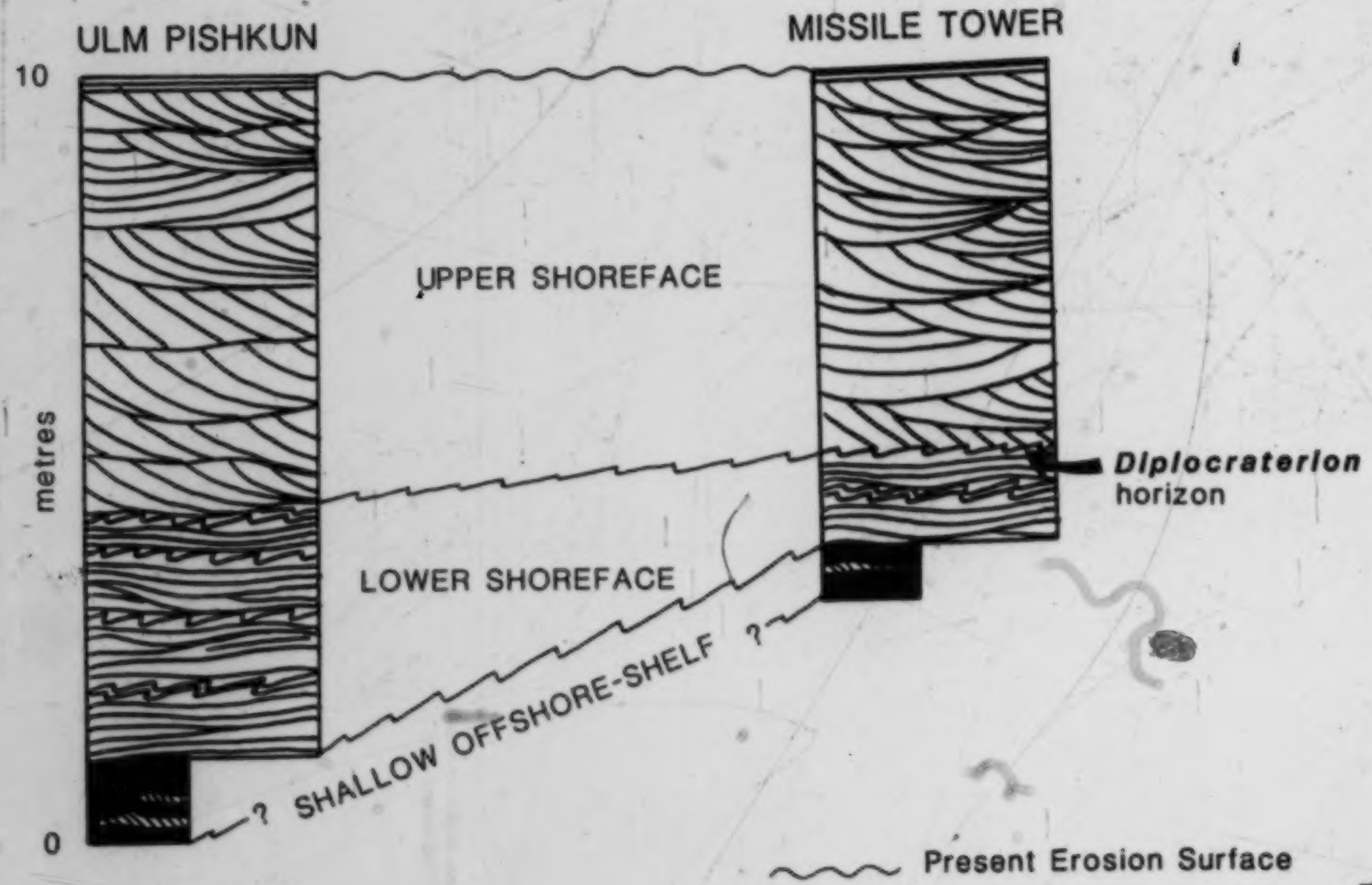
ULM PISHKUN
MISSILE TOWER
10
metres
0
UPPER SHOREFACE
LOWER SHOREFACE
SHALLOW OFFSHORE-SHELF
?
?
*Diplocraterion* horizon
Present Erosion Surface

FIGURE V-9(A): *Diplocraterion* unit occurring at the top of the lower shoreface at the Missile Tower study area

FIGURE V-9(B): *Rosselia* burrows occurring within the *Diplocraterion* unit at the Missile Tower study area. The occurrence of these two forms indicates the progressive evolution of a soft-ground to a semi-consolidated substrate (scale bar is 1.2 cm long).

FIGURE V-9(C): Three distinct *Arenicolites* structures within the *Diplocraterion* unit at the Missile Tower study area. *Arenicolites* are soft-ground burrows occurring within a unit containing abundant semi-consolidated burrow forms (*Diplocraterion*).

FIGURE V-9(D): Laterally migrating limb of a *Arenicolites* burrow observed in the *Diplocraterion* unit at the Missile Tower study area.

FIGURE V-9(E): Large, scratch-marked *Thalassinoides* burrow cast occurring on the base of the *Diplocraterion* unit at the Missile Tower study area (scale bar is 2 cm long).

FIGURE V-9(F): Abundant ropy textured *Palaeophycus* burrow casts observed on the base of the *Diplocraterion* unit at the Missile Tower study area (scale bar is 6 cm long).

A
B
C
D
E
F

FIGURE V-10: Diagrammatic sketches of the development of Bootlegger Member strata at the (1) Ulm Pishkun and (2) Missile Tower study areas. Details of Figures 10A to 10D are given in the text. (A) Palaeotopography at the close of Vaughn Member time; topographic high in the Missile Tower area and a low in the Ulm Pishkun area. (B) Drowning of Vaughn palaeotopography during transgression associated with the advance of the Greenhorn Sea. Transgression lead to the deposition of shallow offshore-shelf deposits at both study areas, but palaeotopography was retained. (C) Shoreline progradation and the development of lower-shoreface depositional environments at both study areas. Sediment by-passing at the topographically higher Missile Tower area enabled the exclusive development of semi-consolidated substrate conditions and the invasion of *Diplocraterion* trace makers. (D) Removal of differential topography and the deposition of equivalent thicknessess upper shoreface strata.

A

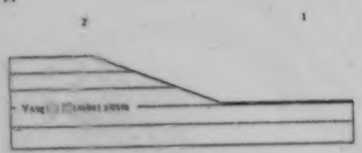
2
1
Vaughn Member zone

B

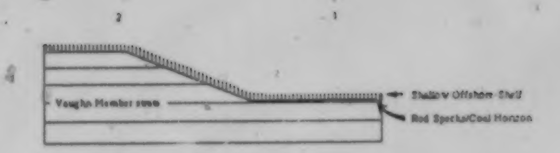
2
1
Vaughn Member zone
Shallow Offshore Shelf
Red Specks/Coal Horizon

C

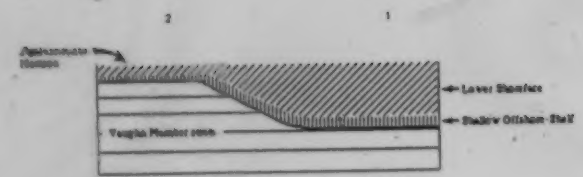
2
1
Horizon
Lower Shaftesbury
Shallow Offshore Shelf
Vaughn Member zone

D

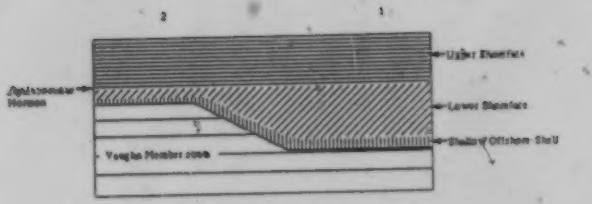
2
1
Upper Shaftesbury
Horizon
Lower Shaftesbury
Shallow Offshore Shelf
Vaughn Member zone

# GENERAL DISCUSSION AND CONCLUSIONS

During the late Jurassic and Cretaceous the western continental margin of North America, due to Pacific Plate collision and subduction, was characterised by the development of the Cordilleran Fold and Thrust Belt. Long-lived build-up and eastward migration of the Fold and Thrust Belt caused the underlying and eastward adjacent lithosphere to subside, thus producing what commonly called the Western Cretaceous Interior Seaway. At its maximum dimensions this seaway extended over 4800 km (north-south) by 1600 km (east-west)(Kauffman, 1985), and into which waters from the Arctic Ocean and Gulf of Mexico periodically migrated into (transgression) and retreated from (regression). Temporal changes from marine to terrestrial depositional conditions within various portions of the trough gave rise to the diverse sedimentary record characterising Cretaceous strata in western North America. One of the most common sedimentary patterns are the typical coarsening- to fining-upward couplets which resulted from marine regression/transgression. Many of the large-scale transgression/regression couplets that have been identified from the Cretaceous Seaway depositional basin have been observed worldwide (Vail *et al.*, 1977), and point to global eustatic sea-level changes during the Cretaceous. However, superimposed on these large-scale events are smaller-scale depositional episodes which owe their existence to intrabasinal events.

The late Albian to early Cenomanian Bootlegger Member represents the uppermost of four stratigraphic members making up the Blackleaf Formation of north-central Montana. In ascending order the four constituent members of the Blackleaf Formation are: Flood, Taft Hill, Vaughn and Bootlegger members. Together these members record the temporal sedimentary influence of two major basin-wide events: the Kiowa-Skull Creek Cyclothem and the younger Greenhorn Cyclothem (Weimer, 1984; Vuke, 1984), which Vail *et al.* (1977) reported to observe on a global scale. Marine deposits of the Flood Member rest unconformably above terrestrial deposits of the Kootenai Formation. This feature represents the initial development of marine depositional conditions in this part of the Creteceous Seaway associated with the early part of the Kiowa-Skull Creek Cyclothem (Kauffman *et al.*, 1977; Vuke, 1984). Transgression continued throughout Flood Member time, but with the onset of regression Flood Member deposition was replaced by Taft Hill Member sedimentation. The glauconitic nature of Taft Hill clastic sediments is proposed to indicate restricted marine conditions (Cobban *et al.*, 1959, 1976) developed as a result of the marine regression (Vuke, 1984). Regression continued into Vaughn Member time and culminated in the development of terrestrial depositional environments. However, these conditions were abruptly terminated, as was the Kiowa-Skull Creek Cyclothem, by the development of a second major transgressive event associated with the Greenhorn Cyclothem. This transgression drowned much of the areally extensive Vaughn Member in north-central Montana and deposited the marine clastic strata of the Bootlegger Member. Transgression continued throughout Bootlegger Member time and extended into the Upper Cretaceous.

The Bootlegger Member crops out near the city of Great Falls and on the northwest slopes of Mt. Lebanon in the Sweetgrass Hills of north-central Montana. It can be identified in the field as that which lies above the red-specks (clinoptilolite crystals) and associated coal marker horizon at the top of the Vaughn Member, and that cropping out beneath the black shales of the Upper Cretaceous Floweree Member of the Marias River shales. The uppermost portion of the Bootlegger Member contains the well known Base of the Fish Scales zone, a common datum for stratal correlations used by Canadian oil geologists. This marker zone has been shown to be contemporaneous from Ft. St. John, British Columbia to Lethbridge, Alberta (Stelck and Armstrong, 1981). However, the similar occurrence of the ammonite *Neogastroplites americanus* in uppermost Bootlegger Member strata suggests that the Base of the Fish Scales marker zone can be extended into at least north-central Montana, a total distance of over 1100 km.

The Base of the Fish Scales marker unit may represent an unconformity. In the eastern portion of the Great Falls study area this marker unit caps Sequence 5, whereas in the western study locations (*eg*. Gordon) it caps Sequence 4 strata. The lack of Sequence 5 strata, excluding the fish scales marker unit, plus the condensed version of Sequence 4 strata in the western study areas, is thought to reflect the erosional bevelling of pre-existing strata during Base of the Fish Scales time. The stratal record in the eastern portion of the Great Falls study area is also affected during this erosional period, although not to the same extent as in the west.

In both the Great Falls and Mt. Lebanon study areas Bootlegger Member strata form a number of sedimentary sequences, five sequences in the Great Falls area and at least three (possibly four) at Mt. Lebanon, characterised by features interpreted to reflect shoaling-upward depositional conditions associated with strandline progradation. Each progradational event, which invariably indicates eastward strandline migration, is subsequently terminated by a transgressive event which displaces the strandline westward. Bootlegger sequences are dominated by sediments deposited during the regressive phase of the sequence, while transgressive deposits tend to be very thin or absent. The nature of the deposits characterising each of the Bootlegger sequences, is for the most part, a direct reflection of the lateral extent of strandline progradation associated with regressive depositional conditions. However, erosion during the ensuing transgression is also instrumental in determining what is preserved of the regressive sedimentary sequence. Transgression usually results in the development of a planar transgressive surface, which may be capped with a thin transgressive lag deposit.

In both study areas, the repetitive nature of sedimentation characterising Bootlegger Member time is suggested to reflect the influence of the ancestral Sweetgrass Arch (Arnott, 1987). Uplift of the arch, which during this part of the Cretaceous may have acted as a forebulge (Lorenz, 1982), resulted in a relative sea level drop and the rapid eastward progradation of the local strandline. Progradation resulted in shoaling depositional conditions and the development of a shoaling-upward sequence. Due to the proximity of the Sweetgrass Arch to both study locations and the position of the local strandlines at the beginning of each Bootlegger Sequence, uplift of the arch, which is thought to be contemporaneous with episodes of Cordilleran thrusting, did not have to be great in order to have a profound effect on local sedimentary patterns. During intervening periods of thrusting quiescence, however, the arch foundered under the effect of sediment loading and elastic lithospheric relaxation. Arch subsidence resulted in a rise of relative sea level, westward displacement of the local strandline and development of transgressive depositional conditions.

Lithologic and biogenic analysis suggests that Bootlegger Member strata deposited during the progradational portion of each sequence indicates deposition within a storm-dominated, nearshore sedimentary environment. Environments of deposition include: shallow offshore-shelf, lower shoreface, upper shoreface, channellized surf zone and foreshore, each characterised by a number of characteristic physical and biogenic sedimentary structures and are listed below;

## SHALLOW OFFSHORE-SHELF

Lithologic characteristics: Interbedded shale and siltstone. Siltstone interbeds exhibit hummocky cross-stratification, gently undulating parallel lamination (GUP lamination), asymmetric and symmetric oscillation ripples, and current ripples. Palaeocurrents are typically offshore-trending and indicate deposition from seaward-moving currents, probably the product of storm-induced coastal set-up. Onshore-trending palaeocurrents are the product of shoaling, onshore waves and the preferential transport of the bottom sediment.

Biogenic characteristics:

in shales: *Teichichnus, Planolites montanus, Chondrites, Gyrolithes*

sandstone soles (horizontal): *Palaeophycus striatus, Palaeophycus tubularis, Thalassinoides, Lockeia, Bergauria, Ophiomorpha nodosa*

sandstone beds (vertical): *Skolithos, Monocraterion, Cylindrichnus, Ophiomorpha nodosa, Arenicolites*

## LOWER SHOREFACE

Lithologic characteristics: Gently undulating parallel lamination (GUP lamination) with rippled bed-tops. Several lines of evidence suggest that these beds were deposited from episodic, upper-flow-regime, unidirectionally-dominated combined flow. The ripple cap, on the other hand, indicates deposition from low flow regime currents associated with the waning stages of the flow. Interbedded with the GUP laminated beds are units of interbedded rippled sandstone and shale. These represent the typical fair-weather record in this lower shoreface environment.

Biogenic characteristics:

in shales: *Teichichnus, Planolites montanus*

sandstone soles (horizontal): *Ophiomorpha nodosa, Ophiomorpha borniensis, Thalassinoides, Palaeophycus tubularis, Palaeophycus striatus, Lockeia, Asterosoma, Planolites montanus, Planolites beverlyensis, Bergauria.*

sandstone beds (vertical): *Arenicolites, Diplocraterion, Cylindrichnus, Monocraterion, Polycladichnus, Skolithos, Ophiomorpha nodosa, Rosselia.* Escape Structures

## UPPER SHOREFACE

Lithologic characteristics: Medium-scale cross-stratified sandstones with interbedded GUP lamination. Palaeocurrent information indicates that sediment transport was typically oblique-onshore (toward the north-west), but was periodically interrupted by eastward transport. The former is associated with the typical northwest attack of shoaling surface gravity waves while the latter is the product of offshore-moving flows associated with storm-induced coastal set-up.

Biogenic characteristics: *Thalassinoides, Arenicolites, Skolithos, Palaeophycus tubularis, Planolites montanus, Planolites beverlyensis, Lockeia, Bergauria, Ophiomorpha nodosa.*

## CHANNELLIZED SURF ZONE

Lithologic characteristics: Interbedded GUP lamination and medium-scale cross-stratified sandstones (approximately 60 : 40 respectively). Palaeocurrent directions from the latter indicate oblique-to-shore sediment transport.

Biogenic characteristics: *Planolites montanus, Thalassinoides*

## FORESHORE

Lithologic characteristics: thin slabs of massive (or planar-laminated) sandstone which commonly form sets with low-angle truncation surface between adjacent and subjacent sets (swash lamination). Also rare medium-scale cross-stratified sandstones.

Biogenic characteristics: *Planolites montanus, Skolithos*

Gently undulating parallel lamination (GUP lamination) is common in the interpreted lower-shoreface depositional environment of the Bootlegger Member. Many features of this problematic structure suggest deposition from offshore-flowing, upper-flow-regime, unidirectionally-dominated combined flow. Unidirectional flow at the seabed is the product of offshore-moving bottom currents generated during coastal set-up, although it may have been greatly enhanced by a shelf turbidity current. The more common occurrence of GUP lamination in lower-shoreface strata and its reduced abundance in shallow-offshore shelf deposits suggests the reduced competence of the unidirectional flow in an offshore direction. In addition, the paucity of hummocky cross-stratification (HCS) on the lower shoreface, but its abundance in offshore-shelf deposits may suggest a progressive increase in the importance of oscillatory flow in environments deeper than the lower shoreface.

Ichnology, or the study of trace fossils, has seen a dramatic explosion during the past decade. This is a direct result of the discovery by researchers of various geologic persuasions of the immense aid these biogenically produced primary structures provide in reconstructing modern and more importantly ancient sedimentary environments. Trace fossils reflect the in-situ behavioural response of a trace maker(s) to a set of environmental conditions, particularly the nature of the substrate. Properly identified, these structures along with various pertinent physical primary structures enable the accurate reconstruction of a sedimentary sequence. In this particular study the trace-fossil record helped verify a storm-dominated interpretation for the deposition of the Bootlegger Member. In addition, the biogenic record was instrumental in explaining a marked stratigraphic thickness disparity measured at two closely spaced study locations (the Ulm Pishkun and the Missile Tower). The exclusive occurrence of an anomalously vertically burrowed *Diplocraterion* and *Arenicolites* horizon at the Missile Tower indicated the presence of a semi-consolidated substrate, a condition that never existed at the Ulm Pishkun. This observation has been interpreted to indicate that sedimentation at the Ulm Pishkun was virtually constant, whereas the Missile Tower was an area of sediment by-pass and not deposition, thereby allowing for the development of a semi-consolidated substrate. With the eventual filling of the topographic low at the Ulm Pishkun and the development of equivalent bathymetric conditions, sedimentation at both study areas proceeded equally.

# REFERENCES

Arnott, R.W., 1987. Stratigraphy of the Lower Cretaceous Bootlegger Member near Great Falls, Montana and its relationship with the ancestral Sweetgrass Arch. Geological Association of Canada, Program with Abstracts, p. 22.

Cobban, W.A., Erdmann, C.E., Lemke, R.W., Maughn, E.K., 1959. Revision of Colorado Group on Sweetgrass Arch, Montana. American Association of Petroleum Bulletin Geologists, v. 43, pp. 2786-2796.

--------, 1976. Type sections and stratigraphy of the members of the Blackleaf and Marias River Formations (Cretaceous) of the Sweetgrass Arch, Montana. U.S.G.S. Professional Paper 974, 66 p.

Kauffman, E.G., 1985. Cretaceous evolution of the Western Interior Basin of the United States. *In* Pratt, L.M., Kauffman, E.G., Zelt, F.B., eds., Fine-grained deposits and biofacies of the Cretaceous Western Interior Seaway: evidence of cyclic sedimentary processes, Society of Economic Paleontologists and Mineralogists field guidebook No. 4, pp. IV-XIII.

-------, Cobban, W.A., Eicher, D.L., 1977. Albian through lower Coniacian strata, biostratigraphy and principals events, Western Interior United States. *In* Evenements de la Partie Moyenne du Cretace (Mid-Cretaceous events), Uppsala-Nice symposia, 1975-1976: Annales duMuseum d'Historie Naturelle de Nice, v. 4, pp. XXIII1-XXIII24.

Lorenz, J.C., 1982. Lithospheric flexure and the history of the SweetgrassArch, northwestern Montana. *In* Rocky Mountain Association of Geologists - 1982 Symposium, Geologic studies of the Cordilleran Thrust Belt, Vol. 1, pp. 77-89.

Stelck, C.R., Armstrong, J., 1981. Neogastroplites from southern Alberta. Bulletin of Canadian Petroleum Geology, v. 29, pp. 399-407.

Vail, P. R., Mitchum, R.M., Thompson, S., 1977. Seismic stratigraphy and global changes of sea level, Part 4: Global cycles of relative changes of sea level. *In* Payton, C.E., ed., Seismic stratigraphy - applications to hydrocarbon exploration, American Association of Petroleum Geologists Memoir 26, pp. 83-97.

Vuke, S.M., 1984. Depositional environments of the Early Cretaceous Western Interior Seaway in southwestern Montana and the northern United States. *In* Stott, D.F., Glass, D.J., eds., The Mesozoic of middle North America. Canadian Society of Petroleum Geologists Memoir 9, pp. 127-144.

Weimer, R.J., 1984. Relation of unconformities, tectonics, and sea-level changes, Cretaceous of Western Interior, United States. *In* Schlee, J.S., ed., Interregional unconformities and hydrocarbon accumulation, American Association of Petroleum Geologists Memoir 36, pp. 7-35.

# VI. APPENDIX I

I(A) The anisotropy of magnetic susceptibility

I(B) Data on magnetic susceptibility and anisotropy of magnetic susceptibility

## APPENDIX I (A): THE ANISOTROPY OF MAGNETIC SUSCEPTIBILITY

Magnetic susceptibility, or what could be more acurrately termed magnetic permeability, is a phenomenon which arises when a sample containing magnetic material is placed within an external magnetic field. In the study of magnetic susceptibility the main variables of interest are:

(1) magnetic field (T)
(2) intensity of magnetization (J)
(3) volume susceptibilty (k)

Volume susceptibility is the most important variable in most geologic studies and is directly related to the size, number and type of the magnetic materials present. By definition it represents the ratio between the measured induced intensity of magnetization (J) and the applied magnetic field (T) (Hood *et al.*, 1979):

$$k = J / T$$

Units of susceptibility are either in cgs (x 10-6 emu/cm$^{-3}$) or SI units, where:

$1\ k_{cgs} = 1 / (4\pi) * k_{SI}$ or,

$k_{SI} = 12.566371 * k_{cgs}$ where SI units are amps /metre (A m$^{-1}$)

The most important feature of magnetic susceptibility, rendering it useful for many geologic studies, is that in almost all cases a preferred directional alignment or anisotropy of magnetic susceptibility exists. This feature indicates the existence of an "easy" or preferred direction of magnetization when placed in an magnetic field, and can arise from two distinctly different sources. The first is a direct consequence of inherent crystalline anisotropy. This feature is a result of the preferred alignment of crystalline axes during crystal growth, which may also be augmented by anisotropic cleavage development (Rees, 1966). Crystalline anisotropy is important in rocks rich in hematite, although hematite is not a particularly abundant mineral in most sandstones (Boetzkes and Gough, 1975). The second and most important source of the anisotropy of magnetic susceptibility is due to shape anisotropy (Khan, 1962; Rees, 1965, 1966; Tarling, 1983). When an induced magnetic field is applied a ferromagnetic particle will attempt to demagnetize that field. However, its ability to do this is a function of the geometry of the grain, being greatest when the field is applied across the shortest dimension of the grain (diamagnetic), and least when applied across the longest dimension (paramagnetic) (Girdler, 1961; Rees, 1965). Shape anisotropy is a common trait of elongate grains composed of cubic crystals, of which magnetite (the most common magnetic mineral in sedimentary rocks) is such an example. Since magnetite has no preferred cleavage direction, cystalline anisotropy can be basically ignored, and virtually all the anisotropy of magnetic susceptibility is due to shape anisotropy (Rees, 1965). It has been shown that magnetite grains can by defined by an ellipsoid of revolution where the demagnetizing factors are related to the directions of the three orthogonal principal susceptibility axes:

$k_{max}$ = maximum principal susceptibility axis

$k_{int}$ = intermediate principal susceptibility axis

$k_{min}$ = minimum principal susceptibility axis

These axes along with their characteristic magnitudes formulate a second-order tensor which accurately describes the orientation of all the magnetic grains within a sample (Granar, 1958; Khan, 1962; Rees, 1965; Stupavsky, 1985). These are:

$k_a$ $k_b$ $k_c$ where, $k_{a,b,c}$ represent the suscseptibility values of the three

a b c principal susceptibility axes and a,b,c their respective angular orientations.

In reality the susceptibility axes correspond very closely to the three mutually orthogonal grain axes defining the length, width and depth of the grain (maximum, intermediate and short dimensions respectively). Collectively all three principal susceptibility axes evaluate the mean susceptibility of the sample:

$$\text{Mean Susceptibility } (k_{mean}) = (k_{max} + k_{int} + k_{min}) / 3$$

During the transport and deposition of a population of sediment grains hydrodynamic forces cause the grains to specifically align their axes to some aspect of the flow. This is a consequence of hydraulic stability and as a result gives rise to a preferential direction of magnetic susceptibility. This process is the basis for the development of sedimentary grain fabric and underlies the use of the anisotropy of magnetic susceptibility by sedimentologists (particularly for the determination of palaeocurrent directions). The development of grain fabric is the result of two main physical forces:

(1) the tangential shear stress generated at the bed by a viscous fluid, and;

(2) the gravitational force which acts normal to the depositional surface.

The tangential shear stress (fluid shear) tends to align the long-axis of the grain in either a parallel-to-flow orientation (Rusnak, 1957; Johansson, 1963, 1976; Allen, 1964; Rees, 1968; Hamilton *et al.*, 1968; Arnott, 1984, 1985; Hand and Arnott, in preparation) or transverse-to-flow orientation (Jeffrey, 1922; Hand, 1961; Khan, 1962; Johansson, 1963, 1976; Lindsay, 1968). Quantitatively the preferential alignment of the grain long axes within a sample has been described by:

$$L = \{(k_{max} - k_{int}) / k_{mean}\} * 100$$ L = magnetic lineation

where, L is a measure of the preferred alignment of maximum susceptibility (the grain long axes).

Large values of L reflect deposition from flows which prior to and during sediment deposition were capable of aligning the sediment grains (reflection of both flow strength and time).

The other major force influencing the development of grain fabric is the gravitational force, acting normal to the boundary. Gravity tends to align the plane containing the long and intermediate grain axes (commonly called the AB plane) parallel to the bed surface. Since the pole of this plane represents the minimum grain axis, a parameter assessing the orientation of several grains' AB planes would provide an indication of the dispersion of the minimum grain axes (and likewise susceptibility) :

$$F = \{[(k_{max} + k_{int}) / 2 - k_{min}] / k_{mean}\}$$ F = magnetic foliation plane

high values of F imply a preferred alignment of the minimum susceptibility axis. Commonly the long-intermediate axes plane is tilted with respect to the horizontal and usually imbricated upstream. Grain imbrication is an attempt by the sediment grain to attain maximum hydraulic stability while under the effect of fluid shear. Since the minimum susceptibility axis is perpendicular to this plane, the angle of grain imbrication is simply:

$\alpha = 90^{o} - I(k_{min})$ where $\alpha$ = angle of imbrication

$I$ = angle of minimum susceptibility axis

A parameter which has come into popular use is the ratio between magnetic lineation and the magnetic foliation:

$$q = L / F$$

and reflects the relative strength of its two constituent variables. Taira and Scholle (1979) suggest that the value of q may carry significance for the depositional environment . They point out that current-deposited sediments are characterised by low q values compared with the typically higher values exhibited by sediment-dispersion deposits. Variation in the value of q were thought to reflect differences in the nature of the sediment supporting and transporting mechanisms which were active prior to and during deposition.

## PROS AND CONS OF ANISOTROPY OF MAGNETIC SUSCEPTIBILITY (AMS)

One of the most positive attributes of this method is the ease of sample preparation and the speed of sample processing. Unlike acetate peel or microscopic methods for determining grain orientation, the AMS method only requires a right cylindrical sample 2.5 cm in diameter and 2.2 cm long. This size requirement (length : width = 0.85 : 1) has been found to give a minimum shape response to the measured susceptibility values (Porath *et al*., 1966), a particularly important phenomenon exhibited by weakly anisotropic samples. Once cored and the appropriate reference lines marked, the cylinder needs only to be fed into the measuring instrument "as is" in order to determine the grain orientation.

Although the AMS method has many advantages it is not without its shortcomings. One of the major problems concerns the basic sampling unit, the 2.5 cm x 2.2 cm cylindrical core. Due to its size the measured anisotropy of magnetic susceptibility is determined for the whole cylinder, so if one is interested in the grain orientation of a unit less than 2.2 cm thick (*e.g.* an individual lamina) this method is not applicable. The other major shortcoming is that the AMS method cannot independently assess multiple orientation modes of the anisotropy of magnetic susceptibility. Consequently, in samples with multiple modes of preferred grain long-axes alignment (*eg.* in planar-laminated sands, long-axes of grains typically show two modes separated by an angle of less than 30$^{\circ}$) this method will only average the multiple modes, thus giving a single composite averaged value.

However, even with its shorcomings the AMS method has been proven to be a powerful and simple tool for the sedimentary geologist. Particularly in the field of palaeogeographic and palaeohydrodynamic reconstruction this method has been proven useful; although its research potential I believe has still not been adequately recognised.

## THE SI-2 SYSTEM

In this study the SI-2 magnetic susceptibility and anisotropy instrument was used (Fig. 1). I would like to thank Dr. M. Stupavsky of Sapphire Instruments for lending me this instrument.

The SI-2 Magnetic Susceptibility And Anisotropy Instrument is compact, sensitive and very simple to use. Its only requirement is the use of a personal computer (equipped with a standard RS 232 serial port) for calculating the susceptibility tensor and storing of the compiled data. It uses a 2.5 cm x 2.2 cm right cylindrical sample core which can be of either consolidated or unconsolidated material. Sample processing time and measurement precision are directly related to the amount of magnetic material (typically magnetite) contained within the sample.

## MAGNETIC SUSCEPTIBILITY MEASUREMENT (MS):

The SI-2 instrument determines the magnetic susceptibility of the sample by comparing the inductance of the measuring coil: first with the sample removed (first air reading, A1), and then with the sample placed in the coil (sample reading, S). In order to check that the accuracy of the measured sample inductance (S) a second air measurement (A2) is made in order to determine the "drift" of the measured inductance over the measuring period (*i.e.* between the A1 and A2 readings). If the drift:

$$\text{Drift (D)} = A1 - A2$$

is too large, a prompt comes onto the screen "DRIFT TOO LARGE" and requires a remeasurement beginning again with the first air reading. If the calculated drift is within acceptable limits the magnetic susceptibility is calculated in terms of A1 and S:

$k = CF * [(SR / A1) * (SR / A1) - 1]$ where, $CF$ = the coil calibration factor

$SR$ = corrected sample reading $(S - 0.5*D)$

or in general terms,

$k_{ij} = M_i / H_j$ where, $k_{ij}$ = the susceptibilty measured with sample coordinates ij

$M_i$ = the induced magnetic moment with the direction i

$H_j$ = the effective applied field with direction j

For an isotropic medium the value of $k_{ij}$ is independent of sample orientation and the induced magnetic moment ($M_i$) is in the direction of the applied field ($H_j$) (coincident with the down-axis trend of the coil axis). However, in an anisotropic medium the value of $k_{ij}$ is dependent upon sample orientation (with respect to the coil axis) and is the basis for the study of the anisotropy of magnetic susceptibility (discussed below).

Precision of the magnetic susceptibility measurement is controlled by four factors. By manipulating various combinations of these factors accurate measurements can be made on even weakly magnetic samples. These factors are:

(1) measurement precision is approximately linearly proportional to the magnetic susceptibilty of the sample (however, this is dependent on the composition of the sample and cannot be adjusted);

(2) precision of the measurement increases as the amount of the coil filled by the sample increases (for weakly magnetic samples smaller coil diameter enhances the measured signal);

(3) precision of the measurement increases proportionately with the measuring time (for weakly magnetic samples, increase the measuring time from 1 to 2 to 4 up to 8 seconds);

(4) precision of the measured value can be improved by signal averaging (signal stacking). The improvement of the signal : instrument noise ratio is approximately proportional to SQR (N), where N is the number of repeat measurements.

## ANISOTROPY OF MAGNETIC SUSCEPTIBILITY MEASUREMENT (AMS):

For most sedimentologic studies the anisotropy of magnetic susceptibility is the parameter of primary importance. As noted above the direction of the maximum susceptibility closely corresponds to the preferential alignment of the magnetic grain long axes within the sample. As this feature can be used for palaeocurrent and palaeohydrodynamic reconstructions, it is obvious that the AMS method is a valuable tool in sedimentary studies.

The SI-2 instrument measures the AMS of a sample by measuring the magnetic susceptibility for 6, 12 or 24 specified sample orientations. Six orientations are the minimum number required to fill the magnetic susceptibility ellipsoid, a symmetric second-order tensor:

$k_{11}$ $k_{12}$ $k_{13}$ where, 1, 2 and 3 represent the x, y, and z
$k_{21}$ $k_{22}$ $k_{23}$ coordinate axes (with respect to the coil axis)
$k_{31}$ $k_{32}$ $k_{33}$

these six elements are equivalent to:

$k_a$ $k_b$ $k_c$ where, $k_{a,b,c}$ represent the suscseptibility values of the three principal susceptibility axes;
a b c a,b,c their respective angular orientations.

The 12 and 24 specimen orientations determine the six tensor elements 2 and 4 times respectively. However, signal stacking (repeat measurements of each of the 6 specified AMS orientations) enables one to stack AMS values in excess of 4 repeat measurements, and is the method used in this study.

The coordinate system used in the analysis is illustrated in Figure 2:

(1) Axis 1 = the orienting line on the surface of the sample (typically the north arrow)

(2) Axis 2 = is $90^{O}$ clockwise with respect to Axis 1

(3) Axis 3 = is $90^{O}$ to both Axes 1 and 2.

(in the Cartesian coordinate system these axes correspond to the x, y and z directions respectively).

If the individual axes are considered unit vectors then the six orientations necessary to fill the susceptibility tensor and their corresponding susceptibility values are:

| | |
|---|---|
| (1) S1 = (1,0,0) | k11 |
| (2) S2 = (1,1,0) / SQR (2) | k12 + (k11 + k22) / 2 |
| (3) S3 = (0,1,0) | k22 |
| (4) S4 = (0,0,1) | k33 |
| (5) S5 = (1,0,1) / SQR (2) | k13 + (k11 + k33) / 2 |
| (6) S6 = (0,1,1) / SQR (2) | k23 + (k22 +k33) / 2 |

IMPORTANT: Each susceptibility orientation is defined with respect to the down-axis trend of the measuring coil axis.

By computing the magnetic susceptibility for each of the 6 sample orientations the direction of the three mean principal magnetic susceptibility axes defining the magnetic susceptibility ellipsoid are determined. Each principal susceptibility axis is represented by an axial vector (axial vectors are composed of a vector and its corresponding antiparallel vector, akin to a bimodal distribution in which the modes are $180^{O}$ apart). The axial vectors defining the three principal magnetic susceptibility axes are:

R1 = (X1, Y1, Z1) and (-X1, -Y1, -Z1) maximum
R2 = (X2, Y2, Z2) and (-X2, -Y2, -Z2) intermediate
R3 = (X3, Y3, Z3) and (-X3, -Y3, -Z3) minimum

Also included in the SI-2 program are a number of statistical packages used to determine the significance of the three calculated principal susceptibility axes. These packages are applicable only when multiple measurements are made of each of the six specified sample orientations (the twelve and twenty-four orientation sequence do not allow repeat measurements). In this study four repeat measurements were made, each with a four-second read time. The calculated values of the three susceptibility axes were evaluated with respect to the radius of the circle of 95% confidence. The physical meaning of this statistical procedure is that one can be 95% confident that the true direction of each of the three magnetic susceptibility axes lies within a 95% confidence circle having the respective determined mean susceptibility direction at its centre and a radius equal to R95, where the radius is given by:

R95 = (1.96 / N) * SQR (sum of squares of the angular deviations)

where: N = the number of repeat measurements
R95 is in degrees.

For a perfectly unimodal distribution R95 = 0, whereas values > 0 reflect the influence of instrument noise and within-sample magnetic susceptibility inhomogeneity. As these influences become progressively stronger the reliability of the calculated principal susceptibility axes becomes increasingly suspect. R95 values based on number of repeated measurements have been tabulated in Harrison (1980). This table indicates that for the four repeated measurements used in this study a 95% confidence level corresponded to a basement R95 value < 46 degrees.

In this study the use of the anisotropy of magnetic susceptibility did not prove to be all that beneficial. This is a direct result of the low abundance of magnetic particles within the clastic sediment composing the Bootlegger Member. As pointed out by Stupavsky (1985), in order for the SI-2 to measure the three susceptibility axes reliably the sample signal : instrument noise ratio should be a minimum of 100 : 1. Since the typical instrument noise level was about 1E-7 SI units, the minimum magnetic sample susceptibility had to be at least or in excess of 1E-5. Unfortunately, most of the Bootlegger Member samples were characterised by magnetic susceptibility values within the 1E-6 range. This low magnetic content translated into calculated principal magnetic susceptibility axes characterised by R95 values typically greater than 46, and consequently are of questionable validity. However, as pointed out in Paper 1 this procedure was useful in identifying transgressive lag deposits. These were characterised by magnetic susceptibilites which were commonly a half to a full order of magnitude higher than the underlying regressive portion of the regressive/transgressive couplet. In addition, anisotropy of magnetic susceptibility indicated that even closely spaced samples illustrate markedly different preferred grain alignment. Together these two characteristics are may indicate reworking of the underlying regressive portion of the regressive/transgressive couplet. Transgression led to the concentrating of magnetic material (due to their high density and resultant hydraulic equivalence) within the lag deposits, thus accounting for the anomalously high value of magnetic susceptibility. Random grain alignment illustrated between adjacent samples would suggest long-term transgressive lag deposition which resulted in the development and superposition of several independent grain fabrics, each possibly related to a particular sedimentation event.

# REFERENCES

Allen, J.R.L., 1964. Primary current lineation in the Lower Old Red Sandstone (Devonian) Anglo-Welsh Basin. Sedimentology, v. 3, pp. 89-108.

Arnott, R.W., 1984. Proximal channel deposits of the Hadrynian Hector Formation, Lake Louise, Alberta. Unpublished MSc. thesis, University of Alberta, 149p.

------, 1985. Depositional characteristics of an Upper Precambrian submarine canyon-fill. Lake Louise, Alberta, Society of Economic Paleontologists and Mineralogists, Prog. with Abstr., p. 7.

Boetzkes, P.C., Gough, D.I., 1975. A spinner magnetometer for susceptibility anisotropy in rocks. Canadian Journal of Earth Sciences, v. 12, pp. 1448-1464.

Girdler, R.W., 1961. The measurement and computation of anisotropy of magnetic susceptibility. The Geophysical Journal of the Royal Astronomical Society, v. 4, pp. 34-44.

Granar, L., 1957. Magnetic measurements on Swedish varved sediments. Arkiv Geofysik. v. 3, pp. 1-40.

Hamilton, N., Owens, W.H., Rees, A.I., 1968. Laboratory experiments on the production of grain orientation in sheared sand. Journal of Geology, v. 76, pp. 465-472.

Hand, B.M., 1961. Grain orientation in turbidites. Compass of Sigma Gamma Epsilon, v. 38, pp. 133-144.

Harrison, C.G.A., 1980. Analysis of the magnetic vector of a single rock specimen. Journal of the Royal Astronomical Society, v. 60, pp. 489-492.

Hood, P.J., Holroyd, M.T., McGrath, P.H., 1979. Magnetic methods applied to base metal exploration. *In* : Hood, P.J., ed., Geophysics and geochemistry in the search for metallic ores, Geological Survey of Canada, Economic Geology Report 31, pp. 77-104.

Jeffrey, G.B., 1922. The motion of ellipsoid particles immersed in a viscous fluid. Royal Society of London Proceedings, Series A, v. 102, pp. 161-179.

Johansson, C.E., 1976. Structural studies of frictional sediments. Geografiska Annaler. Series A, v. 58, pp. 201-301.

-------, 1963. Orientation of pebbles in running water. A laboratory study . Geografiska Annaler, v. 45, pp. 85-112.

Khan, M.A., 1962. The anisotropy of magnetic susceptibility of some igneous and metamorphic rocks. Journal of Geophysical Research, v. 67, pp. 2873-2885.

Lindsay, J.F., 1968. The development of clast fabric. Journal of Sedimentary Petrology, v. 38, pp. 1242-1253.

Porath, H., Stacey, F.D., Cheam, A.S., 1966. The choice of specimen shape for magnetic anisotropy measurements of rocks. Earth and Planetary Science Letters, v. 1, 92p.

Rees, A.I., 1968. The production of preferred orientation in a concentrated dispersion of elongated and flattened grains. Journal of Geology, v. 76, pp. 457-465.

-------, 1966. The effect of depositional slopes on the anisotropy of magnetic susceptibility of laboratory deposited sands, Journal of Geology, v. 74, pp. 856-867.

-------, 1965. The use of anisotropy of magnetic susceptibility in the estimation of sedimentary fabric. Sedimentology, v. 4, pp. 257-271.

Rusnak, G.A., 1957. Orientation of sand grains under conditions of unidirectional flow. Journal of Geology, v. 65, pp. 384-409.

Stupavsky, M., 1985. SI-2 magnetic susceptibility and anisotropy instrument operating manual and handbook, 131 p.

Taira, A., Scholle, P.A., 1979. Deposition of resedimented sandstone beds in the Pico Formation, Ventura Basin, California, as interpreted from magnetic measurements. Geological Society of America Bulletin, v. 90, pp. 952-962.

Tarling, D.H., 1983. Palaeomagnetism: Principals and applications in geology, geophysics and archaeology. Chapman and Hall Ltd., London, 379 p.

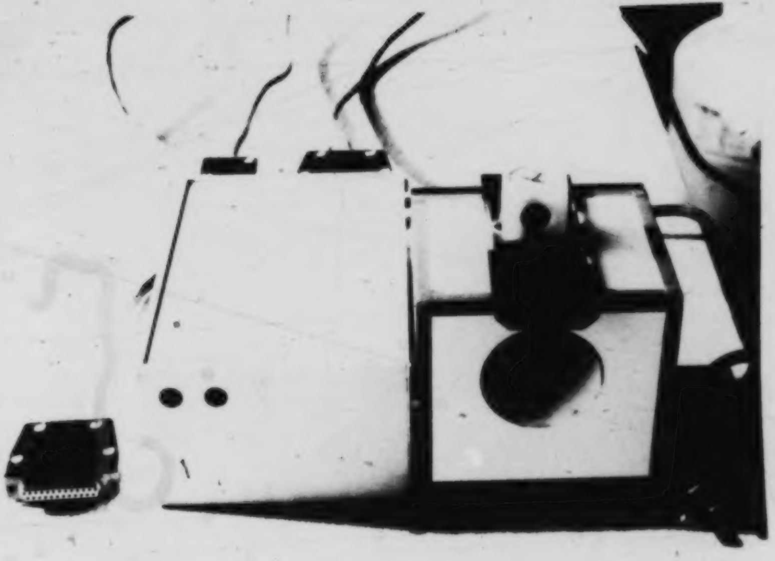

FIGURE VI(A)-1: Photo and diagrammatic sketch of the SI-2 Magnetic Anisotropy and Susceptibility Instrument.

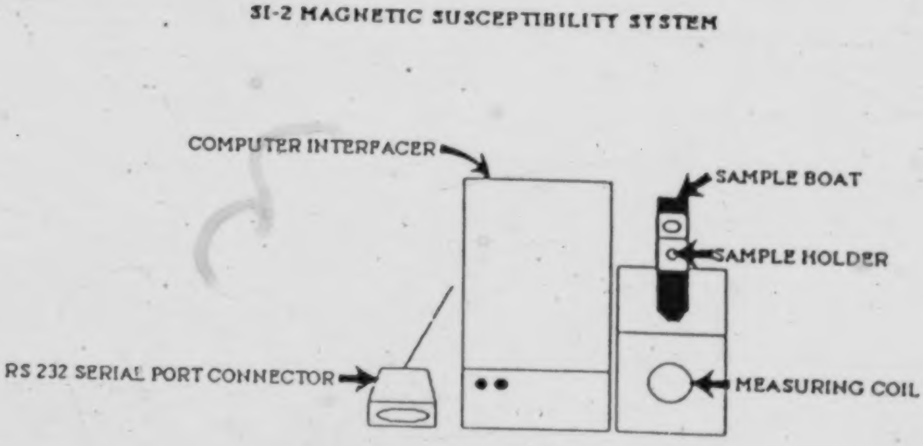
SI-2 MAGNETIC SUSCEPTIBILITY SYSTEM
COMPUTER INTERFACER
SAMPLE BOAT
SAMPLE HOLDER
RS 232 SERIAL PORT CONNECTOR
MEASURING COIL

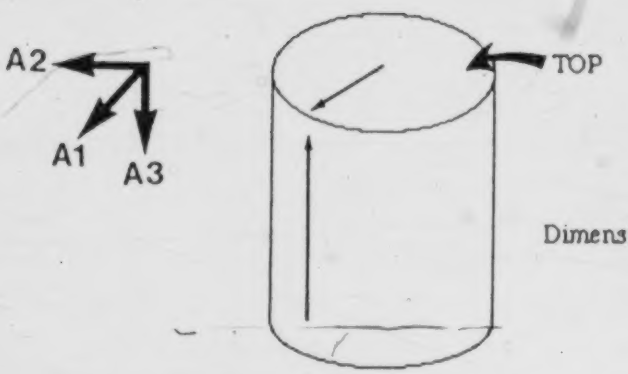

Dimensions: 2.2 cm x 2.5 cm
0.85 in x 1.0 in
(length x width)

SAMPLE COORDINATE SYSTEM

A1 (Axis 1) = orienting line on top of sample (typically the direction of true north marked on the sample in the field).

A2 (Axis 2) = is 90 degrees clockwise from A1 when viewed from the top

A3 (Axis 3) = is 90 degrees from both Axes 1 and 2 and is directed downward

FIGURE VI(A)-2: Sample coordinate system used for measurements of anisotropy of magnetic susceptibility

# APPENDIX I (B): DATA ON MAGNETIC SUSCEPTIBILITY AND ANISOTROPY OF MAGNETIC SUSCEPTIBILITY

The following is a tabulation of data concerning magnetic susceptibility and anisotropy of magnetic susceptibility measured from Bootlegger Member strata outcropping in the Great Falls study area. Most of the data pertain to readings derived from "gently undulating parallel laminated" (GUP lamination) strata from the Ulm Pishkun (i.e. Sections 1-5 and Sections 9-14). Data from Sections 6-8 at the Ulm Pishkun represent planar-laminated foreshore strata. All other data are appropriately described with respect to their location of origin and the nature of the structure sampled.

As can be seen from the data, due to the low abundance of magnetic material in the samples (resulting in a low signal : noise ratio) the calculated susceptibility axes and their preferential orientation are for the most part somewhat questionable. However, in some samples higher magnetic susceptibily measurements enabled a more statistically significant assessment of preferential orientation and thus palaeocurrent direction.

## SCHEME OF DATA PRESENTATION AND DEFINITION OF VARIABLES

### SUSCEPTIBILITY

NR = 4 -- number of repeated measurements

T = 4 seconds -- the length of sample read time

MS (SI v) = the magnetic susceptibility of the sample (measured in one random orientation) measured in SI volume units (SI v)

SDEV (SI v) = standard deviation measured in SI volume units (SI v). This value represents the level of instrument noise

## ANISOTROPY

M = 6 -- the number of sample orientations used to fill the anisotropy tensor

NR = 4 -- the number of repeated measurements for each of the 6 sample orientations

T = 4 seconds -- the sample read time for each measurement

MIN -- DEC = INC = R95 = EV = SD =

INT --

MAX --

MIN, INT AND MAX -- the respective minimum, intermediate and maximum susceptibility axes

DEC -- the declination of that particular susceptibility axes (measured from 0 to 360 degrees)

INC -- the inclination from the horizontal of that particular susceptibility axes (measured from 0 - 90 degrees in which: +ve = downward dip & -ve = upward dip)

R95 -- measure of the radius of the 95 % confidence circle about that particular susceptibility axes (measure of the inhomogeneity of "in-sample" anisotropy)

EV -- measure of the intensity of the signal for that particular susceptibility axes

SD -- measure of the noise level of the instrument

### SITE: ULM PISHKUN - Sec. 1

**SUSCEPTIBILITY**
NR = 4
T = 4 seconds

MS (SI v) = 9.283 x 10-5
SDEV (SI v) = 1.111 x 10-6

**ANISOTROPY**
M = 6
NR = 4
T = 4 seconds

| | | | | | |
|---|---|---|---|---|---|
| MIN -- | DEC = 294.17 | INC = -40.19 | R95 = 42.9 | EV = 8.211 x 10-5 | SD = 8.263 x 10-6 |
| INT -- | 14.98 | 10.70 | 53.0 | 9.195 x 10-5 | 6.49 x 10-7 |
| MAX-- | 272.94 | 47.80 | 38.1 | 1.033 x 10-4 | 7.781 x 10-6 |

### SITE: ULM PISHKUN - Sec. 2

**SUSCEPTIBILITY**
NR = 4
T = 4 seconds

MS (SI v) = 6.705 x 10-5
SDEV (SI v) = 1.264 x 10-6

**ANISOTROPY**
M = 6
NR = 4
T = 4 seconds

| | | | | | |
|---|---|---|---|---|---|
| MIN -- | DEC = 8.02 | INC= -88.47 | R95 = 24.2 | EV = 6.375 x 10-5 | SD = 4.840 x 10-7 |
| INT -- | = 320.20 | 1.04 | 39.7 | 6.546 x 10-5 | 1.108 x 10-6 |
| MAX-- | = 50.22 | 1.11 | 32.0 | 6.735 x 10-5 | 5.358 x 10-7 |

### SITE: ULM PISHKUN - Sec. 2

**SUSCEPTIBILITY**
NR = 4
T = 4 seconds

MS (SI v) = 6.443 x 10-5
SDEV (SI v) = 1.804 x 10-6

**ANISOTROPY**
M = 6
NR = 4
T = 4 seconds

| | | | | | |
|---|---|---|---|---|---|
| MIN -- DEC | = 356.20 | INC = 81.77 | R95 = 5.7 | EV = 5.564 x 10-5 | SD = 3.971 x 10-7 |
| INT -- | = 315.82 | -6.28 | 26.7 | 6.392 x 10-5 | 1.171 x 10-6 |
| MAX-- | = 46.40 | -5.28 | 26.9 | 6.613 x 10-5 | 9.651 x 10-7 |

**SITE**: ULM PISHKUN - Sec. 2

**SUSCEPTIBILITY**
NR = 4
T = 4 seconds

MS (SI v) = 4.558 x 10-5
SDEV (SI v) = 3.128 x 10-7

**ANISOTROPY**
M = 6
NR = 4
T = 4 seconds

| | | | | | |
|---|---|---|---|---|---|
| MIN -- DEC | = 290.16 | INC = -78.17 | R95 = 15.8 | EV = 4.062 x 10-5 | SD = 5.083 x 10-7 |
| INT -- | = 335.77 | 8.33 | 28.0 | 4.380 x 10-5 | 9.754 x 10-7 |
| MAX-- | = 64.53 | -8.33 | 24.8 | 4.558 x 10-5 | 2.364 x 10-7 |

**SITE**: ULM PISHKUN - Sec. 2

**SUSCEPTIBILITY**
NR = 4
T = 4 seconds

MS (SI v) = 1.307 x 10-4
SDEV (SI v) = 1.97 x 10-7

**ANISOTROPY**
M = 6
NR = 4
T = 4 seconds

| | | | | | |
|---|---|---|---|---|---|
| MIN -- DEC | = 9.93 | INC = 75.25 | R95 = 19.7 | EV = 1.229 x 10-4 | SD = 5.011 x 10-7 |
| INT -- | = 29.83 | -13.90 | 19.8 | 1.258 x 10-4 | 9.773 x 10-7 |
| MAX-- | = 298.64 | -4.82 | 2.6 | 1.439 x 10-4 | 8.376 x 10-7 |

**SITE**: ULM PISHKUN - Sec. 3

**SUSCEPTIBILITY**
NR = 4
T = 4 seconds

MS (SI v) = 6.855 x 10-5
SDEV (SI v) = 6.693 x 10-7

ANISOTROPY
M = 6
NR = 4
T = 4 seconds

MIN -- DEC = 54.37 INC = 84.64 R95 = 3.8 EV = 5.428 x 10-5 SD = 4.148 x 10-7
INT -- = 317.17 0.69 32.8 6.490 x 10-5 1.094 x 10-6
MAX-- = 47.10 -5.31 3.4 7.258 x 10-5 5.455 x 10-7

**SITE**: ULM PISHKUN - Sec. 3

SUSCEPTIBILITY
NR = 4
T = 4 seconds

MS (SI v) = 2.824 x 10-5
SDEV (SI v) = 8.164 x 10-6

ANISOTROPY
M = 6
NR = 4
T = 4 seconds

MIN -- DEC = 28.94 INC = -77.79 R95 = 19.9 EV = 3.364 x 10-5 SD = 7.405 x 10-6
INT -- = 353.50 9.99 37.6 4.236 x 10-5 1.189 x 10-6
MAX-- = 84.72 6.93 37.3 4.302 x 10-5 8.875 x 10-7

**SITE**: ULM PISHKUN - Sec. 5

SUSCEPTIBILITY
NR = 4
T = 4 seconds

MS (SI v) = 4.380 x 10-5
SDEV (SI v) = 2.112 x 10-7

ANISOTROPY
M = 6
NR = 4
T = 4 seconds

MIN -- DEC = 32.00 INC = 80.01 R95 = 7.2 EV = 3.320 x 10-5 SD = 3.750 x 10-7
INT -- = 71.00 -7.71 25.6 4.298 x 10-5 4.242 x 10-7
MAX-- = 340.84 -6.30 23.6 4.411 x 10-5 1.049 x 10-6

**SITE**: ULM PISHKUN - Sec. 14

SUSCEPTIBILITY
NR = 4
T = 4 seconds

MS (SI v) = 4.126 x 10-5
SDEV (SI v) = 3.663 x 10-7

ANISOTROPY
M = 6
NR = 4
T = 4 seconds

| | | | | | |
|---|---|---|---|---|---|
| MIN -- | DEC = 317.62 | INC = 81.10 | R95 = 11.5 | EV = 3.635 x 10-5 | SD = 5.680 x 10-7 |
| INT -- | = 302 .29 | -8.58 | 54.4 | 4.119 x 10-5 | 4.150 x 10-7 |
| MAX-- | = 32.64 | -2.31 | 37.6 | 4.222 x 10-5 | 2.129 x 10-7 |

**SITE**: ULM PISHKUN - Sec. 6

SUSCEPTIBILITY
NR = 4
T = 4 seconds

MS (SI v) = 4.507 x 10-5
SDEV (SI v) = 2.116 x 10-7

ANISOTROPY
M = 6
NR = 4
T = 4 seconds

| | | | | | |
|---|---|---|---|---|---|
| MIN -- | DEC = 295.67 | INC = 65.69 | R95 = 22.4 | EV = 4.240 x 10-5 | SD = 1.112 x 10-6 |
| INT -- | = 333.41 | -19.65 | 42.4 | 4.490 x 10-5 | 9.625 x 10-7 |
| MAX-- | = 58.40 | 13.72 | 39.7 | 4.652 x 10-5 | 1.073 x 10-6 |

**SITE**: ULM PISHKUN - Sec. 6

SUSCEPTIBILITY
NR = 4
T = 4 seconds

MS (SI v) = 5.797 x 10-5
SDEV (SI v) = 7.665 x 10-7

ANISOTROPY
M = 6
NR = 4
T = 4 seconds

| | | | | | |
|---|---|---|---|---|---|
| MIN -- | DEC = 37.15 | INC = 58.67 | R95 = 15.2 | EV = 5.683 x 10-5 | SD = 4.976 x 10-7 |
| INT -- | = 54.34 | -30.17 | 45.0 | 5.922 x 10-5 | 4.344 x 10-7 |
| MAX-- | = 319.87 | -7.63 | 45.3 | 5.961 x 10-5 | 2.617 x 10-7 |

**SITE**: ULM PISHKUN - Sec. 6

SUSCEPTIBILITY
NR = 4
T = 4 seconds

MS (SI v) = 4.189 x 10-5
SDEV (SI v) = 5.985 x 10-7

ANISOTROPY
M = 6
NR = 4
T = 4 seconds

| | | | | |
|---|---|---|---|---|
| MIN -- DEC = 328.36 | INC = 72.77 | R95 = 12.5 | EV = 3.784 x 10-5 | SD = 6.135 x 10-7 |
| INT -- = 288.37 | -13.36 | 17.4 | 4.076 x 10-5 | 6.401 x 10-7 |
| MAX-- = 20.94 | -10.66 | 16.1 | 4.254 x 10-5 | 5.012 x 10-7 |

**SITE**: ULM PIASHKUN - Sec. 6

SUSCEPTIBILITY
NR = 4
T = 4 seconds

MS (SI v) = 2.994 x 10-5
SDEV (SI v) = 1.009 x 10-6

ANISOTROPY
M = 6
NR = 4
T = 4 seconds

| | | | | |
|---|---|---|---|---|
| MIN -- DEC = 70.97 | INC = -73.09 | R95 = 28.1 | EV = 2.669 x 10-5 | SD = 1.362 x 10-6 |
| INT -- = 304.87 | -10.15 | 52.8 | 2.882 x 10-5 | 2.899 x 10-7 |
| MAX-- = 32.42 | 13.37 | 43.0 | 3.031 x 10-5 | 7.766 x 10-7 |

**SITE**: ULM PISHKUN - Sec. 6

SUSCEPTIBILITY
NR = 4
T = 4 seconds

MS (SI v) = 3.507 x 10-5
SDEV (SI v) = 4.560 x 10-6

ANISOTROPY
M = 6
NR = 4
T = 4 seconds

| | | | | |
|---|---|---|---|---|
| MIN -- DEC = 33.58 | INC = 82.41 | R95 = 9.9 | EV = 3.311 x 10-5 | SD = 2.557 x 10-7 |
| INT -- = 332.31 | -3.66 | 33.7 | 4.182 x 10-5 | 5.947 x 10-7 |
| MAX-- = 62.74 | -6.63 | 33.9 | 4.268 x 10-5 | 6.528 x 10-7 |

**SITE**: ULM PISHKUN - Sec. 6

SUSCEPTIBILITY
NR = 4
T = 4 seconds

MS (SI v) = 2.035 x 10-5
SDEV (SI v) = 8.279 x 10-7

ANISOTROPY
M = 6
NR = 4
T = 4 seconds

| | | | | |
|---|---|---|---|---|
| MIN -- DEC = 29.92 | INC = 82.85 | R95 = 16.6 | EV = 1.628 x 10-5 | SD = 7.633 x 10-7 |
| INT -- = 312.17 | -1.52 | 48.4 | 1.967 x 10-5 | 1.016 x 10-6 |
| MAX-- = 42.36 | -6.97 | 39.3 | 2.119 x 10-5 | 7.983 x 10-7 |

**SITE**: ULM PISHKUN - Sec. 6

SUSCEPTIBILITY
NR = 4
T = 4 seconds

MS (SI v) = 2.356 x 10-5
SDEV (SI v) = 2.370 x 10-7

ANISOTROPY
M = 6
NR = 4
T = 4 seconds

| | | | | |
|---|---|---|---|---|
| MIN -- DEC = 21.24 | INC = 63.84 | R95 = 20.6 | EV = 2.225 x 10-5 | SD = 3.851 x 10-7 |
| INT -- = 335.94 | -19.05 | 24.2 | 2.434 x 10-5 | 1.804 x 10-7 |
| MAX-- = 72.09 | -17.22 | 16.8 | 2.692 x 10-5 | 2.482 x 10-7 |

**SITE**: ULM PISHKUN - Sec. 6

SUSCEPTIBILITY
NR = 4
T = 4 seconds

MS (SI v) = 6.243 x 10-5
SDEV (SI v) = 4.019 x 10-7

ANISOTROPY
M = 6
NR = 4
T = 4 seconds

MIN -- DEC = 68.99 INC = 84.54 R95 = 8.3 EV = 4.741 x 10-5 SD = 6.004 x 10-7
INT -- = 87.78 -5.17 27.4 6.121 x 10-5 1.281 x 10-7
MAX-- = 357.60 -1.74 27.1 6.298 x 10-5 1.314 x 10-7

**SITE**: ULM PISHKUN - Sec. 6

SUSCEPTIBILITY
NR = 4
T = 4 seconds

MS (SI v) = 3.541 x 10-5
SDEV (SI v) =1.210 x 10-6

ANISOTROPY
M = 6
NR = 4
T = 4 seconds

MIN -- DEC = 321.55 INC = -76.79 R95 = 18.8 EV = 2.979 x 10-5 SD = 9.475 x 10-7
INT -- = 317.02 13.17 42.1 3.427 x 10-5 4.475 x 10-7
MAX-- = 47.26 1.00 39.4 3.514 x 10-5 3.139 x 10-7

**SITE**: ULM PISHKUN - Sec. 6

SUSCEPTIBILITY
NR = 4
T = 4 seconds

MS (SI v) = 3.795 x 10-5
SDEV (SI v) = 8.498 x 10-7

ANISOTROPY
M = 6
NR = 4
T = 4 seconds

MIN -- DEC = 30.63 INC = 86.40 R95 = 11.9 EV = 3.137 x 10-5 SD = 5.414 x 10-7
INT -- = 292.78 0.50 35.3 3.769 x 10-5 7.137 x 10-7
MAX-- = 22.74 -3.56 34.8 3.850 x 10-5 6.518 x 10-7

**SITE**: ULM PISHKUN - Sec. 6

SUSCEPTIBILITY
NR = 4
T = 4 seconds

MS (SI v) = 3.795 x 10-5
SDEV (SI v) = 4.498 x 10-7

ANISOTROPY
M = 6
NR = 4
T = 4 seconds

MIN -- DEC = 33.57 INC = -75.62 R95 = 14.8 EV = 3.215 x 10-5 SD = 6.494 x 10-7
INT -- = 333.63 7.31 31.6 3.677 x 10-5 9.295 x 10-7
MAX-- = 65.23 12.30 36.4 3.820 x 10-5 4.141 x 10-7

**SITE**: MISSILE TOWER SECTION - Sec. 3

SUSCEPTIBILITY
NR = 4
T = 4 seconds

MS (SI v) = 3.440 x 10-5
SDEV (SI v) = 6.853 x 10-7

ANISOTROPY
M = 6
NR = 4
T = 4 seconds

MIN -- DEC = 332.39 INC = -87.19 R95 = 12.9 EV = 2.881 x 10-5 SD = 8.320 x 10-7
INT -- = 88.89 -1.25 44.5 3.392 x10-5 5.389 x 10-7
MAX-- = 358.81 2.50 44.5 3.416 x 10-5 5.518 x 10-7

**SITE**: MISSILE TOWER SECTION - Sec. 3

SUSCEPTIBILITY
NR = 4
T = 4 seconds

MS (SI v) = 5.753 x 10-5
SDEV (SI v) = 1.212 x 10-7

ANISOTROPY
M = 6
NR = 4
T = 4 seconds

MIN -- DEC = 15.53 INC = 86.64 R95 = 6.3 EV = 4.528 x 10-5 SD = 5.811 x 10-7
INT -- = 310.35 -1.41 39.8 5.594 x 10-5 8.864 x 10-7
MAX-- = 40.42 -3.04 39.5 5.753 x 10-5 5.902 x 10-7

**SITE**: MISSILE TOWER SECTION - Sec. 3

SUSCEPTIBILITY
NR = 4
T = 4 seconds

MS (SI v) = 3.883 x 10-5
SDEV (SI v) = 7.901 x 10-7

ANISOTROPY
M = 6
NR = 4
T = 4 seconds

MIN -- DEC = 59.40 INC = -83.65 R95 = 14.0 EV = 3.109 x 10-5 SD = 6.345 x 10-7
INT -- = 56.24 6.33 47.0 3.808 x 10-5 5.309 x 10-7
MAX-- = 326.28 -0.34 45.8 3.884 x 10-5 8.953 x 10-7

**SITE**: WILLOW CREEK RANCH - Sec. 2 (GUP lamination)

SUSCEPTIBILITY
NR = 4
T = 4 seconds

MS (SI v) = 2.611 x10-5
SDEV (SI v) = 6.258 x 10-7

ANISOTROPY
M = 6
NR = 4
T = 4 seconds

MIN -- DEC = 61.51 INC = -80.96 R95 = 9.6 EV = 2.097 x 10-5 SD = 9.312 x 10-7
INT -- = 323.24 -1.32 7.9 2.393 x 10-5 9.996 x 10-7
MAX-- = 53.03 8.93 12.2 2.695 x 10-5 5.452 x 10-7

**SITE**: WILLOW CREEK RANCH - Sec. 2 (GUP lamination)

SUSCEPTIBILITY
NR = 4
T = 4 seconds

MS (SI v) = 7.590 x 10-5
SDEV (SI v) = 7.336 x 10-7

**ANISOTROPY**
M = 6
NR = 4
T = 4 seconds

| | | | | | |
|---|---|---|---|---|---|
| MIN -- | DEC = 296.87 | INC = -85.61 | R95 = 2.4 | EV = 5.626 x 10-5 | SD = 9.672 x 10-7 |
| INT -- | = 354.06 | 2.38 | 10.6 | 7.584 x 10-5 | 5.642 x 10-7 |
| MAX-- | = 83.89 | -3.67 | 10.3 | 7.750 x 10-5 | 5.778 x 10-8 |

**SITE**: WILLOW CREEK RANCH - Sec 2 (FORESHORE)

**SUSCEPTIBILITY**
NR = 4
T = 4 seconds

MS (SI v) = 5.155 x 10-5
SDEV (SI v) = 1.152 x 10-6

**ANISOTROPY**
M = 6
NR = 4
T = 4 seconds

| | | | | | |
|---|---|---|---|---|---|
| MIN -- | DEC = 70.14 | INC = -88.75 | R95 = 13.5 | EV = 4.491 x 10-5 | SD = 9.167 x 10-7 |
| INT -- | = 280.57 | -1.08 | 39.8 | 5.042 x 10-5 | 9.358 x 10-7 |
| MAX-- | = 10.55 | 0.62 | 38.8 | 5.203 x 10-5 | 3.195 x 10-7 |

**SITE**: BLACK HORSE LAKE - SOUTH SIDE - Transgressive sandstone (1)

**SUSCEPTIBILITY**
NR = 4
T = 4 seconds

MS (SI v) = 1.384 x 10-4
SDEV (SI v) = 1.008 x 10-6

**ANISOTROPY**
M = 6
NR = 4
T = 4 seconds

| | | | | | |
|---|---|---|---|---|---|
| MIN -- | DEC = 35.37 | INC = 82.39 | R95 = 1.0 | EV = 9.341 x 10-5 | SD = 3.734 x 10-7 |
| INT -- | = 16.47 | -7.19 | 6.8 | 1.378 x 10-4 | 1.300 x 10-7 |
| MAX-- | = 286.78 | 2.43 | 6.8 | 1.419 x 10-4 | 9.637 x 10-7 |

**SITE**: BLACK HORSE LAKE - SOUTH SIDE - Transgressive sandstone (2)

SUSCEPTIBILITY
NR = 4
T = 4 seconds

MS (SI v) = 4.625 x 10-5
SDEV (SI v) = 1.416 x 10-6

ANISOTROPY
M = 6
NR = 4
T = 4 seconds

| | | | | |
|---|---|---|---|---|
| MIN -- DEC = 316.84 | INC = 64.18 | R95 = 23.6 | EV = 4.190 x 10-5 | SD = 1.208 x 10-6 |
| INT -- = 285.94 | -22.54 | 36.4 | 4.523 x 10-5 | 9.011 x 10-7 |
| MAX-- = 20.97 | -11.91 | 33.7 | 4.839 x 10-5 | 1.468 x 10-6 |

**SITE**: BLACK HORSE LAKE - SOUTH SIDE - Transgressive sandstone (3)

SUSCEPTIBILITY
NR = 4
T = 4 seconds

MS (SI v) = 6.351 x 10-5
SDEV (SI v) = 7.342 x 10-7

ANISOTROPY
M = 6
NR = 4
T = 4 seconds

| | | | | |
|---|---|---|---|---|
| MIN -- DEC = 341.70 | INC = 78.57 | R95 = 1.9 | EV = 4.315 x 10-5 | SD = 5.358 x 10-7 |
| INT -- = 79.43 | 1.56 | 6.8 | 6.074 x 10-5 | 6.705 x 10-7 |
| MAX-- = 349.74 | -11.31 | 6.9 | 6.492 x 10-7 | 5.229 x 10-7 |

**SITE**: BLACK HORSE LAKE - SOUTH SIDE - Transgressive sandstone (4)

SUSCEPTIBILITY
NR = 4
T = 4 seconds

MS (SI v) = 5.682 x 10-5
SDEV (SI v) = 5.279 x 10-7

ANISOTROPY
M = 6
NR = 4
T = 4 seconds

```
MIN -- DEC =  14.75  INC = 80.89  R95 =  6.1  EV = 4.025 x 10-5  SD = 5.299 x 10-7
INT --     = 273.04         1.86         16.3        5.316 x 10-5       2.739 x 10-7
MAX--      =   2.75        -8.90         16.4        5.743 x 10-5       7.688 x 10-7
```

### SITE: BLACK HORSE LAKE - SOUTH SIDE - Transgressive sandstone

SUSCEPTIBILITY
NR = 4
T = 4 seconds

MS (SI v) = 8.086 x 10-5
SDEV (SI v) = 1.061 x 10-6

MS (SI v) = 1.003 x 10-4
SDEV (SI v) = 1.061 x 10-6

### SITE: BLACK HORSE LAKE - NORTH SIDE - Transgressive sandstone (1)

SUSCEPTIBILITY
NR = 4
T = 4 seconds

MS (SI v) = 4.636 x 10-5
SDEV (SI v) = 9.582 x 10-7

ANISOTROPY
M = 6
NR = 4
T = 4 seconds

```
MIN -- DEC = 332.32  INC = 85.31  R95 =  1.6  EV = 3.363 x 10-5  SD = 3.615 x 10-7
INT --     = 334.48        -4.68         43.4        4.669 x 10-5       1.360 x 10-6
MAX--      =  64.45         0.17         49.3        4.802 x 10-5       3.639 x 10-7
```

### SITE: BLACK HORSE LAKE - NORTH SIDE - Transgressive sandstone (2)

SUSCEPTIBILITY
NR = 4
T = 4 seconds

MS (SI v) = 6.546 x 10-5
SDEV (SI v) = 6.852 x 10-7

ANISOTROPY
M = 6
NR = 4
T = 4 seconds

| | | | | | |
|---|---|---|---|---|---|
| MIN -- DEC | = 43.81 | INC = 81.21 | R95 = 5.5 | EV = 5.186 x 10-5 | SD = 6.658 x 10-7 |
| INT -- | = 356.67 | -6.00 | 13.7 | 6.557 x 10-5 | 1.375 x 10-6 |
| MAX-- | = 87.33 | -6.39 | 13.6 | 6.779 x 10-5 | 9.595 x 10-7 |

**SITE**: BLACK HORSE LAKE - NORTH SIDE - Transgressive sandstone (3)

**SUSCEPTIBILITY**
NR = 4
T = 4 seconds

MS (SI v) = 7.971 x 10-5
SDEV (SI v) = 4.629 x 10-7

**ANISOTROPY**
M = 6
NR = 4
T = 4 seconds

| | | | | | |
|---|---|---|---|---|---|
| MIN -- DEC | = 75.37 | INC = 86.65 | R95 = 4.8 | EV = 6.616 x 10-5 | SD = 4.118 x 10-7 |
| INT -- | = 349.01 | -0.24 | 7.0 | 8.002 x 10-5 | 4.384 x 10-7 |
| MAX-- | = 79.03 | -3.33 | 8.0 | 8.257 x 10-5 | 5.347 x 10-7 |

**SITE**: BLACK HORSE LAKE - NORTH SIDE - Transgressive sandstone (4)

**SUSCEPTIBILITY**
NR = 4
T = 4 seconds

MS (SI v) = 5.688 x 10-5
SDEV (SI v) = 8.273 x 10-7

**ANISOTROPY**
M = 6
NR = 4
T = 4 seconds

| | | | | | |
|---|---|---|---|---|---|
| MIN -- DEC | = 284.18 | INC = -78.07 | R95 = 7.9 | EV = 4.895 x 10-5 | SD = 9.240 x 10-7 |
| INT -- | = 334.64 | 7.65 | 42.1 | 5.661 x 10-5 | 8.870 x 10-7 |
| MAX-- | = 63.40 | -9.08 | 44.0 | 5.789 x 10-5 | 4.438 x 10-7 |

**SITE**: BLACK HORSE LAKE - NORTH SIDE - Transgressive sandstone

**SUSCEPTIBILITY**
NR = 4
T = 4 seconds

(5) MS (SI v) = 9.504 x 10-5
SDEV (SI v) = 1.908 x 10-7

(6) MS (SI v) = 1.019 x 10-4
SDEV (SI v) = 4.817 x 10-7

(7) MS (SI v) = 9.836 x 10-5
SDEV (SI v) = 3.662 x 10-7

# VII. APPENDIX II

## III: Flume data from sediment-fallout experiments

As a result of the interpreted importance of upper plane bed conditions during the deposition of GUP lamination this appendix has been included.

## APPENDIX II : FLUME DATA FROM THE SEDIMENT FALLOUT EXPERIMENTS

The following tabulated data are measurements of the anisotropy of magnetic susceptibility (AMS) and magnetic susceptibility (MS) derived from samples taken from flume runs made at Syracuse University from June to December 1986. The experiments were run in order to gain a better understanding of the transition between the Bouma "B" and Bouma "C" divisions, in an attempt to explain the consistent lack of intervening large-scale bedforms. The relevance of this project with respect to the present study is in the fact that turbidites are deposited from waning turbulent suspensions, typically found in ancient and modern deep-sea sedimentary environments. A similar waning turbulent condition has been used to explain the origin of "gently undulating, parallel lamination (GUP lamination), the predominant lithofacies making up the lower-shoreface depositional environment of the Bootlegger Member.

### FLUME EXPERIMENTS:

Runs were carried out in a 9 metre x 54.5 cm flume (Fig. 1). Clear-water runs were initially carried out in order to assess the hydraulic nature of the sand used in the experiments ($\phi_{50} = 2.05\phi$ (0.25 mm)). The actual sediment runs involved the initial generation of an equilibrium bedform, generally taking about an hour or more (length of time required to establish equilibrium is directly related to: (1) the sediment transport capability of the flow; (2) response time of that particular bedform; and (3) how uniform the initial bed surface and bed thickness was over the length of the flume at the beginning of the run). Once equilibrium bedform conditions were achieved sand was introduced into the flow from overhead sand bins (which were filled prior to the run with sediment taken from the flume). A sand flow was achieved by temporarily liquifying the sand with water supplied from overhead hoses (Fig. 2). The temporal length of the sediment injection portion of each run depended on the volumetric rate of sediment supply, ranging from several minutes to less than 2 minutes, bed aggradation rate being directly related. During sediment injection a video tape was made in order to calculate bed accretion rate and view the possible degradation of pre-existing bedforms.

Also during the sediment portion of each run certain variables characterising the nature of fluid flow within the flume were monitored: water depth (D) and volumetric discharge (Q). This was done in order to ensure that the "equilibrium" flow regime developed during the pre-sand-feed portion of each run was maintained during sediment injection. However, the hydraulic grade line (HGL), one of the fluid variables describing the open channel flow, changed dramatically during each sediment run. This observation was a direct result of the downstream thickening of the deposited sediment wedge, which ultimately reflected downstream sediment transport.

After each run was completed and the appropriate measurements made the flume was drained and the sediment was allowed to sit overnight in order for the pore water to escape. Slabs of sediment were then extracted (oriented down-flume) and cemented with dilute Woodworkers Glue (a water-soluble glue; dilution = 15 : 1 (water : glue)). Slabs were then placed on a flat surface and periodically subjected to more glue in order to ensure total impregnation. Eventually the slabs were allowed to dry and solidify. These were then cored and the cores individually placed in the SI-2 AMS instrument for anisotropy of magnetic susceptibility and magnetic susceptibility analysis.

## RESULTS:

(1) Lack of dune bedforms in turbidites is not a result of sediment fallout, BUT is due to a grain size requirement for large-scale bedform development. Therefore during the time when dune-producing conditions are present in most turbidity currents the available sediment grain size population is incapable of producing large-scale (dunes) bedforms.

(2) Plane bed, ripples and dunes are stable under reasonable sediment fallout rates, but all can be eliminated with extremely high volumes of sediment fallout. The angle of climb of all these bedforms is a function of the rate of sediment fallout (or equivalent bed accretion) (Fig. 3A, 3B).

(3) With increasing rate of sediment fallout plane-bed lamination becomes increasingly diffuse, until a limit is reached at which a massive bed is developed (Fig. 4A, 4B, 4C).

(4) The development of plane-bed lamination in a mixed sediment population is the result of downstream-migrating millimetre-high bedforms, which under the effect of sediment fallout are forced to climb and consequently develop fining-upward, climbing parallel bands (Fig. 5).

(5) With increasing flow regime, but always within the upper-plane-bed stability field, the development of planar lamination improves for a given sediment feed rate.

(6) Always within upper-plane-bed field the imbrication of sand grains:

(a) increases with increasing sediment feed

(b) shows a poorly defined increase with flow regime under a given sediment feed rate.

(7) With increasing rate of sediment fallout bed accretion is more rapid at all plane-bed conditions. However, for a given sediment feed rate, bed accretion is inversely related to flow velocity (although always within the upper-plane-bed field).

NOTE: For a description of the variables used in the following tables see APPENDIX I (B).

In all the following tabulated data :

(1) number of sample orientations (M) is 6

(2) number of repeated measurements (NR) is 3

(3) **$0^{o}$ - $360^{o}$** is the reference direction and is always taken as the down-flume direction

## RUN 17

(1)

| | | | | | |
|---|---|---|---|---|---|
| MIN -- | DEC = 54.18 | INC = 78.72 | R95 = 0.4 | EV = 1.349 x 10-3 | SD = 2.483 x 10-7 |
| INT -- | = 293.00 | 5.89 | 4.3 | 1.496 x 10-3 | 1.712 x 10-7 |
| MAX -- | = 22.00 | -9.58 | 4.3 | 1.516 x 10-3 | 9.913 x 10-7 |

(2)

| | | | | | |
|---|---|---|---|---|---|
| MIN -- | DEC = 11.17 | INC = 76.65 | R95 = 0.7 | EV = 1.270 x 10-3 | SD = 4.448 x 10-7 |
| INT -- | = 271.89 | 2.19 | 1.1 | 1.375 x 10-3 | 3.465 x 10-7 |
| MAX -- | = 1.38 | -13.15 | 1.1 | 1.418 x 10-3 | 8.845 x 10-7 |

(3)

| | | | | | |
|---|---|---|---|---|---|
| MIN -- | DEC = 0.56 | INC = 76.48 | R95 = 0.5 | EV = 1.586 x 10-3 | SD = 1.733 x 10-7 |
| INT -- | = 274.41 | -0.52 | 0.8 | 1.714 x 10-3 | 6.113 x 10-7 |
| MAX -- | = 358.26 | -13.15 | 0.7 | 1.771 x 10-3 | 8.520 x 10-7 |

**RUN 19**

(1)

MIN -- DEC = 346.25 INC = 77.70 R95 = 0.8 EV = 1.324 x 10-3 SD = 1.158 x 10-7
INT -- = 272.76 -3.54 1.6 1.398 x 10-3 1.775 x 10-7
MAX -- = 3.50 -11.75 1.6 1.452 x 10-3 7.764 x 10-6

(2)

MIN -- DEC = 340.18 INC = 70.14 R95 = 0.6 EV = 1.255 x 10-3 SD = 2.916 x 10-7
INT -- = 69.05 -0.43 3.3 1.332 x 10-3 5.226 x 10-7
MAX -- = 338.87 -19.85 3.4 1.357 x 10-3 1.107 x 10-6

(3)

MIN -- DEC = 327.42 INC = 78.45 R95 = 0.8 EV = 1.213 x 10-3 SD = 3.571 x 10-7
INT -- = 86.51 5.67 0.9 1.267 x 10-3 4.023 x 10-7
MAX -- = 357.51 -10.02 0.2 1.310 x 10-3 1.000 x 10-6

(4)

MIN -- DEC = 14.40 INC = 77.01 R95 = 1.6 EV = 1.402 x 10-3 SD = 2.712 x 10-7
INT -- = 79.55 -5.53 2.2 1.500 x 10-3 7.108 x 10-7
MAX -- = 348.40 -11.70 1.9 1.537x 10-3 1.048 x 10-7

(5)

MIN -- DEC = 340.18 INC = 77.93 R95 = 0.9 EV = 1.196 x 10-3 SD = 1.197 x 10-7
INT -- = 84.91 3.11 2.1 1.200 x 10-3 7.327 x 10-7
MAX -- = 355.55 -11.64 1.9 1.318 x 10-3 1.409 x 10-6

(6)

| | | | | |
|---|---|---|---|---|
| MIN -- DEC = 16.52 | INC = 76.55 | R95 = 0.6 | EV = 1.443 x 10-3 | SD = 4.171 x 10-7 |
| INT -- = 271.02 | 3.66 | 0.6 | 1.516 x 10-3 | 3.155 x 10-8 |
| MAX -- = 0.18 | -12.92 | 0.4 | 1.557 x 10-3 | 5.629 x 10-7 |

**RUN 20**

(1)

| | | | | |
|---|---|---|---|---|
| MIN -- DEC = 3.52 | INC = 70.78 | R95 = 0.6 | EV = 1.657 x 10-3 | SD = 4.522 x 10-7 |
| INT -- = 270.68 | 0.51 | 1.4 | 1.758 x 10-3 | 4.985 x 10-7 |
| MAX -- = 0.35 | -19.19 | 1.4 | 1.817 x 10-3 | 5.043 x 10-7 |

(2)

| | | | | |
|---|---|---|---|---|
| MIN -- DEC = 352.16 | INC = 73.44 | R95 = 0.5 | EV = 1.934 x 10-3 | SD = 6.325 x 10-7 |
| INT -- = 83.83 | 0.51 | 1.1 | 2.080 x 10-3 | 5.300 x 10-7 |
| MAX -- = 354.00 | -16.54 | 1.1 | 2.133 x 10-3 | 1.210 x 10-6 |

(3)

| | | | | |
|---|---|---|---|---|
| MIN -- DEC = 339.74 | INC = -77.48 | R95 = 0.6 | EV = 1.536 x 10-3 | SD = 4.062 x 10-7 |
| INT -- = 289.41 | 8.06 | 1.1 | 1.650 x 10-3 | 1.410 x 10-6 |
| MAX -- = 20.77 | 9.50 | 1.1 | 1.686 x 10-3 | 1.008 x 10-6 |

(4)

| | | | | |
|---|---|---|---|---|
| MIN -- DEC = 1.51 | INC = -76.75 | R95 = 0.8 | EV = 1.574 x 10-3 | SD = 2.292 x 10-7 |
| INT -- = 89.09 | 0.25 | 0.6 | 1.671 x 10-3 | 4.983 x 10-7 |
| MAX -- = 358.98 | 13.24 | 0.5 | 1.707 x 10-3 | 6.982 x 10-7 |

(5)

MIN -- DEC = 352.48 INC = 73.21 R95 = 0.5 EV = 1.477 x 10-3 SD = 5.056 x 10-7
INT -- = 85.89 1.03 0.6 1.560 x 10-3 4.851 x 10-7
MAX -- = 356.20 -16.75 0.4 1.611 x 10-3 3.952 x 10-7

**RUN 21**

(1)

MIN -- DEC = 357.07 INC = 71.86 R95 = 0.4 EV = 1.778 X 10-3 SD = 1.146 X 10-6
INT -- = 272.57 -1.80 1.0 1.925 X 10-3 2.414 X 10-7
MAX -- = 3.17 -18.08 1.8 1.983 X 10-3 3.459 X 10-7

(2)

MIN -- DEC = 6.14 INC = 75.83 R95 = 0.2 EV = 1.642 X 10-3 SD = 4.514 x 10-7
INT -- 78.37 -4.40 1.0 1.765 x 10-3 9.423 x 10-7
MAX -- 347.31 -13.43 1.0 1.824 x 10-3 6.240 x 10-7

(3)

MIN -- DEC = 359.23 INC = 72.75 R95 = 0.7 EV = 1.522 x 10-3 SD = 2.214 x 10-7
INT -- 284.40 -4.63 0.5 1.622 x 10-3 9.095 x 10-7
MAX -- 15.79 -16.57 0.5 1.682 x 10-3 6.685 x 10-7

**RUN 23**

(1)

MIN -- DEC = 6.74 INC = 76.97 R95 = 0.8 EV = 1.602 x 10-3 SD = 2.303 x 10-7

| | | | | | |
|---|---|---|---|---|---|
| INT -- | 88.00 | -2.06 | 1.5 | 1.699 x 10-3 | 1.878 x 10-7 |
| MAX -- | 357.52 | -12.85 | 1.4 | 1.736 x 10-3 | 1.572 x 10-7 |

(2)

| | | | | | |
|---|---|---|---|---|---|
| MIN -- | DEC = 332.79 | INC = 77.20 | R95 = 0.7 | EV = 1.507 x 10-3 | SD = 5.647 x 10-7 |
| INT -- | 273.78 | -6.79 | 0.9 | 1.567 x 10-3 | 6.526 x 10-7 |
| MAX -- | 5.07 | -10.86 | 0.8 | 1.651 x 10-3 | 5.324 x 10-7 |

(3)

| | | | | | |
|---|---|---|---|---|---|
| MIN -- | DEC = 17.61 | INC = 69.46 | R95 = 0.2 | EV = 1.722 x 10-3 | SD = 3.080 x 10-7 |
| INT -- | 89.07 | -6.79 | 0.4 | 1.837 x 10-3 | 6.121 x 10-7 |
| MAX -- | 356.66 | -19.27 | 0.4 | 1.884 x 10-3 | 4.212 x 10-7 |

### RUN 24

(1)

| | | | | | |
|---|---|---|---|---|---|
| MIN -- | DEC = 0.76 | INC = 78.30 | R95 = 0.6 | EV = 1.420 x 10-3 | SD = 5.937 x 10-7 |
| INT -- | 87.74 | -0.95 | 1.3 | 1.491 x 10-3 | 2.411 x 10-7 |
| MAX -- | 357.42 | -17.67 | 1.2 | 1.552 x 10-3 | 7.616 x 10-7 |

(2)

| | | | | | |
|---|---|---|---|---|---|
| MIN -- | DEC = 38.96 | INC = 74.31 | R95 = 0.2 | EV = 1.889 x 10-3 | SD = 6.534 x 10-7 |
| INT -- | 283.49 | 6.88 | 0.2 | 1.997 x 10-3 | 4.866 x 10-7 |
| MAX -- | 11.76 | -14.02 | 0.3 | 2.076 x 10-3 | 1.622 x 10-7 |

(3)

| | | | | | |
|---|---|---|---|---|---|
| MIN -- | DEC = 0.51 | INC = 74.10 | R95 = 2.1 | EV = 1.525 x 10-3 | SD = 2.759 x 10-7 |
| INT -- | 272.84 | -0.69 | 2.0 | 1.607 x 10-3 | 2.655 x 10-7 |
| MAX -- | 3.04 | -15.87 | 0.7 | 1.648 x 10-3 | 8.019 x 10-7 |

(4)

```
MIN -- DEC = 336.57   INC =  67.56   R95 = 1.3   EV = 1.281 x 10-3   SD = 1.114 x 10-7
INT --       283.48         -13.92         2.1        1.338 x 10-3        3.999 x 10-7
MAX --        17.89         -17.23         1.8        1.378 x 10-3        3.611 x 10-8
```

(5)

```
MIN -- DEC = 348.99   INC = 75.11   R95 = 1.0   EV = 1.137 x 10-3   SD = 3.309 x 10-7
INT --        82.79          1.02         1.0        1.171 x 10-3        1.739 x 10-7
MAX --       353.06        -14.85         0.9        1.229 x 10-3        4.522 x 10-7
```

(6)

```
MIN -- DEC =   4.55   INC = -16.95   R95 = 0.8   EV = 1.534 x 10-3   SD = 9.867 x 10-7
INT --        79.85          -4.45         1.2        1.610 x 10-3        1.182 x 10-6
MAX --       348.53         -16.42         1.0        1.651 x 10-3        6.856 x 10-7
```

TABLE VII-1: Summary table of hydrodynamic conditions during specific upper-plane-bed sediment-fallout flume experiments.

| RUN NO. | BED STATE | Q ($cm^3 / s$) | $\tau_o$ ($dynes / cm^2$) | D (cm) |
|---|---|---|---|---|
| 17 | Plane bed | 80000 | 80.76 | 15.54 |
| 19 | Plane bed | 68000 | 48.61 | 15.99 |
| 20 | Plane Bed | 86000 | 83.11 | 16.95 |
| 21 | Plane Bed | 54000 | 43.54 | 13.06 |
| 23 | Plane Bed | 67500 | 50.59 | 14.74 |
| 24 | Plane Bed | 68000 | 44.29 | 16.13 |

where, Q = discharge (volume/ unit time)

$\tau_o$ = bottom shear stress (force / area)

D = water depth (length)

TABLE VII-2: Grain-imbrication data from specific upper-plane-bed flume runs.
Imbrication was analysed by using anisotropy of magnetic susceptibility.

| RUN | CORE NO. | AXIAL ORIENTATION OF AB PLANE | | AVERAGE PLUNGE |
|---|---|---|---|---|
| | | TREND | PLUNGE | |
| 17 | 1 | 234.18 | 11.28 | 13.33<br>(max = 15.18) |
| | 2 | 191.18 | 13.35 | |
| | 3 | 180.56 | 13.52 | |
| | 4 | 200.41 | 15.18 | |
| 19 | 1 | 166.25 | 12.30 | 13.70<br>(max = 19.86) |
| | 2 | 160.18 | 19.86 | |
| | 3 | 147.48 | 11.55 | |
| | 4 | 194.40 | 12.99 | |
| | 5 | 160.18 | 12.07 | |
| | 6 | 196.52 | 13.45 | |
| 20 | 1 | 183.52 | 19.22 | 15.21<br>(max = 19.22) |
| | 2 | 172.16 | 16.56 | |
| | 3 | 159.74 | 12.52 | |
| | 4 | 178.49 | 13.25 | |
| | 5 | 172.48 | 16.79 | |
| | 6 | 181.11 | 16.93 | |
| | 7 | 163.19 | 11.50 | |
| 21 | 1 | 177.07 | 18.14 | 15.31<br>(max = 18.14) |
| | 2 | 186.14 | 14.17 | |
| | 3 | 179.23 | 17.25 | |
| | 4 | 206.43 | 12.69 | |
| 23 | 1 | 186.94 | 13.03 | 15.71<br>(max = 20.54) |
| | 2 | 152.79 | 14.17 | |
| | 3 | 197.61 | 20.54 | |
| | 4 | 174.46 | 15.85 | |
| | 5 | 163.19 | 16.32 | |

| | | | | |
|---|---|---|---|---|
| 24 | 1 | 180.76 | 17.70 | |
| | 2 | 218.96 | 15.69 | |
| | 3 | 180.51 | 15.90 | 17.28 |
| | 4 | 156.57 | 22.44 | (max = 22.44) |
| | 5 | 168.99 | 14.89 | |
| | 6 | 184.55 | 17.05 | |

where axial orientation of the AB plane represents the trend and plunge of the lineament delineating the maximum strike and dip of the plane containing the maximum (MAX) and intermediate (INT) susceptibility axes

Average Plunge = the average plunge of this lineament which is ALWAYS imbricated upstream

TABLE VII-3: Summary table of bed accretion rate during specific upper-plane-bed sediment-fallout runs.

| RUN NO. | HOLE SIZE (in.) | U (cm / s) | TIME AVERAGE (dA / dt) | RUNNING (dA / dt) | Fr |
|---|---|---|---|---|---|
| 17 | 1/8 | 75 | | 1.49 | 0.58 |
| 19 | 5/32 | 73 | 2.53 | 2.83 | 0.58 |
| 20 | 5/32 | 86 | 2.78 | 3.0 | 0.67 |
| 21 | 5/32 | 77 | 2.53 | 3.1 | 0.71 |
| 23 | 3/18 | 78 | 3.7 | 4.1 | 0.65 |
| 24 | 3/18 | 72 | 4.05 | 4.3 | 0.57 |

where hole size = the size of holes in the bottom of the sediment-feed boxes (a diameter in inches)
U = average flow velocity
dA/dt = accretion rate / minute (measured in cm / min)
Time averaged = assuming constant accretion over the time of the sediment feed (thickness / time)
Running " = incremental thickness / minute (measured from the video tape)
Fr = Froude Number (Fr = SQR (U / gD)) (dimensionless)

FIGURE VII-1: Recirculating flume at Syracuse University (9 m x 54.5 cm).

FIGURE VII-2: Sediment fallout during experimental runs.

FIGURE VII-3(A): Wide-angle view at the completion of a dune bedform run (Run 22).

FIGURE VII-3(B): Close-up of climbing dunes from Run 22.

RUN
10 cm
6

FIGURE VII-4(A): Plane bed run - RUN 17: (dA/dt = 1.49 cm/s).

FIGURE VII-4(B): Plane bed run - RUN 20: (dA/dt = 3.0 cm/s).

FIGURE VII-4(C): Plane bed run - RUN 24: (dA/dt = 4.3 cm/s).

FIGURE VII-5: Development of climbing parallel bands as a result of climbing millimetre-height bedforms formed under upper-plane-bed conditions.

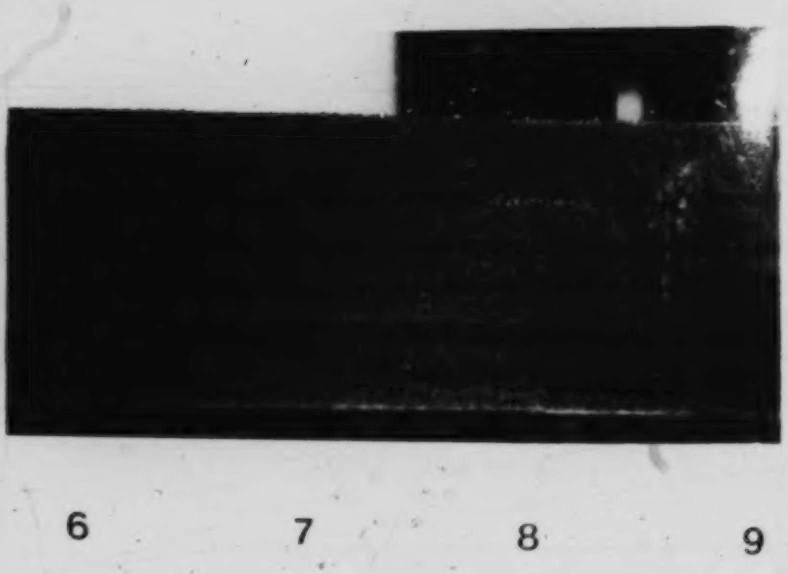
6
7
8
9

# VIII. APPENDIX III

## III: Structural geology of the Bootlegger Member

## APPENDIX III: STRUCTURAL GEOLOGY OF THE BOOTLEGGER MEMBER

The Bootlegger Member, the uppermost of four members making up the Blackleaf Formation, outcrops near the city of Great Falls and within the Sweetgrass Hills of north-central Montana (Fig. 1). Structure of Bootlegger strata in these two areas is distinctly different, being approximately flat-lying throughout most of the Great Falls study area whereas being folded and steeply dipping in the Sweetgrass Hills.

Near Great Falls the dominant structural feature is the southern element of the ancestral Sweetgrass Arch: the South Arch (Fig. 2). This feature which is located immediately southwest of the study area, is a very broad antiform oriented approximately north northwest - south southeast dipping gently toward the northwest. Dips on its limbs are $< 1^{\circ}$ (toward the northeast in most of the study area), resulting in its limited affect on the orientation of Bootlegger strata. Flat-lying strata in the Great Falls area are also a consequence of being located east of the Cordilleran Fold and Thrust Belt (Fig. 2).

In the area near Belt, Montana (within the Great Falls study area) and within the Sweetgrass Hills strata do, although show structural dip, particularly in the latter, where dips reach $42^{\circ}$ from the horizontal. Development of structural dip is not associated with deformation related to the Cordilleran Fold and Thrust Belt or the Sweetgrass Arch, but to the emplacement of post-depositional (*i.e.* post Bootlegger) Tertiary intrusions. The effect of these intrusions are typically localised, but in the case of the Sweetgrass Hills and Belt Butte illustrates their effective doming of the overlying strata.

The Belt Butte, named for a "belt" of basal Bootlegger sandstone surrounding the butte, rises anomalously high around the surrounding area (Fig. 3). On the butte itself strata are approximately horizontal, but on its immediate northeast side strata dip steeply to the horizontal strata on the butte from those dipping steeply on its east side. Also associated with the dipping strata on the east slope is an inferred local syncline axis. However, recent regional mapping by Vuke-Foster and others (person. comm. 1987) have indicated that this syncline may part of a large, approximately 1.2 km wide, circular depression. Strata east and northeast of Belt Butte dip at about $5^{o}$ - $10^{o}$ toward the northeast, although dips decrease with distance northeast from the butte. Strata are abruptly truncated along the western edge of the Tertiary Highwood Mountains. Structural features in the area of the Belt Butte are most likely the result of vertical uplift associated with a Tertiary intrusion (Fig. 5), although the depression may reflect subsidence due to the loss of magma at depth.

Sections at Mt. Lebanon, the easternmost peak of the Sweetgrass Hills (Fig. 6), are exposed in a river valley incised into the axis of a north plunging anticline. Exposed in this valley as well as the Bootlegger Member are the other members of the Blackleaf Formation plus a portion of the uppermost Kootenai Formation. Similar to the scenario developed for Belt Butte, structural development at the Mt. Lebanon section, and actually the ultimate creator of the Sweetgrass Hills is related to uplift by Tertiary intrusions.

FIGURE VIII-1: Location map of the Sweetgrass Hills and Great Falls in north-central Montana.

FIGURE VIII-2: The constituent elements of the Sweetgrass Arch in north-central Montana (Kevin-Sunburst Dome and South Arch) plus the southern portion of the Bow Island Arch of south-central Alberta.

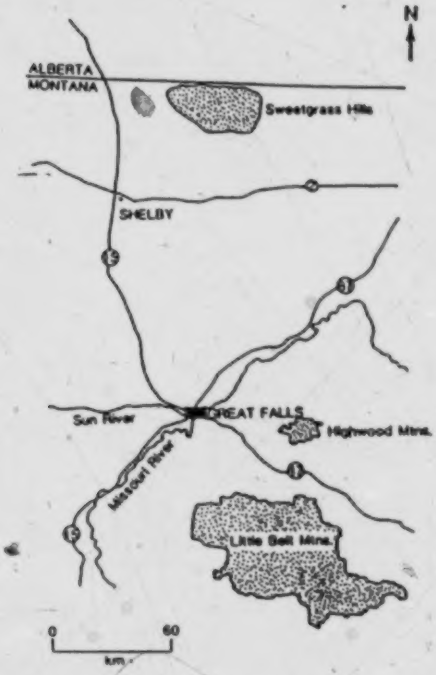
N
ALBERTA
MONTANA
Sweetgrass Hills
SHELBY
Sun River
GREAT FALLS
Highwood Mtns.
Missouri River
Little Belt Mtns.
0
60
km

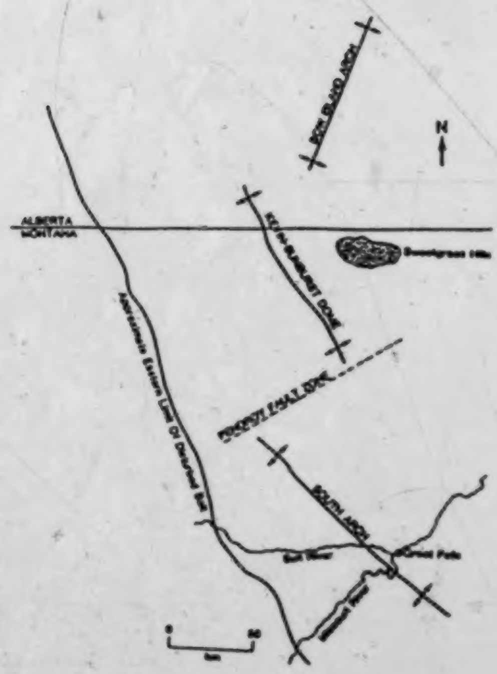
BOW ISLAND ARCH
N
ALBERTA
MONTANA
KEVIN-SUNBURST DOME
Sweetgrass Hills
Approximate Eastern Limit Of Disturbed Belt
PENDROY FAULT ZONE
SOUTH ARCH
Sun River
Great Falls
Missouri River
0
60
km

FIGURE VIII-3: Diagrammatic of the bedding orientations on the northeast slope of Belt Butte.

| SECTION | MEASURED STRIKE AND DIP |
|---|---|
| 1 | horizontal |
| 2 | 152 / 34 / NE  157 / 29 NE<br>157 / 38 NE<br>(average = 155 / 34 NE) |
| 3 | 157 / 29 NE  156 / 34 NE  152 / 37 NE<br>156 / 38 NE  152 / 38 NE  156 / 37 NE<br>153 / 33 NE  150 / 29 NE  157 / 37 NE<br>(average = 154 / 35 NE) |
| 4 | 179 / 38 E  171 / 40 E  180 / 36 E<br>185 / 37 E  170 / 36 E<br>(average = 177 / 37 E) |

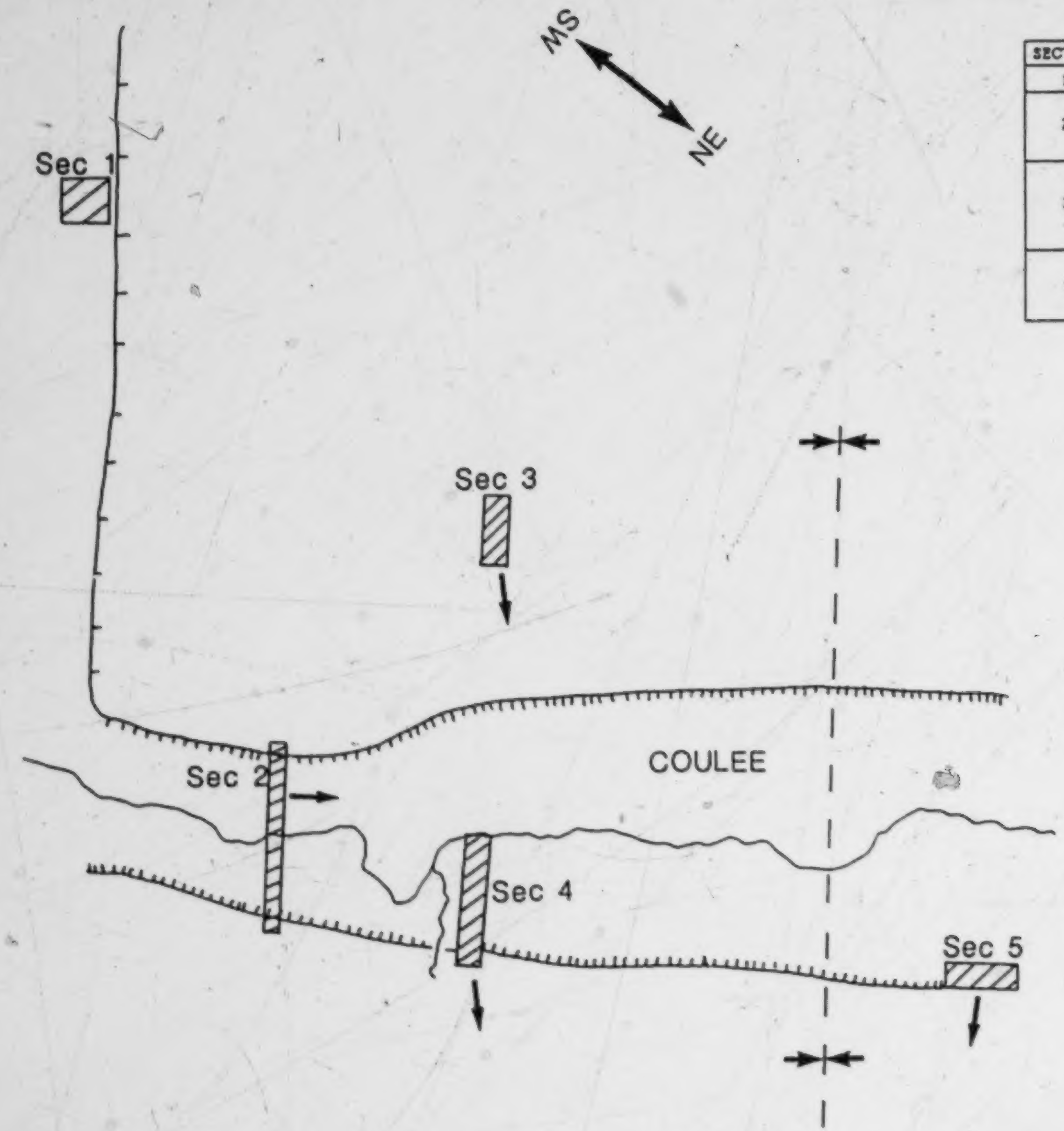
SW
NE
Sec 1
Sec 2
Sec 3
Sec 4
Sec 5
COULEE

inferred syncline axis
average bedding strike and dip
scarp slope

FIGURE VIII-4: Photo of the western slope of Belt Butte. Lower arrow points to the "belt" of basal Bootlegger strata (5 m thick) , while the upper arrow points to the Arrow Creek Bentonite (11 m thick).

FIGURE VIII-5: Diagrammatic sketch of the structure developed on the northeast side of Belt Butte.

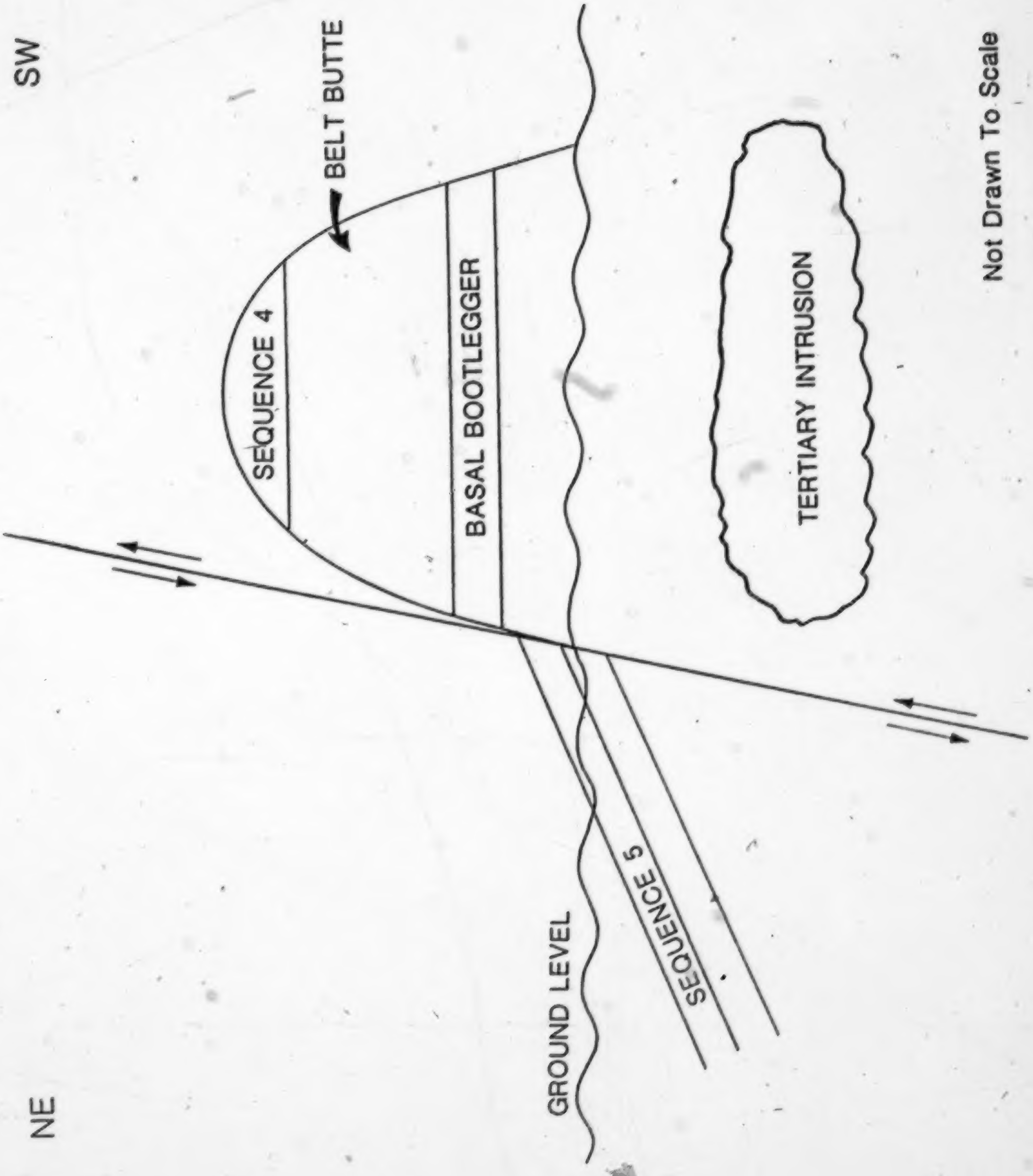
SW
NE
BELT BUTTE
SEQUENCE 4
BASAL BOOTLEGGER
TERTIARY INTRUSION
GROUND LEVEL
SEQUENCE 5

Not Drawn To Scale

12

FIGURE VIII-6: Location of Mt. Lebanon on the east side of East Butte within the Sweetgrass Hills .

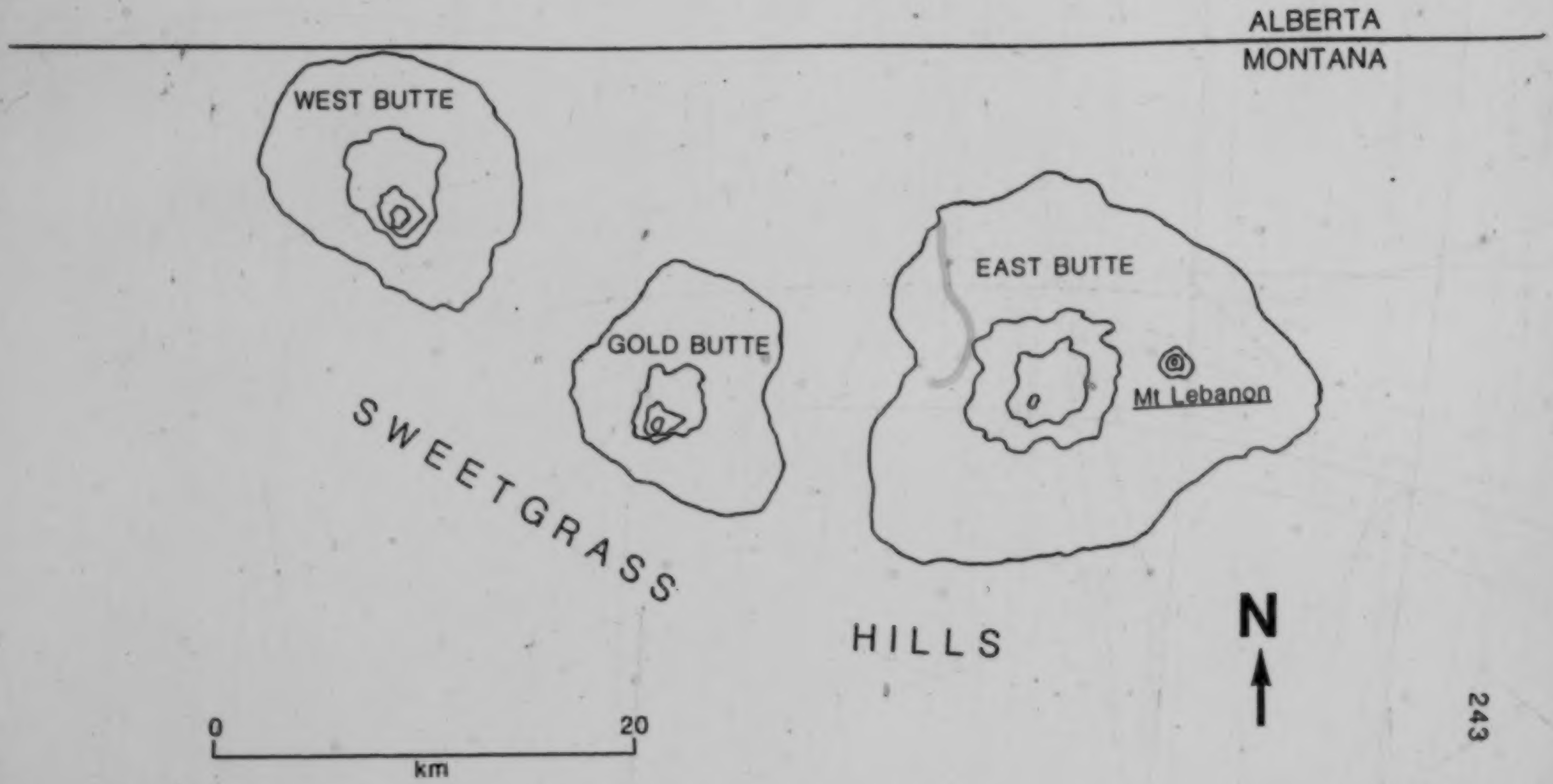
ALBERTA
MONTANA
WEST BUTTE
GOLD BUTTE
EAST BUTTE
Mt Lebanon
SWEETGRASS
HILLS
N
0
20
km

# IX. APPENDIX IV

IV: Measured palaeocurrent data from both the Great Falls and Mt. Lebanon study areas

# APPENDIX IV: MEASURED PALAEOCURRENT DIRECTIONAL DATA

The following appendix is a tabulation of all measured palaeocurrent data from all study areas.

ALL DATA IS LINE OF DIRECTION DATA (*I.E.* ALL DATA IS DESCRIBED BY THE TREND AND PLUNGE OF A LINE). IN THE CASE OF PLANAR DATA (*I.E.* THOSE DESCRIBED BY STRIKE AND DIP OF A PLANAR SURFACE) THIS LINE REPRESENTS THE LINEAMENT WHICH MARKS OUT THE MAXIMUM DIP OF THE PLANE CONTAINING THE CROSS-BED SURFACE *ETC*.).

Unless otherwise stated data represents true sense of direction palaeocurrent directions. In the case of coset measured data the true palaeocurrent direction can only be justfied in a hemispherical sense.

Tabulated data from study areas exhibiting structural dip represents unrotated data. Only measurements obtained from the Sweetgrass Hills study area have been rotated. At all other study locations (*i.e.* in the Great Falls study area) structural dip is always less than $5^{\circ}$ - $8^{\circ}$ (typically toward the northeast) and because of the shallow dip measured palaeocurrent directions have not been rotated. Rotation of Sweetgrass Hills data was accomplished using the rotating program "STEREO" written for a Macintosh Plus computer system. This program only produces a final stereonet representation of the rotated data, but unfortunately does not provide an additional listing of each rotated datum.

Figure 1 is a map locating each of the study locations from which palaeocurrent directions were obtained.

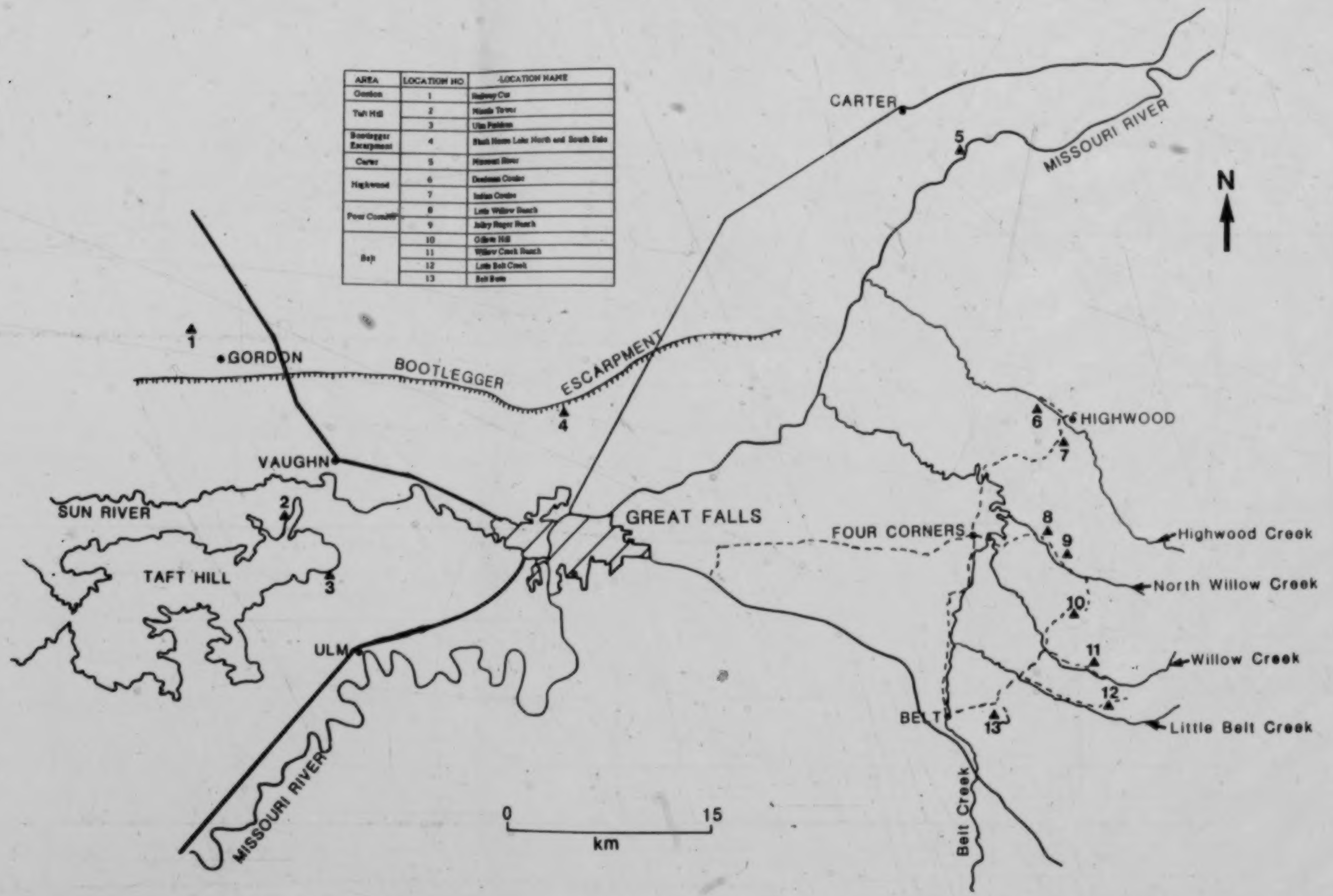

| AREA | LOCATION NO | LOCATION NAME |
|---|---|---|
| Gordon | 1 | Railway Cut |
| Taft Hill | 2 | [illegible] Tower |
|  | 3 | Ulm Pishkun |
| Bootlegger Escarpment | 4 | Black Horse Lake North and South Side |
| Carter | 5 | Missouri River |
| Highwood | 6 | Deadman Coulee |
|  | 7 | Indian Coulee |
| Four Corners | 8 | Little Willow Ranch |
|  | 9 | Jolly Roger Ranch |
| Belt | 10 | Gibson Hill |
|  | 11 | Willow Creek Ranch |
|  | 12 | Little Belt Creek |
|  | 13 | Belt Butte |

CARTER
MISSOURI RIVER
N
1
GORDON
BOOTLEGGER
ESCARPMENT
4
5
6
HIGHWOOD
7
VAUGHN
SUN RIVER
2
TAFT HILL
3
GREAT FALLS
FOUR CORNERS
8
9
Highwood Creek
North Willow Creek
10
11
Willow Creek
12
Little Belt Creek
BELT
13
ULM
MISSOURI RIVER
0
15
km
Belt Creek

FIGURE IX-1: Location map of all study locations in the Great Falls study area from which palaeocurrent information was obtained.

# Measured Palaeocurrent Data From Bootlegger Member Strata

## AREA: TAFT HILL

LOCATION: ULM PISHKUN
STRIKE AND DIP: HORIZONTAL

| SEC. | BED | MEASURED PALAEOCURRENT DIRECTIONS |
|---|---|---|
| 1 | 3 | 78 / 26  112 / 20  138 / 23  124 / 14  63 / 17  47 / 20 |
| | 4 | 167 / 22  115 / 23 |
| | 6 | 313 / 26  247 / 22  265 / 18 |
| | 13 | 125 (flutes) |
| | 16 | 115 / 15  41 / 12  149 / 26  131 26 |
| | 18 | 145 / 18  115 / 10 |
| | 24 | 135 / 24  127 / 16 |
| | 26 | 315 / 12 |
| | 27 | 318 / 17 |
| | 29 | 300 / 10 |
| | 31 | 299 / 26 |
| | 32 | 328 / 17 |
| | | |
| 2 | 7 | 310 / 14  120 / 18 |
| | 10 | 122 / 15 |
| | 18 | 125 / 26 |
| | 19 | 98 / 20  136 / 11  135 / 12 |
| | 20 | 50 / 27  60 / 25 |
| | 22 | 306 / 13 |
| | 23 | 127 / 16 |
| | 24 | 124 / 10  108 / 19 |
| | 25 | 51 / 21  119 / 15 |
| | 26 | 123 / 21 |
| | 29 | 258 / 19  129 / 12  105 / 22  103 / 13  140 / 11  50 / 10  141 / 5 |
| | | 128 / 11 |
| | | 113 / 18  90 / 16  135 / 13  152 / 18  131 / 18  50 / 7  147 / 10  80 / |
| | 19 | 318 / 22 |
| | 30 | 112 / 12  20 / 24 |
| | | 145 (flutes) |
| | 31 | 125 / 15  117 / 8  130 / 17  255 / 22 |
| | 32 | 117 / 31  135 / 18 |
| | 35 | 118 / 17  107 / 31 |
| | 37 | 129 / 27  153 / 20 |
| | 41 | 123 / 14  89 / 22 |
| | | 128 (flutes) |
| | 49 | 130 / 20  120 / 15 |
| | 50 | 120 / 15 |
| | 51 | 304  307  302  314  308  340  307 (ripple trends) |
| | | 325 / 25  326 / 22  312 / 20  316 / 24  318 / 23 |
| | | |
| 3 | 1 | 125 / 35 |
| | 2 | 86 / 20  95 / 16  93 / 21 |
| | 3 | 121 / 23  118 / 22  100 / 17  37 / 22  104 / 23  110 / 12  80 / 18 |
| | 4 | 96 / 20  126 / 26  103 / 23 |
| | 6 | 104 / 17  108 / 24  105 / 15  99 / 11 |
| | 7 | 70 / 17  322 / 13  112 / 17 |

| | | |
|---|---|---|
| | 8 | 285 / 16  137 / 26  260 / 20  265 / 15 |
| | 11 | 150 / 15  144 / 15 |
| | 12 | 126 / 18 |
| | 14 | 302 / 25  325 / 25 |
| | 19 | 310 / 11 |
| | 21 | 323 / 17 |
| 4 | 1 | 108 / 18  79 / 17 |
| | 6 | 294 / 19  50 / 13 |
| | 7 | 141 / 10  148 / 17  155 / 23  102 / 21 |
| | 9 | 95 / 18  120 / 28  130 / 18 |
| | 11 | 111 / 13  92 / 27  98 / 26  92 / 12  111 / 13 |
| | 12 | 260 / 12  230 / 28 |
| | 13 | 300 / 25  287 / 27 |
| | 14 | 109 / 32  112 / 16 |
| | 15 | 112 / 16  121 / 25  105 / 20  118 / 15 |
| | 16 | 145 / 26  117 / 17  83 / 13 |
| | 18 | 130 / 16 |
| | 19 | 95 / 15  123 / 15 |
| | 21 | 96 / 26  114 / 14 |
| | 22 | 115 / 9  105 / 13  122 / 8 |
| | 25 | 116 / 18  82 / 28  63 / 21  142 / 28 |
| | 27 | 291 / 15 |
| | 28 | 107 / 22 |
| | 29 | 105 / 13 |
| | 30 | 322 / 23  122 / 13 |
| | 31 | 82 / 26 |
| | 33 | 49 / 26 |
| | 39 | 130 / 17  160 / 17  110 / 15  123 / 12 |
| | 40 | 132 / 27  123 / 17  101 / 18  66 / 28 |
| | 41 | 339 / 16  323 / 13 |
| | 42 | 111 / 17 |
| | 48 | 85 / 17  103 / 24 |
| | 51 | 54 / 23 |
| | 52 | 131 / 16  90 / 26  105 / 27  66 / 17 |
| | 53 | 148 / 15  76 / 8<br>143 (flutes)<br>125 / 305  133 / 313 (grooves) |
| | 54 | 70 / 16  105 / 9 |
| | 55 | 77 / 20 |
| | 56 | 93 / 13  107 / 29 |
| | 57 | 338 / 16 |
| | 59 | 135 (flutes) |
| | 62 | 324 / 12  119 / 20  120 / 18 |
| | 63 | 133 / 20  87 / 15  125 / 11  147 / 16  83 / 27 |
| | 65 | 319 / 17  313 / 16  307 / 11  330 / 27 |
| | 72 | 315 |
| | 73 | 280 / 23 |
| | 74 | 325 / 19  328 / 16 |
| | 75 | 312 / 16 |
| | 76 | 95 / 13  101 / 15  140 / 14 |
| | 78 | 322 / 12 |

| | | |
|---|---|---|
| 5 | 4 | 70 / 16  100 / 14  122 / 20 |
| | 5 | 95 / 11  67 / 15 |
| | 7 | 101 / 12  121 / 19  127 / 14  128 / 17 |
| | 9 | 90 / 13  103 / 18  98 / 10 |
| | 10 | 105 / 18  70 / 24  50 / 25 |
| | 11 | 120 / 15  95 / 21  150 / 25  155 / 16  103 / 31  105 / 26 |
| | 12 | 131 / 15  115 / 26  144 / 15 |
| | 13 | 107 / 20  115 / 23 |
| | 14 | 84 / 26  77 / 11  115 / 10  116 / 17  109 / 17  105 / 26 |
| | 15 | 90 / 23  85 / 21  100 / 18  63 / 15  65 / 18  100 / 18 |
| | 16 | 52 / 12 |
| | 17 | 117 / 20  75 / 23 |
| | 20 | 72 / 13  100 / 18  100 / 28  108 / 18 |
| | 22 | 110 / 14  103 / 20 |
| | 24 | 90 / 22 |
| | 25 | 90 / 33 |
| | 26 | 112 / 34  100 / 22  133 / 28  108 / 26  120 / 29 |
| | 31 | 85 / 22 |
| | 32 | 95 / 18  105 / 20  105 / 19 |
| | 35 | 104 / 16 |
| | 46 | 130 / 32 |
| 6 | 5 | 153 / 15  151 / 20 |
| | 7 | 162 / 19  161 / 23 |
| | 20 | 279 / 21  267 / 20  258 / 22  263 / 16 |
| 7 | 4 | 128 / 7  97 / 23  88 / 19 |
| | 7 | 141 / 19 |
| | 8 | 75 / 12  75 / 11  68 / 18  84 / 24  120 / 15  94 / 28  90 / 21  85 / 31 |
| | 24 | 321 / 15  320 / 27 |
| 8 | 1 | 172 / 352 (symmetric ripples) |
| | 18 | 120 / 21  146 / 17 |
| | 19 | 332 / 19  323 / 20 |
| 9 | 2 | 138 / 318 (gutter cast) |
| | | 132 (flute) |
| | 3 | 95 / 15  112 / 17 |
| | 4 | 112 / 19 |
| | | 143 (flutes) |
| | 5 | 100 / 12 |
| | 6 | 298 / 20  306 / 22 |
| | 7 | 117 / 15 |
| | 9 | 148 (flutes) |
| | 10 | 303 / 10  312 / 23  309 / 27  312 / 26 |
| | 11 | 122 / 28  128 / 21 |
| | 13 | 125 / 14 |
| | | 128 (flutes) |
| | 14 | 118 / 18  108 / 8 |
| | | 298 / 18  285 / 20 |
| | 16 | 290 / 23 |

| | | |
|---|---|---|
| | 19 | 119/10 90/20<br>290/33 317/20 |
| | 20 | 307/28 291/31 294/21 (back-flow ripples) |
| | 21 | 121/301 (groove) |
| | 27 | 73/12 110/17 |
| | 38 | 258/12 |
| | 39 | 111/16 102/22 |
| | 41 | 107/13 |
| | 42 | 75/11 84/10 73/21 |
| | 44 | 293/16 320/22 301/17 302/22 |
| | 53 | 97/10 93/13 |
| | 54 | 63/11 105/14 77/16 62/24 70/16 |
| | 55 | 74/19 75/14 |
| | 56 | 270/25 278/15 289/27 |
| | 58 | 93/23 105/16 |
| | 59 | 72/15 83/23 97/17 |
| | 60 | 90/22 108/24 78/21 |
| | 61 | 131/16 |
| | 63 | 80/10 108/20 |
| | 68 | 108/22 115/13 103/23 |
| | 70 | 102/10 94/22 |
| | 76 | 345/25 |
| | 77 | 344/22 |
| 10 | 3 | 168 (flutes) |
| | 4 | 310/17 |
| | 5 | 120/16 117/15 122/10 |
| | 6 | 142/24 116/15 |
| | 8 | 297/20 291/14 279/16 299/24 |
| | 13 | 116/21 98/17 126/23 |
| | 19 | 128/28 125/15 110/20 |
| | 20 | 275/17 296/16 |
| | 22 | 247/12 285/18 282/25 |
| | 24 | 92/25 82/20 |
| 11 | 4 | 315/21 294/22 294/22 341/26 |
| | 30 | 160/340 (symmetric ripples) |
| 12 | 3 | 243/32 254/17 263/20 |
| | 11 | 309/25 306/22 314/18 |
| | 13 | 299/15 |
| 13 | 8 | 343/22 |
| | 39 | 28/208 (symmetric ripples) |
| | 51 | 126/306 (symmetric ripples) |
| 14 | 1 | 293/27 310/11 |
| | 2 | 299/18 |
| | 8 | 303 323 330 (ripple trends) |

PARTING LINEATION: Section 1:
138 / 318

Section 2:
119 / 299  116 / 296  131 / 311  130 / 310  138 / 318
135 / 315

Section 3:
131 / 311

Section 6:
110 / 290  104 / 284

Section 9:
158 / 338  144 / 324  134 / 314  133 / 313  149 / 329
157 / 337  148 / 328  136 / 316

Section 14:
130 / 310

Missile Tower Section 3:
160 / 340  166 / 346

COSET MEASUREMENTS:

| SEC. | BED | MEASURED PALAEOCURRENT DIRECTIONS |
|---|---|---|
| 4 | 75 | 322 / 35  312 / 24  320 / 26  313 / 25  312 / 16 |
|  | 83 | 327 / 22  330 / 20  333 / 19  366 / 25  37 / 22  15 / 19 |
| 5 | 55 | 328 / 23  335 / 28  323 / 18  302 / 25  347 / 26  318 / 28  327 / 32 |
|  |  | 325 / 27  342 / 17  344 / 20 |
| 7 | 6 | 328 / 31  322 / 24  324 / 22  331 / 28  333 / 26  323 / 23  321 / 30 |
|  |  | 322 / 22  330 / 20  323 / 28 |
| 8 | 1 | 320 / 28  317 / 17  320 / 24  323 / 22  294 / 11  346 / 25 |
|  |  | 172 / 352 (symmetric ripples) |
|  | 8(a) | 330 / 12  342 / 18  329 / 20  326 / 18 |
|  | 8(b) | 345 / 19  343 / 25  347 / 29  329 / 19  347 / 26  325 / 16  342 / 13 |
|  |  | 336 / 19  348 / 21  341 / 26  340 / 22  338 / 20  342 / 25  350 / 20 |
|  | 14 | 142 / 12  142 / 18  130 / 17  145 / 16  132 / 10  125 / 12  156 / 20 |
|  | 21 | 334 / 16  338 / 13  335 / 10  334 / 21  339 / 23 |
| 9 | 2 | 67 / 8  49 / 10  25 / 17  35 / 5  55 / 7 |
|  | 70(a) | 320 / 18  311 / 15  294 / 17  298 / 17 |
|  | 70(b) | 330 / 21  314 / 18  311 / 21  314 / 18 |
| 10 | 29 | 323 / 14  299 / 20  304 / 18 |
| 11 | 9 | 299 / 26  324 / 24  333 / 22  316 / 15  290 / 13  332 / 25 |
|  | 14 | 55 / 14  115 / 17  102 / 24 |

| | | |
|---|---|---|
| | 15 | 301 / 15 288 / 17 314 / 25 283 / 17 268 / 19 254 / 20 258 / 15 |
| | 16 | 110 / 13 128 / 20 123 / 25 112 / 22 |
| | 18 | 313 / 20 312 / 22 310 / 26 302 / 25 306 / 21 300 / 22 308 / 26<br>299 / 20 303 / 10 288 / 13 311 / 23 302 / 28 |
| | 20 | 298 / 22 303 / 25 291 / 31 299 / 17 296 / 23 317 / 26 303 / 19 |
| | 21 | 294 / 19 326 / 22 306 / 26 306 / 30 |
| | 24 | 134 / 18 123 / 22 137 / 21 |
| | 34 | 118 / 20 142 / 18 137 / 21 122 / 21 127 / 13 |
| | 35 | 295 / 17 304 / 24 324 / 26 308 / 24 315 / 22 324 / 22 |
| 13 | 7 | 328 / 16 331 / 15 314 / 20 336 / 14 329 / 22 |
| | 10 | 324 / 22 313 / 17 316 / 18 317 / 16 329 / 14 |
| | 12 | 342 / 26 316 / 28 317 / 28 323 / 22 |
| | 14 | 256 / 12 244 / 17 258 / 17 256 / 18 |
| | 15 | 309 / 19 325 / 15 |
| | 24 | 324 / 26 325 / 28 331 / 25 |
| | 47 | 15 / 22 30 / 26 28 / 28 24 / 23 25 / 32 |
| | 50 | 305 / 23 311 / 21 327 / 22 322 / 23 308 / 18 |

## AREA: TAFT HILL

**LOCATION:** MISSILE TOWER SECTIONS
**STRIKE AND DIP:** HORIZONTAL

| SEC. | BED | MEASURED PALAEOCURRENT DIRECTIONS |
|---|---|---|
| 1 | (a) | 350 / 23 335 / 19 347 / 28 352 / 17 351 / 22 |
| | (b) | 349 / 20 356 / 21 345 / 20 352 / 23 52 / 13 62 / 12 42 / 8<br>342 / 18 338 / 17 344 / 21 338 / 15 339 / 17 |
| | (c) | 350 / 17 11 / 24 337 / 17 343 / 22 25 / 13 339 / 22 343 / 20 |
| | (d) | 348 / 18 350 / 16 0 / 13 353 / 13 349 / 15 |
| | 11 | 340 /21 355 / 17 345 / 23 340 / 30 349 / 20 |
| 2 | 4 | 338 / 18 335 / 19 6 / 20 35 / 20 340 / 22 3 / 20 355 / 21<br>347 / 20 355 / 15 |
| | 5 | 3 / 14 50 / 23 18 / 18 15 / 20 51 / 25 27 / 18 52 / 28 50 / 23<br>56 / 31 |
| 3 | 3 | 357 / 17 42 / 18 20 / 21 8 / 21 0 / 26 1 / 18 11 / 20 |
| | 6 | 162 / 13 169 / 15 168 / 14 148 / 11 147 / 8 153 / 9 158 / 15 |
| | 7 | 140 / 23 154 / 22 148 / 23 155 / 23 155 / 17 |
| | 10 | 33 / 13 27 / 17 36 / 22 56 / 17 33 / 25 355 / 15 39 / 11 40 / 19<br>41 / 14 27 / 24 38 / 14 37 / 17 |
| | 12 | 45 / 18 42 / 19 45 / 14 44 / 15 |
| | 15 | 57 / 26 58 / 18 54 / 27 64 / 30 55 / 22 8 / 20 |
| | 22 | 22 / 26 328 / 20 17 / 20 352 / 18 37 / 12 3 / 17 55 / 15<br>46 / 15 35 / 26 50 / 31 58 / 28 17 / 27 15 / 23 38 / 28<br>38 / 27 23 / 27 36 / 26 |
| | 24(a) | 312 / 26 308 / 20 304 / 22 306 / 25 308 / 26 345 / 17 322 / 20<br>12 / 21 28 / 12 15 / 22 |
| | (b) | 34 / 22 33 / 21 342 / 16 49 / 19 39 / 13 40 / 16 30 / 22 |

| | |
|---|---|
| (c) | 15 / 23  2 / 26  8 / 20  347 / 18 |
| (d) | 43 / 23  56 / 27  48 / 32  53 / 30  347 / 21  60 / 21  64 / 27  52 / 21  52 / 22  3 / 22 |
| (e) | 353 / 21  340 / 22  357 / 25  6 / 24  13 / 23  350 / 18  335 / 24 |
| (f) | 162 / 8  216 / 17  184 / 16  212 / 18  233 / 9  208 / 15  195 / 12 |
| (g) | 43 / 25  27 / 30  22 / 20  27 / 19  43 / 18  40 / 18 |
| (h) | 45 / 17  28 / 24  40 / 22  66 / 17  39 / 25 |
| (i) | 19 / 20  35 / 29  22 / 23  18 / 22  8 / 28  5 / 23  34 / 18  17 / 24  10 / 24  22 / 25  29 / 25 |
| (j) | 160 / 27  153 / 19  134 / 28  147 / 22  147 / 16 |
| (k) | 20 / 18  52 / 32  57 / 23  23 / 22  17 / 20  68 / 26  8 / 21  45 / 26 |
| (l) | 215 / 18  225 / 10  239 / 18  190 / 9  169 / 10  163 / 18 |
| (m) | 350 / 20  350 / 25  342 / 28  338 / 20  347 / 15  332 / 21  355 / 17 |
| (n) | 169 / 27  153 / 19  154 / 21  141 / 28  144 / 13  150 / 26  143 / 27  159 / 18 |

## AREA: CARTER, MONTANA

**LOCATION:** MISSOURI RIVER
**STRIKE AND DIP:** 143 / 10 NE

| SEC. | BED | MEASURED PALAEOCURRENT DATA |
|---|---|---|
| 1 | 1 | 198 / 14  206 / 9  220 / 16 |
| | 5 | 216 / 10  198 / 26  253 / 15  176 / 22 |
| | 6 | 196 / 16 |
| | 13 | 200 / 12  195 / 10 |
| | 16 | 196 / 18 |
| | 24 | 180 / 22 |
| | 29 | 166 / 12 |
| | 34 | 200 / 18 |
| | 51 | 150 / 17 |
| 2 | 1 | 210 / 16  194 / 14  236 / 20  229 / 16 |
| | 2 | 224 / 20  170 / 8 |
| | 7 | 180 / 22 |
| | 10 | 210 / 16 |
| | 42 | 85 / 17  120 / 10  115 / 22 |
| 3 | | 114 / 20  115 / 34  99 / 24  150 / 22  105 / 27  108 / 37 |

## AREA: HIGHWOOD, MONTANA

**LOCATION:** DEADMAN COULEE
**STRIKE AND DIP:** HORIZONTAL

| SEC. | BED | MEASURED PALAEOCURRENT DATA |
|---|---|---|
| 1 | 2 | 206 / 12  124 / 10  198 / 19  165 / 10  154 / 17 |
| | 6 | 236 / 12  252 / 11  250 / 6  236 / 18 |
| | 7 | 254 / 16  108 / 10  266 / 13 |

**LOCATION: INDIAN COULEE**
**STRIKE AND DIP: HORIZONTAL**

| SEC. | BED | MEASURED PALAEOCURRENT DATA |
|---|---|---|
| 1 | 2 | 144 / 12 |

## AREA: FOUR CORNERS, MONTANA

**LOCATION: NORTH WILLOW CREEK**
**STRIKE AND DIP: 44 / 5 NE**

| SEC. | BED | MEASURED PALAEOCURRENT DATA |
|---|---|---|
| Lower Section | 1 | 14 / 26 |
| Upper Section | 1 | 63 / 11 70 / 8 28 / 5 |
| | 2 | 45 / 16 75 / 9 |
| | 3 | 145 / 19 |
| | 4 | 113 / 26 |
| | 5 | 130 / 9 |
| | 11 | 73 / 14 |

**LOCATION: JOLLY ROGER RANCH**
**STRIKE AND DIP: HORIZONTAL**

| SEC. | BED | MEASURED PALAEOCURRENT DATA |
|---|---|---|
| Upper Section | 1 | 163 / 12 155 / 14 146 / 8 118 / 16 183 / 12 199 / 12 |
| | 2 | 146 / 10 163 / 10 169 / 12 172 / 12 185 / 11 |

## AREA: BELT, MONTANA

**LOCATION: GILLETTE HILL**
**STRIKE AND DIP: 45 / 4 NE**

| SEC. | BED | MEASURED PALAEOCURRENT DATA |
|---|---|---|
| 1 | 2 | 125 / 12 0 / 10 |
| | 10 | 104 / 8 |

**LOCATION: WILLOW CREEK**
**STRIKE AND DIP: 46 / 6 NE**

| SEC. | BED | MEASURED PALAEOCURRENT DATA |
|---|---|---|
| 2 | 6 | 163 / 20 |
| | 8 | 56 / 23 |
| | 9 | 64 / 19 |

**LOCATION: LITTLE BELT CREEK**
**STRIKE AND DIP: 60 / 7 NE**

### ROAD SIDE SECTION

| SEC. | BED | MEASURED PALAEOCURRENT DATA |
|---|---|---|
| 1 | 1 | 170 / 18 175/6 156/11 180/16 147/10 65/23 100/17<br>103/17 167/11 150/17 150/18 161/20 135/15 127/16<br>137/13 146/19 153/15 |
|  | 2 | 162/13 155/13 248/11 162/16 158/13 80/19 174/17<br>115/23 183/9 72/11 75/16 |
|  | 4 | 153/8 |
|  | 9 | 271/22 |
|  | 10 | 113/11 157/13 |
|  | 12 | 300/11 |

### WAVY CONGLOMERATE SECTION

|  |  |  |
|---|---|---|
| 2 | 3 | 30 / 230 (symmetric ripples)<br>172 / 20 |
|  | 5 | 175 / 20 |
|  | 6 | 185 / 26 |

**LOCATION: BELT BUTTE**
**STRIKE AND DIP: HORIZONTAL**

### BASAL BOOTLEGGER - the belt around Belt Butte

| SEC. | BED | MEASURED PALAEOCURRENT DATA |
|---|---|---|
| 1 | 1 | 210/21 165/8 155/22 158/10 150/15 160/15 177/16<br>195/27 189/7 97/11 167/14 160/13 174/12 181/28<br>182/16 |
|  | 12 | 310/12 |
|  | 14 | 343/17<br>1/22 355/17 (trough cosets)<br>0/180 (symmetric ripples) |
|  | 16 | 187/16 |
|  | 20 | 285/22 |
|  | 21 | 310 / 19 (trough coset) |
|  | 22 | 3 / 183 (symmetric ripples) |
|  | 26 | 283 / 10 |
|  | 27 | 65 / 10 |
|  | 30 | 281 / 13 (trough coset) |
| 2 | 1 | 254/17 246/8 114/10 50/26 108/10 100/10 176/5<br>97/12 177/20 30/18 199/10 217/10 |

UPPER SECTION - the fish scale and ammonite beds

| SEC. | BED | MEASURED PALAEOCURRENT DATA |
|---|---|---|
| 1 | 3 | 150 / 17  110 / 20  205 / 11  135 / 7  135 / 10  183 / 11  62 / 9 |
| | | 150 / 8  166 / 5  176 / 15  205 / 15  150 / 11  202 / 5  175 / 8 |
| | | 173 / 17  32 / 10  70 / 18  46 / 14 |

## AREA: BOOTLEGGER ESCARPMENT

**LOCATION: BLACKHORSE LAKE FLAT**
**STRIKE AND DIP: HORIZONTAL**

NORTH SIDE

| SEC. | BED | MEASURED PALAEOCURRENT DATA |
|---|---|---|
| 1 | 2 | 245 / 17  190 / 14  250 / 24  241 / 28  167 / 12  244 / 15  179 / 10 |
| | | 235 / 16  228 / 23 |
| | 3 | 250 / 24  203 / 18  200 / 26 |
| 2 | 4 | 246 / 9  250 / 13  253 / 8 |
| | 7 | 93 / 273  (symmetric ripples) |
| | | 112 / 292  "  " |
| | | 109 / 289  "  " |
| 4 | 3 | 11 / 191  (symmetric ripples) |
| | | 36 / 213  (symmetric ripples) |
| 5 | 2 | 129 / 309  (symmetric ripples) |
| | | 120 / 300  "  " |
| | 4 | 178 / 30  180 / 33  148 / 27  193 / 32  167 / 29  175 / 24  200 / 27 |

SOUTH SIDE

| SEC. | BED | MEASURED PALAEOCURRENT DATA |
|---|---|---|
| 1 | 1 | 233 / 14  238 / 21  238 / 24  195 / 23  153 / 23  154 / 23  150 / 25 |
| | | 228 / 22 |
| | 2 | 215 / 18  235 / 20  237 / 21  243 / 26  243 / 19  176 / 13  240 / 20 |
| | | 240 / 27  206 / 15  223 / 27  158 / 15  232 / 15  216 / 13  146 / 15 |
| | | 222 / 17  170 / 12 |
| | 5 | 215 / 27 |
| | 9 | 149 / 27  138 / 18 |
| | | 326 / 22  312 / 20  316 / 24  318 / 28 |
| | | 43 / 223  (symmetric ripples) |
| | | 0 / 180  "  " |
| | | 175 / 355  "  " |
| | | 48 / 228  "  " |
| | | 40 / 220  "  " |

## AREA: GORDON, MONTANA

LOCATION: RAILWAY CUT
STRIKE AND DIP: HORIZONTAL

| SEC. | BED | MEASURED PALAEOCURRENT DATA |
|---|---|---|
| 1 | 2 | 153 / 12 171 / 20 85 / 17 82 / 14 78 / 10 |
| | 7 | 90 / 5 50 / 18 158 / 15 |
| | 9 | 286 / 9 92 / 15 140 / 17 127 / 12 |

## AREA: SWEETGRASS HILLS

LOCATION: MT. LEBANON
STRIKE AND DIP: 295 / 42 NE

| SEC. | BED | MEASURED PALAEOCURRENT DATA |
|---|---|---|
| 1 | 9 | 11 / 25 |
| | 10 | 359 / 44 |
| 2 | 1 | 355 / 61 347 / 48 |
| | 2 | 19 / 48 355 / 61 350 42 28 / 25 |
| | 3 | 359 / 46 350 / 47 15 / 45 286 / 30 354 / 50 1 / 56 11 / 52 7 / 46 25 / 65 |
| | 20 | 22 / 61 37 / 65 |

A SCHMIDT EQUAL AREA PROJECTION stereonet representation of the rotated Sweetgrass Hills palaeocurrent data is given in Figure 2.

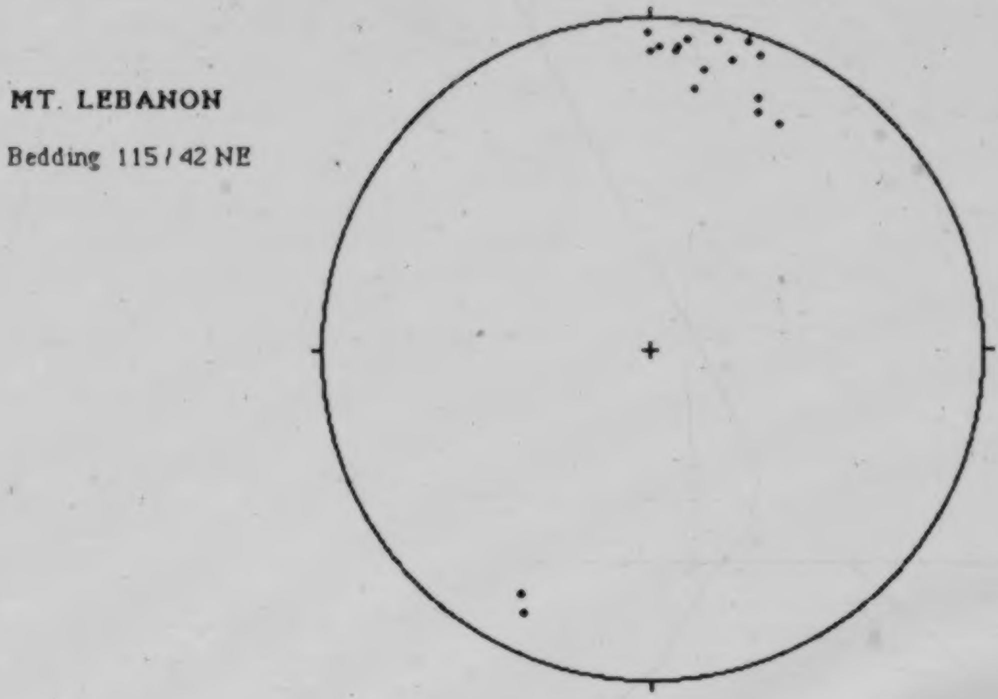

FIGURE IX-2: A Schmidt Net representation of the rotated palaeocurrent data from Mt. Lebanon.

TABLE IX-2: Pebble imbrication measurements of Sequence 3 conglomerate: Little Willow Ranch Section.

## CONGLOMERATE CAPPING BOOTLEGGER SEQUENCE 3

**LOCATION: NORTH WILLOW CREEK** - Little Willow Ranch
**STRIKE AND DIP: HORIZONTAL**

### TROUGH

160 / 28
284 / 23
103 / 32
20 / 37
300 / 28
10 / 38
230 / 46
340 / 27
17 / 13
152 / 27
118 / 27
280 / 22
301 / 36
237 / 26
300 / 8
296 / 11
304 / 34
112 / 17
236 / 26
05 / 52
312 / 49
265 / 11
330 / 60
235 / 23
282 / 21

### CREST

253 / 20
54 / 28
300 / 27
212 / 42
40 / 10
21 / 21
288 / 18
257 / 19
343 / 35
21 / 29
336 / 20
270 / 34
132 / 11
342 / 14
249 / 22
351 / 19
295 / 32
22 / 13
287 / 31
251 / 22
40 / 21
335 / 17
170 / 10
19 / 31
352 / 30

### TROUGH

05 / 19
296 / 44
313 / 22
340 / 18
112 / 10
111 / 39
145 / 16
155 / 24
04 / 18
310 / 66
293 / 35
356 / 24
92 / 31
23 / 24
10 / 49
200 / 25
262 / 47
291 / 26
115 / 14
254 / 22
190 / 47
90 / 32
339 / 16
317 / 19

304 / 72

CREST

311 / 33
52 / 19
203 / 29
00 / 32
137 / 4
48 / 11
12 / 39
166 / 7
47 / 39
271 / 21
338 / 47
222 / 34
315 / 28
349 / 34
247 / 64
40 / 23
100 / 32
14 / 22
208 / 46
290 / 73
353 / 36
334 / 19
27 / 38
138 / 53
100 / 58
62 / 53

TOTAL NUMBER OF CLAST IMBRICATION MEASURMENTS = 101

Wavelength of the symmetric wave-like transgressive lag feature = 1.4 m , 1.12 m
Amplitude of wave crest = 7 cm
Clasts are mostly black chert pebbles (white chert, sandstone and siltstone clasts are common)
Outcrop is weathered and intensely iron stained

A MATRIX-SUPPORTED CONGLOMERATE (MSC)
Bed is 9 cm thick in trough and 15 cm thick in the crest
Matrix is 1 mm sandstone
Size of ten largest clasts ($D_{10}$) = 6.5, 4.0, 3.5, 2.7, 4.0, 3.0, 2.9, 2.5, 3.0, 2.6 cm

Figure 3 = rose diagram plot of the above data

PEBBLE IMBRICATION DATA

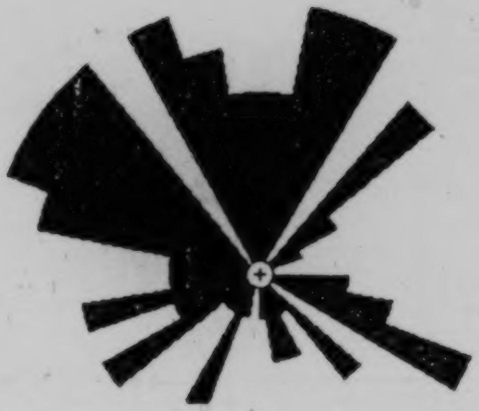

N = 101

NORTH WILLOW CREEK - LITTLE WILLOW RANCH

FIGURE IX-3: Rose diagram of pebble imbrication data of conglomerate outcropping at the Little Willow Ranch study area.

TABLE IX-3: Pebble imbrication measurements of Sequence 3 conglomerate:

Little Belt Creek - Section 2(a).

**LOCATION: LITTLE BELT CREEK - Section 2 (a)**
**STRIKE AND DIP: HORIZONTAL**

## CREST

19 / 29
00 / 10
332 / 29
10 / 21
206 / 21
336 / 23
63 / 17
13 / 18
19 / 26
40 / 28
97 / 27
11 / 13
00 / 21
281 / 25
34 / 51
36 / 33
00 / 26
12 / 4
165 / 11
32 / 13
140 / 22
214 / 40
49 / 7
21 / 9
12 / 10

## TROUGH

13 / 42
15 / 27
53 / 37
54 / 27
115 / 18
345 / 25
345 / 28
335 / 19
328 / 16
27 / 26
352 / 25
22 / 9
14 / 31
62 / 27
08 / 46
40 / 14
00 / 22
349 / 26
25 / 21
333 / 10
348 / 11
25 / 16
59 / 42
52 / 53
52 / 39

## CREST

335 / 30
325 / 16
333 / 27
08 / 12
03 / 28
338 / 32
332 / 33
342 / 7
41 / 36
350 / 37
75 / 25
50 / 35
04 / 14
68 / 18
68 / 17
334 / 40
143 / 34
84 / 17
07 / 13
16 / 24
117 / 32
70 / 26
346 / 24
34 / 33
354 / 17

TROUGH

98 / 57
95 / 13
27 / 4
99 / 40
92 / 40
18 / 9
345 / 22
22 / 15
58 / 33

86 / 62
72 / 30
343 / 14
36 / 6
351 / 14
21 / 30
64 / 11
292 / 28

80 / 41
298 / 20
320 / 17
77 / 16
210 / 51
294 / 7
126 / 29
143 / 19

TOTAL NUMBER OF CLAST IMBRICATION MEASUREMENTS = 100
Wavelength of the symmetric wave-like transgressive lag feature = 1.1 m, 0.95 m, 0.84 m
Amplitude of wave crests = 7.5 cm

A MATRIX-SUPPORTED (MSC) AND IN SOME PLACES A CLAST-SUPPORTED (CSC) CONGLOMERATE

Matrix is 1 mm sandstone
Crests of waves are oriented $18^{o}$ - $198^{o}$
Size of ten largest clasts ($D_{10}$) = 6.0, 5.0, 5.2, 6.7, 4.2, 5.7, 6.0, 5.6, 5.6, 5.3 cm

Figure 4 = rose diagram plot of the above data

***NB* : THE ABOVE PEBBLE IMBRICATION DATA REPRESENTS THE LINEAMENT MARKING OUT THE MAXIMUM DIPPING PEBBLE PLANE (IN MOST CASES THIS LINEAMENT REPRESENTS THE PEBBLE "AB" PLANE WITH AN UPSTREAM B-AXIS IMBRICATION)**

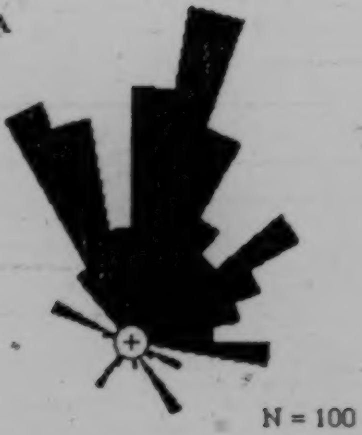

FIGURE IX-4: Rose diagram of pebble imbrication data of conglomerate outcropping at the Little Belt Creek study area .